# Functional characterization of a new IgM- and IgA-enriched immunoglobulin preparation

Schmidt, Carolin

(2020)

# Functional characterization of a new IgM- and IgA-enriched immunoglobulin preparation

Dissertation
Carolin Schmidt

TECHNISCHE UNIVERSITÄT DARMSTADT

**Vom Fachbereich Chemie**
**der Technischen Universität Darmstadt**

zur Erlangung des Grades
Doctor rerum naturalium
(Dr. rer. nat.)

**Dissertation**
**von Carolin Schmidt**

Erstgutachter: Prof. Dr. Harald Kolmar
Zweitgutachter: PD Dr. med. Dr. med. habil. Jörg Schüttrumpf

Darmstadt 2020

**Tag der Einreichung:** 22. September 2020

**Tag der mündlichen Prüfung:** 23. November 2020

## Erklärung zur Dissertation

### Erklärung gemäß §8(1) Promotionsordnung

Hiermit erkläre ich, dass ich die vorgelegte Dissertation selbstständig und nur mit den mir zulässigen Hilfsmitteln angefertigt habe. Die Dissertation wurde in der vorgelegten oder einer ähnlichen Fassung zu keinem früheren Zeitpunkt an einer in- oder ausländischen Hochschule eingereicht. Die schriftliche Version stimmt zudem mit der elektronischen Version überein. Die identische elektronische Version für die Durchführung des Promotionsverfahrens liegt vor.
Außerdem erkläre ich, noch keinen Promotionsversuch unternommen zu haben.

Darmstadt, 22. September 2020
Ort, Datum

Unterschrift

### Erklärung gemäß §9 Promotionsordnung

Hiermit versichere ich, dass ich die vorliegende Dissertation selbstständig angefertigt und keine anderen als die angegebenen Quellen und Hilfsmittel verwendet habe. Alle wörtlichen und paraphrasierten Zitate wurden angemessen kenntlich gemacht. Die Dissertation wurde in der vorgelegten oder einer ähnlichen Fassung zu keinem früheren Zeitpunkt an einer in- oder ausländischen Hochschule eingereicht.

Darmstadt, 22. September 2020
Ort, Datum

Unterschrift

## Zusammenfassung

Die Entwicklung und die funktionelle Charakterisierung von Immunglobulin (Ig) Präparaten, die aus menschlichem Blutplasma gewonnen werden, sind von hoher klinischer Relevanz für die Therapie von Patienten, die an Antikörpermangel, Autoimmun- oder an Entzündungserkrankungen leiden. Gegenwärtig werden hauptsächlich intravenös verabreichte Immunglobulin G (IgG) Präparate (IVIgs) zur Behandlung eines breiten Spektrums pathologischer Zustände, wie primärer und sekundärer Immundefekte (PID; SID), aber auch zur Immunmodulation eingesetzt. Dennoch besteht die Notwendigkeit, eine effizientere Ausnutzung des Plasmas zu erreichen sowie die Wirksamkeit polyklonaler Ig-Präparate zu verbessern, ohne den Plasmabedarf zu erhöhen. Insbesondere Fraktionen, die IgA- und IgM-Moleküle enthalten, können aufgrund ihrer vielseitigen pharmakologischen Effekte vorteilhaft sein und therapeutisch genutzt werden.

Trimodulin (Wirkstoffname, welcher der Abgrenzung zu einem Standard-IVIg-Präparat dient) ist ein neues Ig-Präparat aus menschlichem Blutplasma, für die intravenöse Anwendung und ist in seiner Zusammensetzung einzigartig, da es im Vergleich zu den bisher auf dem Markt verfügbaren Standard-IVIg-Präparaten neben IgG auch definierte Mengen an IgM- sowie IgA-Molekülen enthält. Es wurde für die Behandlung von Patienten mit schweren Infektionen entwickelt und bereits in einer klinischen Phase II Studie (CIGMA Studie) getestet, in der ein vielversprechendes Potenzial für die Therapie von Patienten mit schwerer ambulant erworbener Lungenentzündung (sCAP) nachgewiesen werden konnte. Aufgrund der Neuheit und der Komplexität des Ig Präparates, das neben IgG auch IgM und IgA Moleküle enthält, besteht jedoch Bedarf an einem detaillierteren Verständnis der komplexen Wirkungsweise von Trimodulin, sowohl hinsichtlich seiner antimikrobiellen als auch seiner immunmodulatorischen Eigenschaften. Insbesondere das Komplementsystem ist ein wichtiges Werkzeug des humoralen Immunsystems, da seine Aktivierung über verschiedene Effektorfunktionen zur Abtötung eindringender Krankheitserreger führt. Es kann allerdings auch schädlich für den Wirt sein, wenn das Immunsystem überaktiviert ist und zu Gewebeschäden sowie zu multiplem Organversagen führen. Daher ist es wichtig, dass die Aktivierung sowie die Hemmung des Komplementsystems ausbalanciert sind. Es wurde die Hypothese aufgestellt, dass Trimodulin eine ambivalente Wirkung hinsichtlich der Komplementaktivierung aufweist, um die Neutralisierung eindringender Mikroorganismen zu gewährleisten, aber auch um den Wirt vor Entzündungsreaktionen zu schützen, die durch ein überaktiviertes Immunsystem verursacht werden können.

Um zu überprüfen, ob die Aktivierung des Komplementsystems gehemmt werden kann, wurde die Bindung von Trimodulin an aktivierte Komplementfaktoren (C3b, C4b, C5a und C3a) in ELISA Tests untersucht. Es wurde gezeigt, dass Trimodulin sowohl mit C3b- als auch mit C4b-Molekülen interagieren kann, indem es diese bindet sowie überlagert. Die Zugabe einer IVIg-Kontrolle (Intratect) zeigte nur geringe Effekte und die Abnahme der C3b sowie C4b Detektion war nach Gabe des IgM- und IgA-angereicherten Präparats deutlich erhöht. Darüber hinaus zeigte sich ein Trend zur Verringerung der C5a Detektion nach Trimodulin Gabe, wohingegen keine Interaktion von Trimodulin mit aktivierten C3a-Molekülen nachgewiesen werden konnte. Des Weiteren wurde mit Hilfe eines komplementabhängigen Zytotoxizitätstests (CDC) untersucht, ob Trimodulin die Aktivierung des Komplementsystems auch funktionell verhindern kann. Daher wurde die komplementabhängige Zytotoxizität von Zielzellen (Ramos-Zelllinie) nach Zugabe von Trimodulin gemessen, wobei eine deutliche Reduktion der Zytotoxizität von Ramos-Zellen festgestellt werden konnte. Diese Ergebnisse zeigten erstmalig, dass Trimodulin dazu in der Lage ist, aktivierte Komplementfaktoren zu hemmen, was zur Verhinderung von Entzündungsreaktionen bei Patienten mit einer überstimulierten Immunantwort eingesetzt werden könnte. Darüber hinaus zeigten die Ergebnisse ebenfalls deutlich die Vorteile der Verwendung von Trimodulin zur Reduzierung der Überstimulation des Komplementsystems, gegenüber einem Standard-IVIg-Präparat auf, welches keine verminderte Zytotoxizität in diesem Test bewirkte.

Weiterführend wurden zwei Opsonophagozytose-Tests (OPAs) entwickelt, um zu analysieren, ob Trimodulin, welches neben IgG und IgA auch ≈ 23% IgM enthält, dazu in der Lage ist, das Komplementsystem zu aktivieren und die Opsonophagozytose von Krankheitserregern zu induzieren. Generell können IgM Moleküle das Komplementsystem im klassischen Weg deutlich effektiver aktivieren als IgG Moleküle. Der Opsonophagozytose-Test, der mit lebenden *E. coli* Bakterien durchgeführt wurde,

war allerdings nicht dazu geeignet die Aktivierung des Komplementsystems und die damit verbundene Einleitung der Opsonophagozytose durch Trimodulin zu zeigen. Es wurde ausschließlich die IgG-vermittelte Phagozytose der Bakterien detektiert. Weiterhin wurde vermutet, dass dies auf eine starke unspezifische Abtötung durch die verwendete Komplementquelle zurückzuführen ist, die auch in Abwesenheit von Trimodulin eine große Anzahl an *E. coli* Bakterien neutralisierte. Aus diesen Gründen wurde ein zweiter Opsonophagozytose-Test unter Verwendung von *S. aureus* Biopartikeln etabliert und die Fähigkeit von Trimodulin Opsonophagozytose einzuleiten, in einem Durchflusszytometer (FACS) evaluiert. Die Analyse zeigte, dass Trimodulin dazu in der Lage war, das Komplementsystem konzentrationsabhängig zu aktivieren und dadurch die Opsonophagozytose von *S. aureus* Biopartikeln durch Effektor Zellen (HL-60-Zelllinie) in niedrigen Konzentrationen auszulösen. Zusätzlich wurde festgestellt, dass Trimodulin in hohen Dosen auch im Opsonophagozytose-Test das Komplementsystem hemmte.

Die Ergebnisse dieser Doktorarbeit unterstützen die Theorie, dass Trimodulin eine ambivalente Wirkung hinsichtlich der Komplementaktivierung besitzt und stehen im Einklang mit verschiedenen Studien, die ebenfalls duale Mechanismen von Ig-Präparaten hinsichtlich der Aktivierung und der Hemmung des Komplementsystems zeigen. Darüber hinaus wird vermutet, dass die Behandlung mit Trimodulin dazu beitragen könnte, Entzündungsreaktionen, die durch eine Überstimulation des Komplementsystems verursacht werden, zu reduzieren und gleichzeitig die Neutralisierung schädlicher Krankheitserreger sicherzustellen. Des Weiteren gibt die Arbeit durch die Bestätigung der Aktivierung sowie Inhibierung des Komplementsystems durch Trimodulin neue Einblicke in dessen Wirkungsweise und zeigt entscheidende Vorteile der Verwendung eines IgM- und IgA-angereicherten Präparats im Vergleich zu einem Standard-IVIg-Präparat auf.

## Abstract

The development and the functional characterization of human plasma-derived immunoglobulin (Ig) preparations are of high clinical relevance for the therapy of patients who suffer from antibody depletion, autoimmune or inflammatory disorders. Currently, mainly intravenous immunoglobulin G (IgG) preparations (IVIgs) are in use to treat a broad range of pathological conditions, like primary and secondary immunodeficiencies (PID; SID), but also for immunomodulation. Nevertheless, there is a need to improve the exploitation of the plasma as well as the efficacy of polyclonal Ig preparations without an increase in plasma demand. Especially fractions containing IgA and IgM molecules may be advantageous, because of their versatile pharmacological effects that could be exploited therapeutically.

Trimodulin (name of the active substance, for differentiation from a standard IVIg preparation) is a new plasma-derived Ig preparation for intravenous application and is unique, as it contains besides IgG also defined amounts of IgM as well as IgA molecules compared to currently available standard IVIg preparations. It was developed for the treatment of patients with severe infections and was already tested in a phase II clinical trial (CIGMA study), where a promising potential in the therapy of patients with severe community-acquired pneumonia (sCAP) could be demonstrated. Based on the novelty and complexity of this Ig preparation that contains besides IgG also IgM as well as IgA molecules, there is still a need for a detailed understanding of the complex mode of action (MoA) of trimodulin regarding its antimicrobial as well as its immunomodulatory mechanisms. Particularly the complement system is an important tool of the humoral immune system, because its activation leads to the killing of invading pathogens via various effector functions. Nevertheless, it can also be harmful to the host when the immune system is over-activated and can lead to tissue damage as well as multiple organ failure. Therefore, it is important that the complement system is balanced between activation and inhibition. It was hypothesized that trimodulin exhibits an ambivalent effect regarding complement activation to ensure the neutralization of invading microorganisms but also to protect the host against inflammation caused by a hyper-activated immune system.

In order to evaluate the ability to inhibit complement activation, the binding of trimodulin to activated complement factors (C3b, C4b, C5a and C3a) was analyzed in ELISA settings. It was demonstrated that trimodulin is able to interact with C3b as well as C4b molecules by binding and an overlay of these complement factors. The addition of an IVIg control (Intratect) showed only slight effects and the decrease in the detection of C3b as well as C4b was obviously stronger with the IgM- and IgA-enriched preparation. Moreover, a trend in reducing the detection of C5a with trimodulin was revealed, whereas no interaction of trimodulin with activated C3a molecules could be demonstrated. Furthermore, a complement-dependent cytotoxicity (CDC) assay was used to analyze if trimodulin can even functionally prevent complement activation. Therefore, the CDC of target cells (Ramos cell line) was measured after addition of trimodulin and an obvious reduction in the CDC of Ramos cells was detected. This demonstrated for the first time that trimodulin is able to inhibit activated complement factors, which could be used to prevent inflammation in patients with an over-stimulated immune response. Furthermore, the results clearly showed the benefit of using trimodulin to prevent the over-stimulation of the complement system, over a standard IVIg preparation that was not able to reduce the CDC in this assay.

In order to analyze if trimodulin, which contains besides IgG and IgA also ≈ 23% IgM, is able to activate the complement system and to induce the opsonophagocytosis of pathogens, two opsonophagocytosis assays (OPAs) were developed. In general, IgM molecules are able to activate the complement system via the classical pathway more effectively than IgG molecules. The OPA using living *E. coli* bacteria unfortunately did not depict the opsonophagocytic capacity of trimodulin, but showed only the IgG-mediated phagocytosis of the bacteria. This was assumed to be due to a high non-specific killing of the used complement source, which destroyed high amounts of *E. coli* bacteria even in the absence of trimodulin. For this reason, a second OPA was established by using *S. aureus* bioparticles and the opsonophagocytic capacity of trimodulin was evaluated in a fluorescence-activated cell sorter (FACS). The analysis showed that trimodulin was able to activate the complement system concentration-dependently and thereby to trigger the opsonophagocytosis of *S. aureus* bioparticles by effector cells

(HL-60 cell line) in low concentrations. Additionally, it was detected that even in the OPA setting trimodulin was able to inhibit the complement system in high doses.

The results of this PhD thesis obviously support the theory that trimodulin exhibits an ambivalent effect regarding complement activity and are in accordance with various studies that also show dual mechanisms of Ig preparations in activating and inhibiting the complement system. Moreover, it is assumed that the treatment with trimodulin could help to reduce inflammation caused by an over-stimulation of the complement system and simultaneously ensuring the neutralization of harmful pathogens. Furthermore, the PhD thesis gives new insights in the MoA by confirmation of the complement activating as well as inhibitory capacity of trimodulin and emphasizes the crucial advantages of using an IgM- and IgA-enriched preparation compared to a standard IVIg preparation.

## Table of contents

# 1. Introduction

## 1.1. The human immune system

The primary function of the immune system is to protect the host against invading pathogens that are harmful to the body, like bacteria, viruses, parasites and fungi. It is a network of cells, tissues and organs to control and eliminate such disease-causing organisms. By using a complex array of protective mechanisms, it is able to detect specific structural features (antigens) of the pathogens and can therefore distinguish between self and non-self. This is a very important function, to avoid excessive damage to the body's own tissues and cells[1,2]. Generally, the immune system is divided into the innate and the adaptive immune responses. Both parts stay in constant interaction by using an elaborate communication network. The innate immune response is the early first line of defense against invading microbes. Involved cell types react quickly and include macrophages, dendritic cells, natural killer cells, granulocytes and mast cells. They are able to recognize pathogenic structures in an unspecific way and react to signaling molecules released by the body. Epithelial barriers, soluble proteins and bioactive small molecules (e.g. complement proteins or cytokines) also belong to the innate immune system. It causes inflammation by eliminating infectious agents, but also helps to activate the cells of the adaptive arm. This part of the immune system exhibits highest specificity for its targets, but reacts slower than the innate response. The main cell types of the adaptive immune system are B and T lymphocytes, which express antigen-specific receptors on their surfaces. The major functions of the T cells are the killing of pathogens and infected cells as well as the control of the adaptive response. B cells primarily secrete antibodies that attach to the infectious agents. Once exposed to an antigen, the adaptive arm forms immunological memory, ready to remember specific pathogens for the next infection[3].

The two arms of the immune system are often described as distinct mechanisms, but they usually act together. An important example of the elaborate collaboration of the innate and adaptive arm is the clearance of immune complexes by the complement system and antibodies that bind specifically to a certain pathogen. The synergy of both parts of the immune system is a fundamental process that is necessary for a functional immune response[4,5].

## 1.2. The complement system

The complement system is a tightly regulated network of more than 30 soluble and membrane-associated proteins that provides a first-line defense against invading microorganisms[6,7]. It was discovered as heat-sensitive component of normal plasma that complements the antibacterial activity of antibodies. However, today it is well established that it can be activated early in infection even in the absence of antibodies. As part of the non-specific humoral immune response, it is rapid and efficient in protecting the host through the immediate activation of components that are present in the blood as inactive proenzymes, called zymogens. Although it belongs to the innate immunity, it influences the adaptive arm by the interaction with cell surface receptors of immune cells as well as by augmenting the opsonization of bacteria through antibodies. Therefore, it is an important effector component of both, the innate and the adaptive immune system[8–11].

The complement proteins react in a cascade like manner with one another and are activated by proteolytic cleavage at site of infection, where they induce inflammatory events to help immune cells fighting pathogens and maintain homeostasis. This enzymatic cascade proceeds by the cleavage of a zymogen precursor, which becomes an active enzyme by itself and goes on with the activation of the next complement zymogen in the pathway. Hence, the cascade amplifies itself and leads to a large cytolytic and inflammatory response to infectious organisms[12]. This is caused by the generation of proinflammatory mediators like C3a and C5a, so-called anaphylatoxins, by opsonization of pathogenic surfaces with complement opsins, like C3b and C4b and by the formation of the membrane attack complex (MAC), which is the terminal component of the cascade and leads to the lysis of targeted cells[13].

### 1.2.1. Mechanisms of activation

The complement system can be activated via three different pathways: the classical, lectin and alternative pathway (Figure 1)[7,12].

The classical pathway is antibody dependent and starts with the recognition of a pathogen or a foreign antigen by IgG or IgM. This emerging immune complex triggers the activation of the first complement component, the C1 complex[11]. It consists of one C1q molecule as well as two molecules of the serine proteases C1r and C1s and binds to the Fc portion of the Igs attached to pathogenic surfaces. Thus, the serine proteases are autocatalytically activated and in turn cleave their substrates C4 and C2 into the fragments C4b, C4a and C2b, C2a. C4b, which is covalently bound to the surface of the pathogen, assembles with the serine protease C2b and leads to the generation of the C3 convertase. The consequent cleavage of the C3 molecule forms the opsonin C3b and the anaphylatoxin C3a and marks the point at which the three complement pathways converge. With the production of C3b molecules and their deposition on the pathogenic surface, the microorganisms are effectively opsonized and further complement activation takes place. In contrast, the generation of C3a leads to local inflammatory responses[13,14]. The C3b molecule then interacts and assembles with the C3 convertase and therefore induces a change in the specificity regarding the cleavage preferences. It is now able to bind and cleave the C5 molecule and therefore generates the C5b fragment and the anaphylatoxin C5a. C5b is responsible for the recruitment of the terminal factors C6, C7, C8 and C9 of the cascade. All these components build together the MAC C5b-9 that forms pores into the membrane of the pathogens, leading to subsequent lysis[15]. It is well established that IgM is more efficient in activating the complement system than IgG. In general, C1q needs two or more IgG molecules in a specific distance to each other for activation of the complement cascade, because of low binding affinity to some IgG subclasses. The energy that is required for C1q activation is only achieved by the binding of two or more IgG molecules. Compared with this, just one pentameric IgM molecule, comprising 10 antigen-binding sites, bound to the surface of a microorganism, is sufficient for classical pathway activation. IgA, IgD and IgE have not the ability to activate the complement system via the classical effector arm[12].

As the classical pathway needs C1q for activation, the lectin pathway requires a similar molecule, called mannose-binding lectin (MBL), which is composed of globular lectin domains and collagen-like arms. This protein binds directly to foreign cells and recognizes mannose residues on microorganism surfaces. It is also capable of binding to IgA on the surface of microorganisms, thereby activating the lectin pathway[16]. In addition, ficolins resemble C1q and can activate the lectin pathway as well. The MBL-associated serine proteases (MASP), MASP-1 and MASP-2, can in turn bind to MBL and ficolin molecules and autoactivate when these complexes bind to a foreign cell. This in turn leads to the cleavage of classical pathway components. Homologous to C1s, MASP-2 is responsible for the C4 and C2 fragmentation, while MASP-1 cleaves C3[8,17,18]. After that, the following steps of the complement cascade are indistinguishable from the classical effector arm.

In comparison to the activation of the classical and lectin pathway, the alternative pathway does not require specific binding to a foreign protein. The pathway starts with the spontaneous hydrolysis of factor C3 to C3($H_2O$) that associates with the serine protease complement factor B. Another component, factor D, then proteolytically cleaves factor B to Bb and Ba. Bb stays in complex with C3($H_2O$) and is a serine protease. It cleaves C3 into C3b, which binds to factor B and generates more C3 convertases. This amplification loop is stabilized by the serum protein properdin, which also enhances the reaction. The generation of more C3b fragments then leads to the assembly of the C5 convertase, C3bBbC3b. After that, the progress of the alternative pathway is homologous to the MAC formation in the classical pathway[15,19]. In addition, Hiemstra *et al.* described the formation of a C3/C5 specific convertase after the incubation of alternative pathway components C3, factor B and D as well as Properdin with deposited IgA. These results revealed that IgA is also capable of activate the complement pathway via the alternative arm[20].

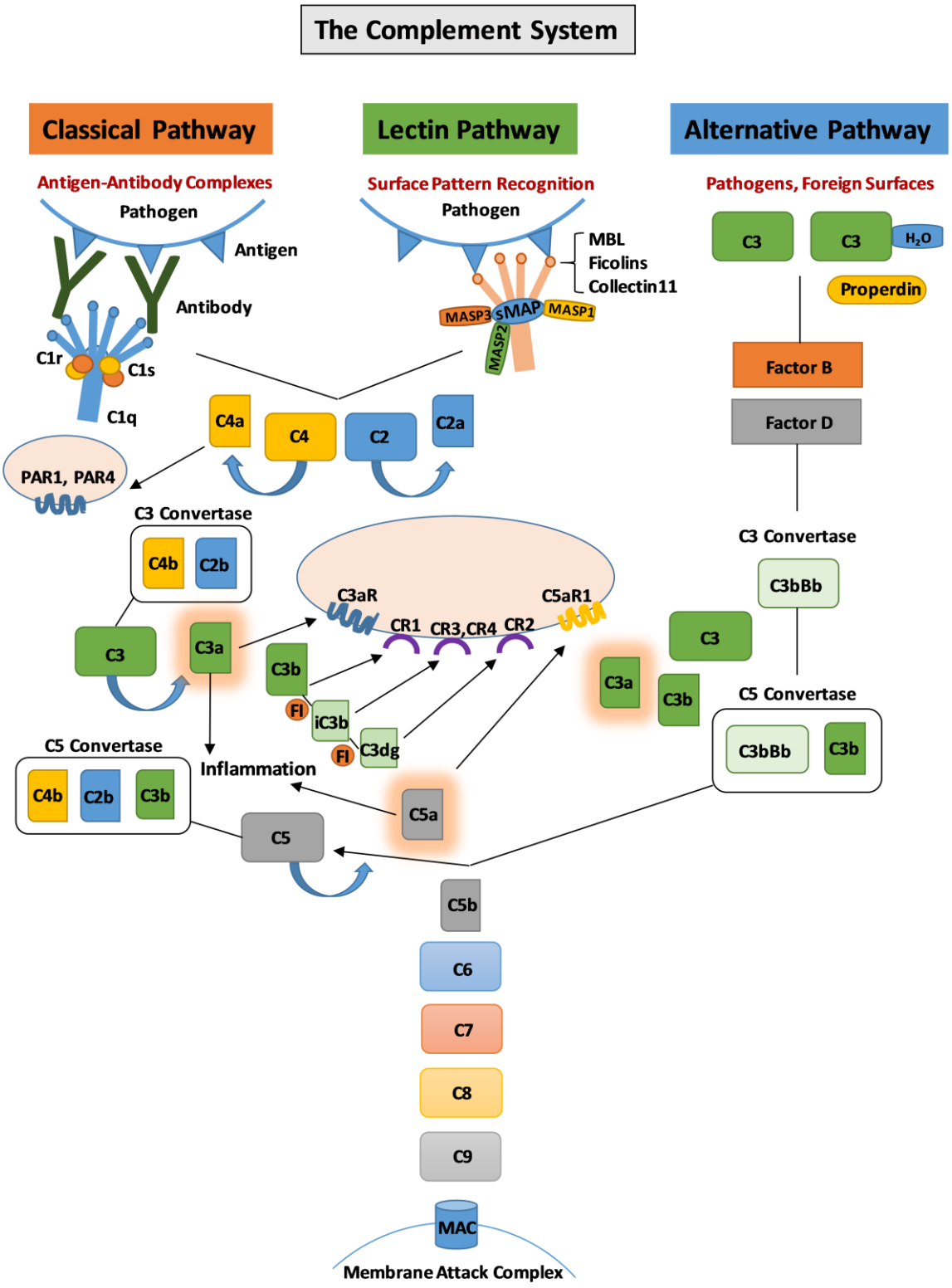


**Figure 1** Overview of the complement cascade. The complement system can be activated via the classical, lectin and alternative pathway. The binding of C1q to its ligands, such as immune complexes, triggers classical pathway activation. The lectin pathway is activated by the binding of MBL ficolins or collectins to a pathogen. Activation of the alternative pathway occurs spontaneously and is initiated by the hydrolysis of factor C3 to C3($H_2O$). All pathways converge at the point of C3 activation that is cleaved into the opsin C3b and the anaphylatoxin C3a. C5 convertases lead to the formation of C5a as well as C5b. The latter generates together with C6-9 the MAC, which in turn forms pores into the membrane and lyses the target cells[21]. CR = complement-receptor; FI = factor I; MAC = membrane attack complex; MASP = MBL-associated serine proteases; MBL = mannose-binding lectin; PAR = protease-activated receptor.

### 1.2.2. The complement system and inflammation

The activation of the complement cascade leads to a variety of antimicrobial functions to protect the host from pathogens that are harmful to the body[6,9,11,22,23]. However, this activation can also induce inflammatory reactions due to the generation of powerful immune effectors, like the anaphylatoxins C5a and C3a. Already low concentrations of these factors are enough to induce acute inflammation and anaphylactic reactions[24]. C3a and C5a are released after the cleavage of C3 and C5 with their specific convertases and are able to activate immune cells and non-myeloid cells that express the specific anaphylatoxin receptors (C3aR and C5aR) on their surfaces[23]. These receptors can be found on leukocytes, macrophages, mast cells, hepatocytes, lung epithelial cells, endothelial cells, astrocytes and microglial cells[25]. C3a and C5a are the most extensively studied anaphylatoxins and show a great array of biological activities[22]. They induce the chemotaxis of phagocytes (neutrophils, eosinophils and monocytes) to the site of infection, thereby activating the effector cells and inflammatory mediators, like cytokines, lysosomal proteases and reactive oxygen species (ROS) are released[6,26]. These events lead to smooth muscle contraction, increased vascular permeability and cause inflammatory cell migration. Moreover, C3a and C5a can induce histamine release by mast cells, leading to vasodilation and extravasation of fluid[23,27]. In addition, the binding of the anaphylatoxins to effector cells (e.g. macrophages, mast cells, B and T lymphocytes) leads to the generation of cytokines, which in turn induces an amplification of the inflammatory response. This interplay between the complement system and proinflammatory cytokines can also lead to an enhanced anaphylatoxin receptor expression on inflammatory cells[27,28]. In case of excessive complement activation, all the indicated mechanisms can be harmful to the host and lead to tissue damage and multiple organ failure[9,24,26,29].

The anaphylatoxins show differences in their biological activity: C5a is the most active and stable anaphylatoxin, whereas C3a is up to 200-times less potent[12]. In addition, C5a exhibits a stronger chemotactic influence on phagocytic cells at already very low concentrations. Both anaphylatoxins are quickly converted into C3a-desArg and C5a-desArg after generation in plasma. This is performed by carboxypeptidase N and B, which cleave the C-terminal arginine. Differences to C3a and C5a are a weaker proinflammatory activity of C5a-desArg and the inability of C3a-desArg to bind to the C3aR[22,23]. Furthermore, there are evidences that C3a can also exhibit anti-inflammatory activities as an antagonist to C5a. It seems that C3a can react dichotomous to an injury or inflammatory infections, depending on particular conditions. On the one hand, C3a is able to prevent neutrophil migration and accumulation in an acute setting of inflammation, thus leading to reduced inflammation. On the other hand, in chronic phases of inflammation, the proinflammatory actions of C3a are triggered. This dual role of C3a seems also to be dependent of the involved cell types and is important for the development of therapeutics[23,30,31]. Nevertheless, deregulated complement activity contributes to the pathogenesis of a number of chronic inflammatory diseases. Excessive activation or insufficient control are key mediators for an immune imbalance between inflammatory cells, complement system and tissue damage that lead to hypersensitivity reactions, respiratory distress syndrome, neurodegenerative diseases, endotoxic shock and multiple organ failure[24,26,32–34].

### 1.2.3. Inhibition of the complement system

The complement system has to be tightly regulated, in order to prevent undesired as well as indiscriminated effects that are harmful to host cells. Pro-inflammatory mechanisms mainly induced by anaphylatoxins can damage host tissues and cells, when the immune system is over-stimulated, due to uncontrolled activation of the complement system. Therefore, it is necessary to control complement activation by a variety of membrane-bound and soluble inhibitors. This ensures that healthy host surfaces are not affected by uncontrolled attacks of the complement system, but at the same time permits the efficient activation to defense foreign targets[35]. An important modulator of the complement response is the C1 inhibitor (C1INH), which is able to bind and to inactivate the two molecules C1r and C1s of the classical pathway. It can also inhibit MASP-1 and MASP-2 of the lectin pathway irreversibly. The key regulators for the alternative pathway are complement factor H (CFH) and complement factor I (CFI) that interact with the factors C3b as well as C4b. As a plasma serine protease, CFI degrades C3b to iC3b

and further into C3dg as well as C3c, with the help of specific cofactors. It is also able to cleave C4b and the C3 convertase C4b2a, whereas CFH induces the dissociation of the C3bBb convertase into C3b and Bb and therefore downregulates the alternative pathway. The regulation of the terminal MAC is controlled by vitronectin (protein S), which inhibits the polymerization of C5b-7 and clusterin that prevents the insertion of this complex into cell membranes. Moreover, CD59 is the key modulator of the terminal pathway, which prevents the C5b-9 formation by blocking the C9 incorporation into C5b-8[36–38].

However, insufficient regulation of the complement cascades can lead to a number of inflammatory and autoimmune diseases[39]. Therefore, it is important to discover new drugs that are not only able to activate but also to inhibit as well as modulate the complement system. The development of drug candidates can be divided into different categories regarding their function: protease inhibitors, soluble complement regulators, therapeutic antibodies, complement component inhibitors and receptor antagonists. In general, it is important to specifically target particular factors for each indication and to preserve immunomodulatory as well as defensive mechanisms of complement[40].

## 1.3. Immunoglobulins

Igs are heterodimeric glycoproteins, produced and secreted by plasma cells[41,42]. They can be divided into natural and adaptive antibodies, due to their different origin[42]. Natural antibodies (mostly IgM) are spontaneously produced without antigen exposure, are polyreactive and the first line of defense in a newborn organism. Compared to this, adaptive Igs are produced by B2 B-cells after the binding of an antigen to a B-cell receptor (BCR) and are specific to this certain antigen[43].

In general, Igs are roughly Y-shaped molecules, consisting of two large heavy and two small light chains connected by disulfide bonds as well as noncovalent interactions (Figure 2). Moreover, they are separated in a NH2-terminal variable domain, where antigen binding occurs and COOH-terminal constant regions for effector functions, like complement activation or Fc receptor binding[41]. The region, where the antigen binding takes place, is also called Fab-domain and differs from the Fc-domain, where the effector functions are triggered. A flexible polypeptide chain, called the hinge-region, joins the Fab and the Fc domain. In addition, the light chains consist either of a kappa or lambda chain and contain one variable (VL) and one constant domain (CL), whereas the heavy chains exhibit one variable (VH) and three or four constant regions (CH)[44]. The five different Ig isotypes with their specific functions are determined by the structure of the heavy chains (alpha, gamma, delta, epsilon or mu) and can be divided into IgA, IgG, IgD, IgE and IgM[45].

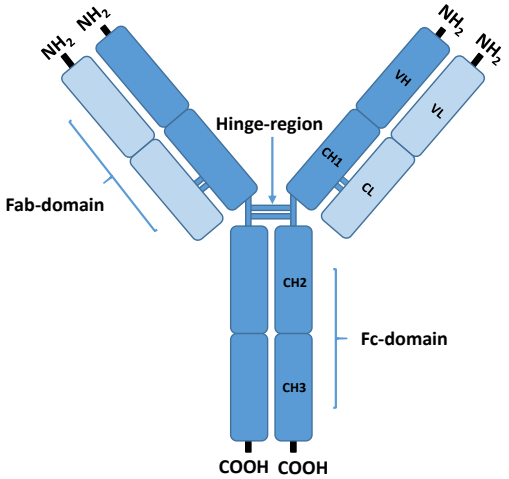


**Figure 2** Basic structure of an Ig, depicted by IgG. Igs consist of two heavy (dark blue) and two light chains (light blue). Each chain has amino terminal variable regions (Fab-domain), where antigen binding occurs and carboxyl terminal constant regions, where effector functions are triggered (Fc-domain). The light chain has one variable region (VL) and one constant region (CH), whereas the heavy chain is composited of one variable region (VH) and three constant regions (CH1-3). The Fab and the Fc domain are linked by a flexible hinge-region with disulfide bonds. Light and heavy chains are also connected by disulfide bonds[41,44].

### 1.3.1. Immunoglobulin G

IgG is the predominant isotype found in human serum and the most extensively studied Ig class. The molecular weight of IgG is approximately 150 kDa and the serum concentration amounts to 9 mg/mL. Moreover, it has the longest half-life among all Ig isotypes. Due to differences in the structure and function of the heavy chains, it is divided into four subclasses ($IgG_1$, $IgG_2$, $IgG_3$ and $IgG_4$), each triggering specific responses to an antigen[42,46]. In general, the most important effector functions of IgG are caused by the activation of the complement system and the binding to Fc-γ receptors (FcγR). FcγRs, which are found on B cells as well as most innate immune cells, are distinguished by their structure in FcγRIII (CD16), FcγRII (CD32) as well as FcγRI (CD64) and specifically bind to the Fc-domain of IgG[47]. The subclasses $IgG_3$ as well as $IgG_1$ bind to all Fc-γ receptors. $IgG_4$ is able to bind to FcγRII and III and $IgG_2$ exclusively to FcγRII[41]. Concerning complement interaction, $IgG_4$ is the only subclass that is not able to activate the complement system, whereas the affinity for C1q of the classical complement pathway is highest for $IgG_3$, followed by $IgG_1$ and $IgG_2$. Moreover, the most well-known effector functions, mediated by the Fc-domain of IgG are antibody-dependent cell-mediated cytotoxicity (ADCC), antibody-dependent cellular phagocytosis (ADCP) and CDC, which also link the innate and the adaptive immune responses[48]. $IgG_1$ is the most abundant antibody subclass and the primarily isotype that reacts to soluble and membrane-bound protein antigens. In addition, a deficiency of $IgG_1$ causes hypogammaglobulinemia, where the level of total IgG is decreased[49]. The main function of $IgG_2$ is the binding to bacterial capsular polysaccharide antigens, whereas $IgG_3$ induces mainly effector functions and is a pro-inflammatory antibody with a relatively low half-live. Additionally, viral infections mostly cause the production of $IgG_3$ and $IgG_1$. Finally, $IgG_4$ antibodies are often generated after repeated or long-term exposure to an allergen and are the primarily isotype that responses due to therapeutic proteins (e.g.FVIII)[46,50]. Next to the induction of effector functions, IgG molecules are also able to neutralize toxins as well as viruses directly and are therefore potent mediators of host protection[41].

### 1.3.2. Immunoglobulin A

IgA is the predominant antibody found in secretions on mucosal surfaces. It is produced in high amounts by a remarkable energy consumption, which suggests that it is of high relevance for the immune defense[51]. Monomeric IgA, which is divided into the subclasses IgA1 and IgA2 in humans, is located in the serum and has a molecular weight of approximately 160 kDa. With a concentration of 2-3 mg/mL, it is the most abundant Ig in serum, after IgG. The secretory form of IgA is mainly dimeric, stabilized through disulfide linkages as well as a joining chain (J-chain) and has approximately 385 kDa[42]. It is transported to mucosal surfaces by the binding to the polymeric Ig rector (pIgR), which is expressed on the basolateral surface of epithelial cells, thereby receiving the extracellular part of the pIgR, known as secretory component[52]. The main function of IgA is to protect the mucosal barrier from pathogens like bacteria as well as viruses and exhibits strong anti-inflammatory properties in the secreted form[53]. It is able to prevent the attachment to host cells by the direct binding to pathogens and the associated neutralization as well as blocking of their activation. Moreover, secretory IgA can also inhibit the entrance of pathogens to the intestinal lumen by immune exclusion, a process by which the accessibility of epithelial receptors is prevented[54]. In addition, the pIgR can transport immune complexes composed of polymeric IgA and the specific pathogen that are formed in the lamina propria by transocytosis into the lumen[52]. However, IgA can also lead to inflammatory mechanisms, by its immune activating functions and the binding to specific receptors[55]. The Fcα receptor I (FcαRI), also known as CD89, is a mediator of effector functions induced by the binding of clustered IgA on the surface of a pathogen. It is expressed on neutrophils, monocytes, eosinophils as well as some macrophages and dendritic cells[56,57]. The binding can lead to the phagocytosis of target cells, the release of cytokines, the production of activated oxygen species and the initiation of ADCC[52]. Moreover, IgA does not activate the complement system via the classical pathway. It can only induce activation by triggering the lectin and the alternative pathway, but this does not seem to be a major effector mechanism of IgA[16,20]. In general, it is a poor activator of the complement system and there is evidence that IgA can even inhibit complement activation induced by IgG or IgM antibodies in an environment with less antigen[58].

### 1.3.3. Immunoglobulin M

IgM is the first antibody that is produced in response to infectious antigens. The monomeric form of IgM is present on naïve B lymphocytes and serves as B cell receptor with a molecular weight of 180 kDa. Compared to this, the secreted form is found mainly as a pentamer and occasionally as a hexamer, has a molecular weight of approximately 970 kDa and an average serum concentration of 1.5 mg/mL[42,59]. The pentamer is composed of 5 monomers linked by disulfide bonds and a J-chain. This specific structure leads to the availability of 10 antigen binding sites that exhibit a relatively low affinity, but a wide range of avidities. Additionally, the high valency allows IgM to bind to pathogens more efficiently than other Igs and this facilitates agglutination, which is an important mechanism for antigen neutralization by providing phagocytosis and the clearance of pathogens. Moreover, the majority of IgM is polyreactive[60]. In general, IgM is able to block pathogens from binding to targets cells (direct neutralization), but not as effective as IgG or IgA. However, the polymeric character makes IgM a potent activator of complement, because one single molecule is able to activate the classical pathway[61]. Compared to this, C1q needs two or more IgG molecules in a specific distance to each other, to become activated. This is an important function of IgM, because complement activation links the innate and the adaptive immune response and leads to pathogen opsonization as well as neutralization. IgM can also modulate effector functions by binding to its recently discovered Fc$\mu$ receptor (Fc$\mu$R). This receptor is expressed on B, T as well as natural killer cells (NK cells), but is not present on monocytes, granulocytes, erythrocytes, and platelets[62]. In general, Fc$\mu$R binds IgM attached to membrane components by its Fab domain more efficiently than free IgM. Furthermore, it is assumed that the Fc$\mu$ receptor activated by IgM, plays a role in B and T cell regulation[63–65]. In addition, IgM is able to contribute to the mucosal immunity, by binding to the pIgR and the associated transport to mucosal surfaces[66]. Due to its multiple functions, IgM plays an important role in early immunity but also in the long-term protection against various pathogens[60].

## 1.4. Immune effector cells

It is essential for the host immunity to recognize and neutralize pathogens that are harmful to the body. Effector functions caused by the activation of specific immune cells (e.g. phagocytes, NK cells, mast cells) are of high relevance, besides the direct inhibition by antibodies or the cellular cytotoxicity caused by the activation of the complement system in response to invading microorganisms. Immune effector cells exhibit the potential to capture and destroy pathogens by mechanisms like phagocytosis, degranulation or intracellular degradation, but can also mediate inflammation. They are attracted by a stimulus and actively respond to it[2,67].

### 1.4.1. Neutrophil granulocytes

Neutrophils are the major pathogen-fighting immune cells and the most abundant cell type in the blood[68–70]. Besides eosinophils and basophils, they are one type of granulocytes, which belong to the white blood cells and are also known as polymorphonuclear cells (PMNs). Their primarily function is the killing of pathogens and the protection of the host as first line of defense of the innate immune system. During a bacterial infection, they are generated at a rate of $10^{12}$ per day[68]. Neutrophils exhibit three antimicrobial functions, thereby linking the innate and the adaptive immunity: phagocytosis, degranulation as well as the release of extracellular neutrophil traps (NETs). Phagocytosis is the process by which an opsonized pathogen is ingested into the vacuole of a phagocyte and is destroyed at low pH and by specific enzymes, after the formation of a phagolysosome. In neutrophils this process is very rapid, compared to the phagocytosis induced by other immune cells (e.g. macrophages)[70]. Additionally, ROS are generated by the activation of a NADPH oxidase during phagocytosis by neutrophils. They are released into the phagolysosome as well as to the outside of the neutrophils, where they can also affect neighboring cells. ROS is suggested to kill pathogens directly and therefore supports the antimicrobial functions of neutrophils[68,71]. A further effector function is the degranulation of neutrophils that destroys pathogens by the release of granules, which contain proteinases as well as antimicrobial peptides. After

the fusion of the neutrophil granulocyte with a plasma membrane the release of the granules occurs, which are classified in three different types due to their specific function. Moreover, NETs are used to bind and kill bacteria as well as fungi extracellularly, when the ingestion of large foreign particles is inhibited. For this purpose, long chromatic fibers that contain also granules of the neutrophils, are ejected after the membrane breaks and trap the microorganisms[68]. This process is known as NETosis. It is a form of active cell death, distinct from apoptosis and necrosis, which requires the generation of ROS as well as NADPH[72]. However, neutrophils can also mediate inflammation by the production as well as release of pro-inflammatory cytokines[73]. Due to their numerous functions, neutrophils play an essential role for pathogen destruction and are important effector cells of the immune system.

## 1.5. Antibody mediated effector functions

The immune system exhibits various functions to respond to and destroy invading pathogens. One mechanism is the direct binding and the neutralization of microorganisms by antibodies. Moreover, there are also indirect mechanisms, known as antibody mediated effector functions, by which the killing of a pathogen is mediated. These functions are mainly triggered by the interaction of complement or Fc receptors with the Fc-part of an antibody and link the innate and the adaptive immune system. This leads to the activation or inhibition of specific pathways in various immune effector cells. ADCC, ADCP as well as CDC are the best-known effector functions induced by the binding of Fc receptors to antibodies[48]. In the following paragraphs, direct as well as indirect mechanisms (Figure 3) of pathogen destruction triggered by Igs are described in detail.

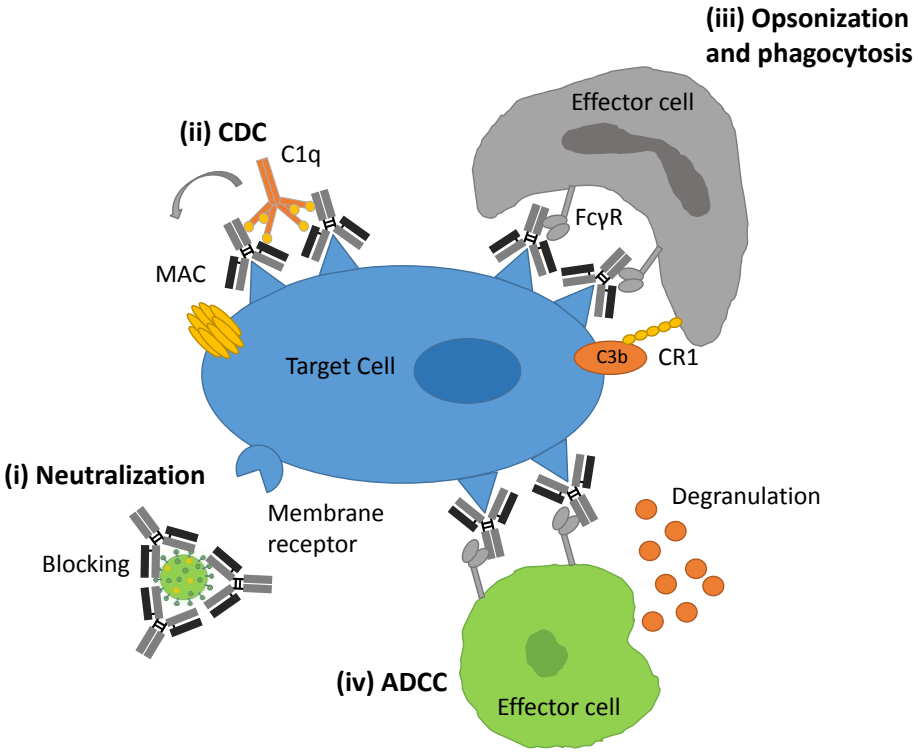


**Figure 3** Antibody mediated functions to destroy pathogens. Antibodies exhibit direct and indirect mechanisms to mediate the destruction and clearance of invading microorganisms. (i) Direct binding and neutralization prevents the infection of the cell by pathogens. (ii) CDC induces the formation of the MAC and leads to the lysis of bacteria. (iii) Opsonization and phagocytosis induces the ingestion of a microorganism covered with specific opsonins on its surface (antibodies and complement factors) by an activated phagocytic cell. (iv) ADCC occurs when the Fc part of an antibody is bound by Fc receptors on an effector cell, which induces the lysis of a pathogen[48].

### 1.5.1. Direct neutralization

Antibodies are able to prevent invading pathogens from infecting host cells in the absence of effector cells or molecules (e.g. complement) by direct binding. This process is known as neutralization and is caused by Igs that block the attachment of the microorganisms to host tissues (see Figure 3)[74]. It is an important function for viral protection, by binding the virus particle, which sterically hinders the interaction of the pathogen with host receptors[75]. Therefore, the elimination of the pathogen can be induced before a serious infection develops. Moreover, bacteria can cause damage to the host by the release of specific toxins. A toxin operates by the attachment to receptors on the target cell. Neutralizing antibodies prevent this attachment by rapidly binding to the receptor-binding site of the toxin with high affinity. In general, IgA neutralizes toxins mainly on mucosal surfaces, whereas IgG is responsible for toxin neutralization in tissues[45]. In addition, the adhesion of bacteria to host surfaces is a critical step in the pathogenesis of bacterial infections. Molecules, called adhesins, cause the binding to the cells and are therefore targets of neutralizing antibodies[76].

### 1.5.2. Complement-dependent cytotoxicity

CDC is an important effector function to eliminate pathogens and neoplastic cells that can be harmful to the body. It is initiated by the activation of the complement system that leads to the formation of the MAC and target cell death (see Figure 3). The classical, the lectin as well as the alternative pathway can induce CDC[77,78]. CDC is also an important function of therapeutic antibodies that can activate the classical pathway, triggered by immune complexes consisting of IgM, $IgG_1$, $IgG_3$ and to a lesser extent $IgG_2$ as well as the pathogen. This leads to the binding of C1q and to the opsonization of the foreign cell with activated complement components[79,80]. By the terminal insertion of the MAC, ions and water can enter the cell and cause a lethal colloid-osmotic swelling. The CDC affects the cell organelles by dilation of the rough endoplasmic reticulum, disruption of the Golgi complex, swelling of mitochondria and lysis of the plasma as well as nuclear membranes. In addition, ROS are generated and a number of intracellular signals were triggered. Nucleated cells require the presence of multiple MACs because otherwise, they can endocytose the MAC and the damage will be repaired[78,81,82]. When complement activation is dysregulated, many malignancies can occur. Under specific conditions, the system can destroy normal tissues and cellular debris, which is unsuccessfully removed, accumulates. This dysfunction can lead to autoimmune diseases as well as inflammatory pathologies. Therefore, it is important to find agents that inhibit CDC as well as antibodies that activate the complement system[83].

### 1.5.3. Opsonization and phagocytosis

Opsonization is an antimicrobial process that promotes the covering of pathogen surfaces with opsonins, like antibodies or complement factors. It is a mechanism by which the phagocytosis of foreign particles is induced as well as facilitated[45,84,85]. In general, opsonins create a bridge between the particle being ingested and the phagocytic cell. They bind to antigens on the pathogens and are recognized by complement as well as Fc receptors on effector cells, like neutrophils or macrophages. This in turn induces the phagocytic process[45]. Phagocytosis mediates the clearance of microbial particles as well as apoptotic cells (see Figure 3)[48]. The effectivity of this process is increased by the engagement of multiple ligands on the opsonized cells with multiple receptors on the phagocytes as well as by the aggregation (also known as crosslinking) of phagocytic receptors that are capable of lateral membrane diffusion. After recognition of the immune complexes, signaling pathways are activated by which the actin skeleton of the effector cell is regulated and the plasma membrane is able to engulf the pathogen. A new vesicle, the phagosome is built, which matures and transforms. Fusion as well as fission reactions of the phagosome with early endosomes, late endosomes and finally lysosomes take place. The mature condition of the phagosome is called phagolysosome, which contains a different composition of the membrane with an acidic and degenerative environment inside for the digestion of the internalized contents[84,85] . Opsonization and phagocytosis (opsonophagocytosis) are important effects that regulate and control tissue homeostasis and the immune response. Nevertheless, it can also mediate inflammation

by the release of cytokines through phagocytes and this attracts further effector cells as well as plasma proteins to the site of infection[73].

## 1.6. Antibody mediated immunomodulation

As mentioned in the previous chapters, the activation of the hosts' immune system by direct mechanisms or indirect effector functions is a fundamental process for the killing and destruction of pathogens that are harmful to the body. Nevertheless, a permanent stimulation, autoimmune reactions or a hyper-responsiveness of immune cells lead to an excessive activation of the whole immune system and to strong reactions that may be directed against the host[86]. A higher production and the uncontrolled release of cytokines cause the up-regulation of inflammatory reactions and this contributes to the emergence of pathological pain. Moreover, it can lead to tissue damage, hemodynamic changes, organ failure and finally to death[87]. There is evidence that administered polyclonal or monoclonal antibody preparations exhibit a therapeutic effect by initiation of the immune response, but also by the down-regulation of harmful effects caused by inflammation, autoimmunity and hypersensitivity[88–91].

### 1.6.1. Anti-inflammatory mechanisms of Ig preparations

In general, Ig preparations are used as replacement therapy in immunosuppressed patients and in high doses as anti-inflammatory therapeutics in autoimmune diseases. The letter is mediated by various molecular mechanisms that affect the innate as well as the adaptive immune response[92]. Igs are able to block Fc receptors on effector cells for antibody recognition. These receptors are important for the opsonophagocytosis of pathogens that enter the hosts' immune system. By preventing the binding to Fc receptors, the Fc-mediated phagocytic process is inhibited, which is an important effect regarding autoimmune diseases[93]. Moreover, Ig preparations can inhibit the complement cascade by binding to activated complement factors and preventing their deposition on tissues and cells[94–96]. This mechanism will be described in detail in paragraph 1.6.2. Further effects are the modulation of pro-inflammatory as well as anti-inflammatory cytokine production, the neutralization of autoantibodies as well as an increased expression of the inhibitory Fc-receptor (FcγRIIB)[89,91–93].

### 1.6.2. Neutralization of complement factors by Ig preparations

The activation of the complement system is not always beneficial for the host and can lead to a number of severe diseases under inappropriate circumstances. Despite the protective function of the complement system in immunity, it can induce autoimmune reactions or the over stimulation of the innate immune system that is harmful and cause self-damaging as well as inflammation[11,17,94,97]. The neutralization of the components of the complement system is therefore of high clinical relevance.

It has been postulated, that high-dose IVIgs as well as IgM-enriched and IgA-enriched preparations can affect the complement system in an anti-inflammatory manner, by blocking its activation[95,98–101]. Basta *et al.* described the interaction of IVIgs with C3b and C4b molecules, as well as with C3a and C5a in the fluid phase. Fc-specific binding of opsins and F(ab)´2-mediated binding of the anaphylatoxins, that inhibited the complement cascade directly, could be shown in *in vitro* experiments[11,17,96]. Moreover, Rieben *et al.* examined the complement inhibitory capacity of different IVIgs as well as IgM- and IgA-enriched Ig preparations and could show that the inhibitory effects regarding C3 and C4 were best for an IgM- and IgA-enriched preparation in comparison to pure IVIgs, but also IgG-dependent effects were revealed. These results were confirmed in an *in vivo* rat model[99]. Additionally, Miletic *et al.* showed a higher capacity of IgM and IgA in inhibiting complement C4 uptake onto sensitized sheep erythrocytes as target cells than IgG[102]. Furthermore, Roos *et al.* analyzed IVIg preparations for their capacity to block complement activation in pig xenografts, transplanted into primates. They showed a dose-dependent inhibition by the preparations as well as a stronger inhibitory capacity of IgM compared to IgG[98]. The study of Mollnes *et al.* focused on the inhibition of complement-mediated red cell lysis by Igs and they concluded that this was mainly due to the binding and blocking of the C1q molecule, which is dependent on the IgG isotype. Furthermore, they reported that $IgG_3$ proteins were the most potent inhibitors,

followed by $IgG_1$, whereas $IgG_2$ and $IgG_4$ did not exhibit inhibitory capacity[103]. The inhibitory effect of IVIgs regarding complement was also tested in an experimental stroke setting in mice. After the administration of IVIg, complement-mediated neuronal cell death was prevented and the general functional outcome in murine stroke improved, leading to the hypothesis that this was due to the efficacy of IVIgs to bind activated complement components[104]. In addition, Esen *et al.* demonstrated neuroprotective effects of IVIgs in a rat model of sepsis by complement inhibition. These effects were ascribed to a reduction of the C5a anaphylatoxin and a resulting inhibition of inflammation as well as apoptosis[105].

The previously described studies show a strong influence of different Ig preparations on complement inhibition in settings simulating an over-stimulated immune system. This inhibitory effect was due to the direct binding of complement factors by Igs. Moreover, the results indicated a stronger effect of IgM- and IgA-enriched preparations on complement inhibition compared to IVIgs.

## 1.7. Acute lower respiratory tract infections

Acute lower respiratory tract infections (LRIs) are a substantial public health problem worldwide. In 2015, approximately 2.74 million people died, because of infections of the lower respiratory tract[106]. The mortality caused by these infections is still high and the burden of disease even increased in the last years in people older than 70. LRI include pneumonia, but also croup, tracheobronchitis, as well as bronchiolitis[107,108]. In general, the patients' outcome is dependent on the virulence of the organism, which is responsible for the infection as well as the inflammatory response in the lung. Inflammation of the pulmonary system develops when high amounts of virulent microbes colonize the lung and the immune system is overstimulated. This in turn can finally lead to lung injury as well as abnormal pulmonary function[109].

### 1.7.1. Severe Community-Acquired Pneumonia

One of the most common causes of death within LRIs is the community-acquired pneumonia (CAP)[110,111]. Generally, a pneumonia is described as an infection of the lung parenchyma, where the immune system is overwhelmed with the defense of invading pathogens. The main pathogen is *Streptococcus pneumoniae* followed by *Haemophilus influenzae* and *Staphylococcus aureus*. Symptoms like fever, cough with purulent sputum, dyspnea and pleuritic chest pain are common [112,113]. An overall increased progress of disease and a higher mortality rate is called sCAP, where patients require admission to an intensive care unit (ICU) and often have to be ventilated[114]. Despite the availability and the improvement of pneumococcal polyvalent vaccine-based immunization strategies as well as of antibiotic treatment, the morbidity and mortality in sCAP is still high[115,116]. Challenges of the therapy against pneumonia are the increasing resistance of the bacteria to antibiotics as well as the development of new contagious and deadly pathogens[115,117]. In addition, patients with severe infections often suffer from transient antibody depletion. It was shown that the antibody serum concentrations correlate with disease severity and that there is a need for replacement therapy[118]. In general, it is of high relevance for sCAP patients to obtain an effective treatment that activates the immune system and destroys relevant pathogens because, high bacterial load that cannot be cleared completely as well as a resulting over-activation of the hosts' immune defense can lead to harmful effects for the patient. Activation of the complement cascade as well as the release of cytokines and the subsequent recruitment of effector cells that in turn secrete cytokines, are key events that trigger inflammation[116]. Pneumolysin, a virulence factor of *Streptococcus pneumoniae* activates the classical complement pathway, whereas the alternative pathway is triggered by teichnoic acid, a polymer component of the pneumococcal cell wall[119]. Unsuccessful treatment with antibacterial agents together with antibody depletion can therefore aggravate the situation and lead to the development of a hyper-inflammation, which causes the systemic spread of the disease, pulmonary damage and at worst sepsis and multi-organ failure. Because of these difficulties in antimicrobial therapy, mortality in sCAP remains high and there is a need for adjunctive therapies that also target inflammatory responses[115,120–122]. One mechanism of agents that are able to reduce inflammation is the inhibition of activated complement factors. There is evidence that

neutralization of complement component C5a by specific inhibitors protects the patient against lung and extrapulmonary organ injury in pneumonia-induced sepsis[123]. Therefore, it may improve the patient outcomes by targeting directly the host response rather than the microorganisms. Related to this, various Ig preparations have been examined for their potential as add-on therapies in patients with sCAP. It could be shown that such preparations can prevent nonspecific complement activation, besides the improvement of pathogen opsonization as well as the neutralization of endotoxins and superantigens[96,98,99,12411,98,99,124].

## 1.8. Coronavirus Disease 2019

The outbreak of the coronavirus disease 2019 (COVID-19) was caused by the novel severe acute respiratory syndrome coronavirus 2 (SARS-CoV-2)[125,126]. It was primarily identified in China, has rapidly spread all over the world and finally caused a pandemic[127–129]. In the past, coronaviruses were responsible for the severe acute respiratory syndrome (SARS) pandemic of 2003 as well as for the Middle East respiratory syndrome in 2012 (MERS)[117,130,131]. SARS-CoV-2 is an RNA viruses that is comprised of an envelope, is non-segmented and rapidly trasmitted[128]. The symptoms of COVID-19 are fever, cough, myalgia, fatigue as well as headaches, hemoptysis and diarrhea[132]. Most patients show a mild to a moderate progress of the disease, but in 5-10% of the cases severe diseases like pneumonia, respiratory failure or acute respiratory distress syndrome (ARDS) develope[133]. It is also known that the virus invades the lung parenchyma and causes severe interstitial inflammation of the lungs, seen in computer tomography images[134]. This is due to the over-stimulated immune responses that trigger mediator cascades (complement, coagulation and cytokine storm) as well as to the lytic effects of the virus, which is harmful to host cells[125,135,136]. High levels of pro-inflammatory cytokines, like tumor necrosis factor (TNF), interleukin-1β (IL-1β) as well as interleukin-6 (IL-6) were found in patients with SARS-CoV-2[132]. These pro-inflammatory cytokines are mainly produced by immune cells and are able recruit other immune cells to the site of inflammation. When the immune system is permanently activated and a loss of negative feedback occurs, pro-inflammatory cytokines are excessively produced and lead to an exponential growth of inflammation. This can result in a cytokine storm, which causes increased vascular hyperpermeability and at worst multiple organ failure.[137] There is evidence that cytokine storm is a major cause for lung injury and ultimately for ARDS in critically ill COVID-19 patients[132]. Therefore, it is important that the treatment of SARS-CoV-2 positive patients include a therapeutic reduction of the uncontrolled and excessive immune response to save the patient's lives. Moreover, various studies described that complement activation in COVID-19 patients can also cause inflammatory responses and an inhibition of the complement system could have positive effects for the disease progression. Gralinski *et al.* already analyzed the role of the complement system in SARS-CoV infections of 2003. By using a model with SARS-CoV infected mice he was able to demonstrate a direct activation of the complement system in the lung at day 1 of infection. It was suggested that this activation mediates systemic pro-inflammatory responses like the recruitment of neutrophils and inflammatory monocytes as well as the release of cytokines and chemokines[138]. Additionally, the activation of the complement system was also analyzed by Gao *et al.* relating to SARS-CoV, MERS-CoV as well as to the new SARS-CoV-2 infections. It was reported that the nucleocapsid (N) proteins of the analyzed coronaviruses, are all able to bind to MASP-2 of the lectin pathway and thereby aberrantly activating the complement system that leads to inflammatory lung injury[139]. Moreover, first clinical studies in patients with mild and severe COVID-19 infections detected increased levels of complement factor C5a compared to healthy individuals, which was suggested to contribute to lung as well as endothelial damage[140]. In addition, Magro *et al.* detected thrombotic microvascular injury in patients infected with SARS-CoV-2 accompanied by the deposition of complement (C5b-9, C4d, MASP-2), which was associated with an increased activation of the clotting pathway leading to hypercoagulability[141]. These findings leads to the assumption that uncontrolled complement activation by SARS-CoV-2 plays a major role in the development of inflammation as well as multiple organ failure. Additionally, the complement system is also able to interact and activate the coagulation system. It was shown that C5a for e.g. can increase the activity of tissue factor, which is an important coagulation protein and that the inhibition of complement is associated with a reduced expression of this factor[142,143]. In COVID-19 patients, excessive intravascular coagulation as well as

thrombus formation was detected[144]. It was assumed that the increase in coagulation was caused by an increased complement activity[141]. For the described reasons, it could be a promising treatment, to reduce or inhibit complement activation by monoclonal antibodies or plasma derived Ig preparations next to the standard antiviral therapies that directly neutralize aberrantly activated complement factors. Therefore, the effects of complement inhibition in COVID-19 patients should be evaluated in future studies[145–148].

## 1.9. Plasma derived immunoglobulin preparations

Plasma-derived Igs are of high relevance for e.g. the destruction and clearance of pathogens, the therapy of autoimmune diseases and for immunomodulation. By exhibiting multiple effector functions, they protect the host against infections and control the immune response in order to prevent over-stimulatory processes[149]. Moreover, the development of plasma-derived Ig preparations that contain highly purified antibody molecules, which are isolated and pooled from thousands of healthy donors, are used as replacement therapy in immunodeficient patients as well as for the treatment of inflammatory disorders[150–152]. Due to the pooling, the preparations contain a considerably higher amount of Igs that contain various specificities compared to one individual[149]. Plasma-derived Ig preparations are produced by chromatographic purification and the removal of potential pathogens and impurities is ensured by various processes as well as by controls during manufacturing[153,154]. The products are either administered by intravenous, intramuscular or subcutaneous infusion. Currently, mainly IVIgs are in use, but there is a need for the better exploitation of the plasma, which contains additionally fractions of IgA and IgM. The production of alternative Ig preparations with other compositions is an important step for new indications and therapies[149].

### 1.9.1. Intratect

Intratect is a human plasma-derived polyvalent IVIg preparation developed as replacement therapy for PID and SID. Meanwhile, IVIgs are used for autoimmune and inflammatory diseases as well[155–157].Therefore, new indications for Intratect like chronic inflammatory demyelinating polyneuropathy (CIDP) and multifocal motor neuropathy (MMN) were approved. IVIg preparations in general, contain >95% IgG, exhibit a distribution of the IgG subclasses that is comparable to the composition in normal serum and have a minimal amount of aggregates. It is a critical step in the manufacturing process of IVIgs that the functionality of the IgG molecules as well as the safety of the product is maintained.

For Intratect production, the method of Cohn (fractionated precipitation) was modified for the separation of the precipitates by using filter instead of centrifugation techniques[116]. The efficacy, safety as well as the pharmacokinetic profile of Intratect was tested in clinical trials in patients with PID, SID and autoimmune disorders. The data suggests that the preparation is well tolerated, safe and effective for this indications with mild and transient adverse reactions[158–160]. Moreover, the immunomodulatory effects of Intratect were also examined regarding its complement inhibitory capacity. Spycher *et al.* analysed the complement inhibitory capacity of different IVIg preparations in an ELISA system and confirmed that Intratect was able to inhibit the deposition of C3b as well as iC3b concentration-dependently. Nevertheless, the product was not as effective in inhibiting complement as the other IVIg preparations that were tested in this study[100].

### 1.9.2. Trimodulin

Trimodulin (name of the active substance) is a human plasma-derived polyvalent Ig preparation for intravenous administration (IV) and comprises ≈ 23% IgM, ≈ 21% IgA and ≈ 56% total IgG. It was specifically developed for the treatment of severe infections and already tested in a phase I and II clinical trial. Due to the three antibody isotypes that are present in the product, three relevant mode of actions are described, divided in antimicrobial and immunomodulatory functions: on the one hand, trimodulin can initiate the opsonization and clearance of pathogens as well as the neutralization of their virulence factors. On the other hand, it is able to modulate the host inflammatory responses.

The three Igs of trimodulin show a large variety of activities and are important for antimicrobial activities. IgM is the first Ig that arises in a humoral immune response following infection or immunization by an antigen and can be divided into natural and immune IgM[161]. Both forms have specific functions regarding pathogen-associated infections. Natural IgM is able to facilitate the removal of apoptotic cells, bacterial debris, dead virus particles and their toxins. In the pentameric structure, IgM exhibits 10 antigen binding sites and has therefore a higher valency than other Igs. A single IgM pentamer can activate the complement system via the classical pathway, whereas IgG needs two and more molecules. This high valency makes IgM more efficient in antigen binding than other Igs, although it has a lower affinity[60]. In addition, the activation of the complement system increases the pathogen lysis via CDC[23]. IgA, secreted on mucosal surfaces and in plasma, protects against microorganisms and toxins as well as prevents their attachment to mucosal surfaces[58]. Its receptor is expressed on neutrophils that can be activated to mediate phagocytosis. The secretory form of IgA (sIgA) has a polymeric character and is more effective than monomeric IgA in preventing bacterial or viral infection[41,51]. It induces complement activation via the alternative and the lectin pathway, therefore mediating pathogen lysis via CDC[16,20]. IgG shows highest specificity for its targets and induces phagocytosis as well as ADCC of pathogens by binding to their specific receptors on effector cells[41,46]. Moreover, it has various immune modulating activities in autoimmune and inflammatory disorders[155,162].

In the CIGMA study, which was a randomized, placebo-controlled, double-blind, multicenter, phase II trial, the efficacy and safety of trimodulin as add-on therapy in mechanically ventilated sCAP patients was evaluated. In *post hoc* analyses, it could be shown that the mortality of the patients was significantly reduced in subsets with elevated baseline C-reactive protein (CRP) levels and/or reduced IgM levels[163]. CRP is an acute-phase inflammatory protein that increases up to 1000-fold in response to bacterial infections[164]. The advantages shown in the trimodulin-treated patients are an indicator for the important antimicrobial as well as immunomodulatory functions of the product and support its mode of action.

Several studies done in the past, showed the pharmacological effect of trimodulin: the product is able to bind to the first complement component of the classical pathway, C1q, therefore activating the proteolytic cascade and leading to opsonization of pathogens. Moreover, it can bind bacterial and viral pathogen-associated molecular patterns (PAMPS) to restrict dysregulated inflammatory responses. This antimicrobial functions support the host immune system, especially in immune-compromised patients. In addition, trimodulin shows important immunomodulatory effects: it can affect the cytokine network[165], influences the toll-like receptor (TLR) expression on monocytes[165] and interacts with activated complement components, which can prevent or correct systemic hyper-inflammatory responses as well as infection-related tissue damage[166].

## 2. Aim of the thesis

The aim of this PhD thesis was to functionally analyze the new IgM- and IgA-enriched Ig preparation trimodulin, for an improved understanding of its complex MoA of not only IgG, but also IgM and IgA. In general, plasma-derived Ig preparations exhibit a variety of functions that can help people who suffer from antibody-depletion, inflammatory or autoimmune diseases[155–157,167,168]. For this reason, there is strong interest in the development, characterization and the clinical uses of such preparations[149].

Trimodulin is being developed for the treatment of severe infections and was already tested in a phase II clinical trial with sCAP patients. It was seen that the 28-day mortality of subsets with elevated CRP and/or reduced IgM levels could be obviously reduced after trimodulin addition[163]. Currently, trimodulin is also tested in a multinational phase II clinical trial for the treatment of severe COVID-19 patients. Moreover, pre-clinical *in vitro* as well as *in vivo* studies investigated various pharmacological effects of this Ig preparation. On the one hand, trimodulin shows antimicrobial functions: it is able to bind C1q, the first component of the classical complement pathway, induces the opsonization of gram-positive and gram-negative bacteria, viruses and fungi and is able to trigger the IgG-mediated phagocytosis of pathogens (data not published). On the other hand, trimodulin can also operate via its immunomodulatory mechanisms: it reduces the production of pro-inflammatory cytokines[165], is able to modulate the phenotype of monocytes[165], inhibits T cell activation[165] and was shown to interact with the complement system[166]. These mechanisms are caused by the individual functions of the IgM, IgA and IgG molecules, which are present in trimodulin.

Nevertheless, there is still a need for a better understanding of the correlation between the antimicrobial and immunomodulatory effects to obtain detailed insights in the MoA of trimodulin. Therefore, this PhD thesis pursued the aim to analyze the ambivalent effects of trimodulin that are responsible for balancing the activation and the inhibition of the immune system. Moreover, it was also important to analyze the influence of the enriched IgM and IgA proportion in trimodulin and to compare it with a normal IVIg preparation. For this reason, Intratect was used in this PhD thesis as IVIg control.

Initially, it was analyzed if trimodulin is able to bind and inhibit the activated complement factors C3b, C4b, C3a and C5a. The opsonins (C3b and C4b) as well as the anaphylatoxins (C3a and C5a) play an important role in the activation of the complement system and in the defense against invading pathogens[12]. However, they can also be harmful to the host, when the complement system is over-activated. Especially C5a and C3a can trigger various inflammatory effects that can lead to tissue damage and multiple organ failure[24]. Due to the interactions of trimodulin with activated complement factors that were seen in ELISA experiments of Rieben *et al.*[166], it was hypothesized that trimodulin is also able to functionally inhibit activated complement factors. The ability of trimodulin to decrease the activation of the complement system would be beneficial for patients with autoimmune diseases or inflammatory disorders that attack the bodies' own cells and tissues. Particularly in diseases like sCAP or COVID-19, it is known that the immune system can be over-stimulated, which leads to systemic inflammation and can promote mortality[125,135,136,169]. In order to prove the hypothesis that trimodulin can inhibit activated complement factors, the binding of the Ig preparation to the various complement components was tested and subsequently, the functional effect determined by using a CDC assay. This was the first time that trimodulin was functionally analyzed concerning complement system inhibition.

Certainly, the activation of the immune system in order to destroy invading pathogens is also an important MoA of Ig preparations. It is known that IVIgs are able to induce the phagocytosis of microorganisms, by binding to effector cells like neutrophils or macrophages and to trigger their clearance[48]. The IgG-mediated phagocytosis of trimodulin could already be shown in pre-clinical experiments (data not published). Nevertheless, there is a need to analyze the ability of trimodulin, to additionally activate the complement system, which triggers effector functions like opsonophagocytosis or CDC of pathogens and therefore facilitates their neutralization[48]. In general, IgM molecules are better activators of the classical complement pathway than IgG molecules, whereas IgA does not have the ability to induce this pathway[12]. In order to analyze, if trimodulin is able to trigger the opsonophagocytosis of pathogens, an OPA was developed. It was hypothesized that trimodulin, which contains high amounts of IgM and IgA molecules, is a better complement activator and therefore induces a stronger opsonophagocytosis than Intratect that is only compromised of IgG molecules.

This PhD thesis analyzed for the first time the dual role of trimodulin regarding complement activation and therefore gave new insights in the MoA of this preparation.

# 3. Material

## 3.1. Chemicals and reagents

| Product | Manufacturer | Order number |
|---|---|---|
| 0.4% Trypan Blue Solution | Corning | 25-900-CI |
| All Blue Prestained Protein Standards | Bio-Rad | 1610373 |
| Aqua | B. Braun | 0082479E |
| Bond-Breaker TCEP solution | Thermo Scientific | 77720 |
| Bovine serum albumin | Sigma-Aldrich | A9647 |
| Carbonate-Bicarbonate Buffer (capsule) | Sigma-Aldrich | C3041-50CAP |
| Dulbecco's PBS (w/o $Ca^{2+}$ w/o $Mg^{2+}$ ) | Life technologies | 14190144 |
| Gelatin | Sigma-Aldrich | 48723-500G-F |
| Gelatin Veronal Buffer with $Mg^{2+}$ and $Ca^{2+}$ ($GVB^{++}$) | Boston Bio Products | IBB-300X |
| Hanks' Balanced Salt Solution (10x) with $Mg^{2+}$ and $Ca^{2+}$ | Thermo Scientific | 14065056 |
| HEPES Buffer Solution (1 M) | Life technologies | 15630-056 |
| Methanol | Merck | 1.06009.1011 |
| NuPage Antioxidant | Thermo Scientific | NP0005 |
| NuPage LDS Sample Buffer (4x) | Thermo Scientific | NP0007 |
| NuPage MOPS SDS Running Buffer (20x) | Thermo Scientific | NP0001 |
| NuPage Transfer Buffer | Thermo Scientific | NP0006 |
| PBS (10x), pH 7.4 | Thermo Scientific | 70011044 |
| Propidium iodide | Invitrogen | P1304MP |
| Odyssey Blocking Buffer | Li-Cor | 927-40000 |
| TBS-T concentrate (20x) | In-house preparation | 1083 |
| TMB substrate | In-house preparation | 1077 |
| TMB substrate buffer | In-house preparation | 1076 |
| TMB substrate stopping solution | In-house preparation | 1078 |
| Triton X-100 | Sigma-Aldrich | T8787-50ML |
| Tween 20 | Sigma-Aldrich | P1379-25ML |
| Zymosan A (from *Saccharomyces cerevisiae*) | Sigma-Aldrich | Z4250-250MG |

## 3.2. Consumables

| Product | Manufacturer | Order number |
|---|---|---|
| 15 mL conical tube | Falcon | 352096 |
| 50 mL conical tube | Falcon | 352070 |

| | | |
|---|---|---|
| 24 well F-bottom plate | Corning | 353047 |
| Bolt Bis-Tris Plus Gels, 15 well (8%) | Thermo Scientific | NW00085BOX |
| Cell culture flask T-25 | Eppendorf | 0030710029 |
| Cell culture flask T-75 | Eppendorf | 0030711025 |
| Cell culture flask T-175 | Eppendorf | 0030712013 |
| Cluster tubes, 1.2 mL, 96 well, PP | Corning | CLS4401-960EA |
| Combitips advanced, 5 mL | Eppendorf | 0030089456 |
| Combitips advanced, 10 mL | Eppendorf | 0030089464 |
| Counting Chamber Neubauer Improved C-Chip | Carl Roth | PK36.1 |
| Deep well plate, 96 square well | VWR | 732-3323 |
| Drigalski spatula | VWR | 612-2688 |
| epT.I.P.S. Biopure, 0.1-20 $\mu$l | Eppendorf | 0030075323 |
| epT.I.P.S. Biopure, 2-200 $\mu$l | Eppendorf | 0030075021 |
| epT.I.P.S. Biopure, 50-1000 $\mu$L | Eppendorf | 0030075358 |
| Inoculation loop | VWR | 612-9352P |
| Micro cuvette | VWR | 634-0675 |
| Microplate, 96 well, Nunc MaxiSorp, PS, F-Bottom | Thermo Scientific | 44-2404-21 |
| Microplate, 96 well, PS, U-bottom | Greiner | 650101 |
| Microplate, 96 well, PS, V-bottom | Greiner | 651101 |
| Microplate sealing tape | VWR | 319-1250 |
| Mini orbital shaker | VWR | 444-0270 |
| Pierce Nitrocellulose Membrane | Thermo Scientific | 88013 |
| Pierce Western Blot Filter Paper | Thermo Scientific | 84783 |
| Safe-Lock Tubes, 1.5 mL | Eppendorf | 0030120086 |
| Serological pipette, 5 mL | VWR | 612-5523P |
| Serological pipette, 10 mL | VWR | 612-5827P |
| Serological pipette, 25 mL | VWR | 612-5828P |
| Serological pipette, 50 mL | VWR | 612-5546P |

### 3.3. Devices

| **Product** | **Manufacturer** |
|---|---|
| Amersham Typhoon 5 Imager | GE Healthcare |
| Axiovert 40c | Zeiss |
| Cell Freezing Container Cool Cell LX | Corning |
| Clean bench Herasafe | Thermo Scientific |

| | |
|---|---|
| Thermomixer Comfort | Eppendorf |
| FACS Canto II | BD |
| HERACell 240i $CO_2$ Incubator | Thermo Scientific |
| Heraeus Multifuge 3S Plus | Thermo Scientific |
| Heraeus Multifuge X3R | Thermo Scientific |
| Ice Basin , 4 L | NeoLab |
| Infinite F200 | Tecan |
| Low Speed Orbital Shaker | Corning |
| Magnetic stir bar | VWR |
| Magnetic stirrer | VWR |
| Microcentrifuge 220 R | Hettich |
| Microplate shaker | VWR |
| Microplate washer 405TSUVS | Biotek |
| Multipette | Eppendorf |
| Olympus IX53 microscope | Olympus |
| Power Supply | Bio-Rad |
| Research pipette (12-channel) 30-300 $\mu$L | Eppendorf |
| Research plus pipette 0.5-10 $\mu$L | Eppendorf |
| Research plus pipette 1-20 $\mu$L | Eppendorf |
| Research plus pipette 10-100 $\mu$L | Eppendorf |
| Research plus pipette 20-200 $\mu$L | Eppendorf |
| Research plus pipette 100-1000 $\mu$L | Eppendorf |
| Spectral Photometer UV-3100PC | VWR |
| Ultrasonic bath | VWR |
| Vortex shaker | IKA |
| Water Bath | Grant |
| X Cell II Blot Module | Thermo Scientific |
| X Cell SureLock Mini-Cell Electrophoresis Chamber | Thermo Scientific |

### 3.4. Software

| **Product** | **Manufacturer** |
|---|---|
| Amersham Typhoon Control Software | GE Healthcare |
| BD FACSDiva | BD |
| FlowJo X | Tree Star |
| GraphPad Prism | GraphPad Software |

| | |
|---|---|
| Image Quant TL | GE Healthcare |

### 3.5. Cell culture reagents

| Product | Manufacturer | Order number |
|---|---|---|
| Dimethylformamide | Sigma-Aldrich | 227056-100ML |
| Dimethyl sulfoxide | Sigma-Aldrich | D2650-100ML |
| Fetal bovine serum | Life technologies | 10270106 |
| RPMI-1640 Medium | ATCC | ATCC 30-2001 |
| Penicillin-Streptomycin | Sigma-Aldrich | P0781-100ML |

### 3.6. Bacteria culture reagents

| Product | Manufacturer | Order number |
|---|---|---|
| Glycerol, pure, 83.5-88.5% aqueous solution | Acros organics | 277360010 |
| LB agar plates (Miller) | VWR | 102502ZA |
| LB broth (Miller) | Alfa Aesar | H26676.36 |

### 3.7. Buffer protocols

| Formulation Buffer Intratect pH 5.0 |
|---|
| 0.32 M glycine |
| In distilled water |

| Formulation Buffer trimodulin pH 4.3 |
|---|
| 0.32 M glycine |
| In distilled water |

| TBS-T Washing Buffer |
|---|
| 1x TBS-T concentrate (20x) |
| In distilled water |

| Western Blot Buffer |
|---|
| 10% methanol |
| 0.1% antioxidant |
| 1x Transfer Buffer |
| In distilled water |

### 3.8. Kits

| Product | Supplier | Order number |
|---|---|---|
| Human C3a ELISA Kit | BD | 550499 |
| Human C5a ELISA Kit | BD | 557965 |

### 3.9. Cell lines

| Product | Supplier | Order number |
|---|---|---|
| HL-60 cells | ATCC | ATCC CCL-240 |
| Ramos Cells | ATCC | ATCC CRL-1596 |

### 3.10. Bacteria

| Product | Supplier | Order number |
|---|---|---|
| *E. coli* (K12) | ATCC | ATCC 10798 |
| *Staphylococcus aureus* bioparticles, Alexa Fluor 488 conjugate | Thermo Scientific | S23371 |

### 3.11. Antibodies

| Product | Manufacturer | Order number |
|---|---|---|
| CF488A Donkey Anti-Goat Antibody | Biotium | 20016. |
| CF555 Donkey Anti-Mouse Antibody | Biotium | 20037. |
| CF640R Donkey Anti-Rabbit Antibody | Biotium | 20178. |
| Goat anti-human IgG/IgA/IgM antibody mix | Abcam | 102416 |
| Goat anti-rabbit antibody (HRP) | Agilent | P044801-2 |
| Mouse anti-human CD11b (Pacific Blue) | BD | 558123 |
| Mouse anti-human CD16 (V500) | BD | 561393 |
| Mouse anti-human CD20 (APC) | BD | 559776 |
| Mouse anti-human CD32 (PE) | BD | 550586 |
| Mouse anti-human CD35 (FITC) | BD | 555452 |
| Mouse anti-human CD64 (Alexa Fluor 700) | BD | 561188 |
| Mouse anti-human CD71 (APC) | BD | 561940 |
| Mouse anti-human IgM antibody (clone AF6) | 2BScientific | 2BS-SM100101 |
| Mouse IgG1 κ Isotype Control (Alexa Flour 700) | BD | 557882 |
| Mouse IgG1 κ Isotype Control (FITC) | BD | 555748 |
| Mouse IgG1 κ Isotype Control (Pacific Blue) | BD | 558120 |
| Mouse IgG1 κ Isotype Control (V500) | BD | 560787 |

| | | |
|---|---|---|
| Mouse IgG2a κ Isotype Control (APC) | BD | 555576 |
| Mouse IgG2b κ Isotype Control (APC) | BD | 555745 |
| Mouse IgG2b κ Isotype Control (PE) | BD | 555743 |
| Rabbit anti-human C3c antibody | Agilent | F020102-2 |
| Rabbit anti-human C4c antibody | Agilent | F016902-2 |
| Rabbit anti-human C5a antibody | Thermo Scientific | PA5-35000 |
| Rabbit anti-human IgG antibody | Abcam | ab97156 |
| Rabbit anti-mouse IgG antibody (HRP) | Abcam | ab6728 |

### 3.12. Serum and complement

| Product | Manufacturer | Order number |
|---|---|---|
| EDTA-plasma | In-house preparation | n/a |
| Purified C5a | Sigma-Aldrich | 204902 |
| Normal human serum | In-house preparation | n/a |
| Human serum IgG/IgM depleted | Pel-Freez | 34014 -10 |

### 3.13. Antibody preparations

| Product | Manufacturer | PZN |
|---|---|---|
| MabThera (Rituximab, 100 mg) | Roche Pharma AG | 08709896 |

### 3.14. Plasma products

| Product | Manufacturer | Lot |
|---|---|---|
| Intratect | Biotest AG | B791256 |
| trimodulin | Biotest AG | B588016 |
| | | B588026 |
| | | B588036 |
| | | B588039 |

Intratect (50 g/L) is a normal human IVIg preparation containing ≈ 96% IgG. Trimodulin (50 g/L) is an IgM/IgA-enriched Ig preparation with ≈ 23% IgM, 21% IgA and ≈ 56% total IgG.

# 4. Methods

## 4.1. Cell culture techniques

All cells were cultured under controlled conditions, at 37 °C and 5% $CO_2$ in a humidified incubator. Every 3-4 days they were subcultured, thereby transferred to a new culture bottle and fresh medium was added.

### 4.1.1. Determination of cell count

For determination of the cell count, a Neubauer chamber was used. The counting grid of this chamber consists of 3 x 3 large squares, each with an area of 1 $mm^2$. The central large square, which is divided into 5 x 5 medium squares and each of them again divided into 4 x 4 smaller squares, is used for the counting of platelets as well as red blood cells. The four large squares in the corners of the chamber comprises a volume of 0.0001 mL, are divided into 16 smaller squares with 0.25 mm side length and used for the counting of white blood cells as well as most cell-line derived cells. In order to determine the cell count, samples were 2-fold diluted in 0.2% trypan blue solution. This dye exclusively labels dead cells, because it cannot pass the membrane of intact cells and cannot enter the cytoplasm. Samples with higher cell densities were pre-diluted in phosphate-buffered saline (PBS). After dilution, 10 $\mu$L of the sample was added to the chamber and the cells counted using a light microscope. The bright viable cells were excluded from the dark blue labeled dead cells and the cell concentration, the absolute cell number as well as the viability determined by the following formulas:

$$\text{Cell concentration [cells/mL]} = \frac{\text{Number of viable cells} \cdot \text{Dilution factor}}{\text{Number of squares} \cdot 0.0001\ \text{mL}}$$

$$\text{Absolute cell number} = \text{Cell concentration} \cdot \text{total volume}$$

$$\text{Viability [\%]} = \frac{\text{Number of viable cells}}{\text{Number of total cells}} \cdot 100$$

### 4.1.2. Cryopreservation

For long-term storage, cells of a low passage number were centrifuged at 350 x g for 5 min and adjusted to $1 \cdot 10^6$ cells/mL in cryopreservation medium, containing 95% culture medium and 5% Dimethyl sulfoxide (DMSO). 1 mL aliquots were generated and frozen for 24 h at -80 °C in a cell-freezing container, to ensure a temperature decrease of 1 °C per min. After that, the cells were transferred to a -150 °C refrigerator.

### 4.1.3. Ramos cells

The Ramos cell line is a human B lymphocytic cell line that originates from Burkitt's lymphoma and express the surface antigen CD20[170–172]. Ramos cells were routinely used to analyze antibodies to induce cell death by binding to CD20[173,174]. In the CDC assay, the cells were used to evaluate the effects of trimodulin on CDC of the Ramos cells, caused by the activation of the complement cascade through binding of the chimeric monoclonal antibody Rituximab to CD20.

### 4.1.4. Cultivation of Ramos cells

Frozen cryovials were rapidly thawed in a 37 °C water bath and the cells transferred to a 15 mL conical tube, containing 9 mL of pre-warmed RPMI-1640 medium, supplemented with 10% fetal bovine serum (FBS) and 1% penicillin-streptomycin. After centrifugation of the cells at 350 x g for 5 min, they were resuspended in 10 mL supplemented RPMI-1640 medium and transferred to a T-25 cell culture flask. The cells were incubated in a 37 °C humidified incubator, containing 5% $CO_2$ and subcultured every 3-4 days. They were counted and $1.5 \cdot 10^5$ cells/mL were transferred to a new T-75 cell culture flask.

After thawing, cells were subcultured at least three times prior to their first use in the CDC assay and a maximum of 25 passages was performed.

### 4.1.5. HL-60 cells

The HL-60 cell line is a human leukemia cell line, with a neutrophilic promyelocytic morphology and was obtained from peripheral blood[175]. The cells differentiate to mature granulocytes by the addition of DMSO or retinoic acid to the culture medium[176,177]. Moreover, the treatment with 12-O-tetradecanoylphorbol-13-acetate (TPA) leads to monocytic, macrophage-like and eosinophil phenotypes[178]. These characteristics have made the cell line an attractive model for myeloid cell differentiation and for cytokine research[179]. In this study, HL-60 cells were used as effector cells in the OPA after differentiation to mature neutrophil-like granulocytes.

### 4.1.6. Cultivation of HL-60 cells

In order to cultivate the HL-60 cells, frozen cryovials were rapidly thawed in a 37 °C water bath. After thawing, the cells were transferred to a 15 mL conical tube, containing 9 mL of pre-warmed IMDM medium, supplemented with 20% FBS and 1% penicillin-streptomycin. Subsequently, the cells were centrifuged at 350 x g for 5 min and transferred to a T-25 cell culture flask. They were incubated for 3-4 days at 37 °C and 5% $CO_2$ in a humidified incubator. For subculturing, they were counted and set to $2 \cdot 10^5$ cells/mL by transferring the required amount of cell suspension to a new T-75 cell culture flask and adding supplemented IMDM medium.

After thawing, cells were subcultured at least three times prior to their first use in the OPA assay and a maximum of 25 passages was performed.

## 4.2. Bacterial culture of *E. coli* (K12)

In order to use the gram-negative bacterium *E. coli* (K12) in the OPA assay, the microorganisms were cultured under controlled conditions. *E. coli* are rod-shaped, facultative anaerobe bacteria with peritrichous flagella for motility or are non-motile[180]. They colonize the lower intestine of endothermic organisms, as part of the normal microbiota, where they can suppress the growth of pathogenic bacteria and synthesize vitamins[181,182]. However, harmful serotypes can lead to various infections of the enteric, urinary, pulmonary and the nervous system[183]. The reference strain K12 was one of the first microorganisms targeted for genome sequencing and therefore helped to understand the genetics, molecular biology, physiology and biochemistry of this bacterium[184]. In the present study, *E. coli* (K12) was used as a model-organism for the phagocytosis of microorganisms by trimodulin in the OPA assay.

All steps, described in the following paragraphs (inoculum, master stock and assay stock preparation) were performed under a clean bench.

### 4.2.1. Inoculum preparation

To dissolve the lyophilized pellet of *E. coli* (K12), the vial was opened and 5-6 mL lysogeny broth (LB) medium were pipetted to a 15 mL conical tube. 1 mL was taken out to resuspend the bacteria and transferred to the tube, containing the residual medium. The tube was incubated for 24 h at 37 °C and shaking (≈ 140 rpm).

### 4.2.2. Master stock preparation

A master stock preparation is used as an internal reference standard and is directly made from the reference culture vial (ATCC). It is stored as liquid suspension at -150 °C and used for the production of assay stocks. The assay stocks in turn are used in the individual tests.

In order to produce master stocks of the *E. coli* culture, the liquid over-night inoculum was mixed with 80% glycerol. 500 $\mu$L of the suspension was distributed to 1.5 mL safe-lock tubes and stored in a -150 °C freezer.

### 4.2.3. Assay stock preparation

For assay stock preparation, a small piece of ice was removed from the frozen master stock vial and was distributed on a LB agar plate with a Drigalski spatula, which was streaked out onto a 2$^{nd}$ and 3$^{rd}$ LB agar plate. The plates were incubated upside-down at 37 °C overnight. After that, 20 colonies were harvested by using a sterile inoculation loop and were transferred to a 50 mL conical tube, containing 50 mL LB medium. The tube was incubated in a 37 °C water bath for 3-8 h until an optical density (OD), measured at a wavelength of 600 nm, between 0.5 and 0.8 was reached. 10 mL of the suspension were removed from the top of the tube and were transferred to a new 50 mL conical tube. Subsequently, 5 mL of 80% glycerol were added as well as 10 mL fresh LB medium, resuspended and 0.5 mL distributed to 1.5 mL safe-lock tubes. The aliquots were stored at -150 °C.

## 4.3. Purification of blood components and activity testing

Whole blood is a mixture of various components that can be separated by centrifugation due to their different relative density and gravities. The components are divided into plasma, platelets and leucocytes as well as red blood cells (RBCs) (Figure 4)[185]. Blood plasma is the liquid protein-rich fraction of whole blood and serves as solution in which the cells as well as the platelets are suspended. Serum is collected after clotting of whole blood and remains as fluid after centrifugation. In comparison to plasma, it is free of fibrinogens and clotting factors[186].

Since complement components can be found in plasma and serum, the collection of these blood components is an important method for the analysis of the factors in different *in vitro* tests.

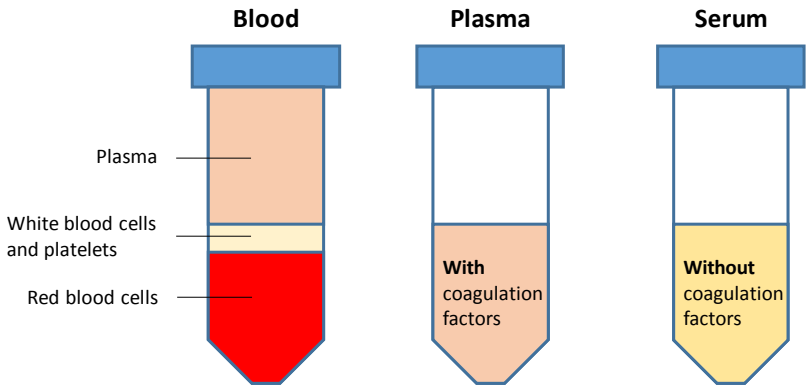


**Figure 4** Purification of blood components by centrifugation of whole blood. Due to their different gravities, plasma, white blood cells and platelets as well as RBCs can be separated after centrifugation of whole blood. In comparison to plasma, serum is devoid of fibrinogens as well as coagulation factors[185,186].

### 4.3.1. Ethylenediaminetetraacetic acid (EDTA)-plasma collection

The plasma was collected by using EDTA-treated tubes for blood sampling. EDTA is an anticoagulant, which has the ability to chelate calcium ions necessary for the coagulation cascade, thereby preventing blood from clotting[187]. Whole blood, collected from 10 different donors, was centrifuged for 30 min at 4 °C and 1000 x g. The following steps were performed on ice under a clean bench. The supernatant of each vial was collected by using a 5 mL serological pipette and was pooled in a 50 mL conical tube. Subsequently, the serum was again centrifuged for 15 min at 4 °C and 2570 x g. The supernatant was transferred to a new 50 mL conical tube, distributed in 1.5 mL safe-lock tubes and stored at -80 °C.

### 4.3.2. Serum collection

In order to isolate normal human serum (NHS), whole blood was collected from 10 different donors in tubes without anticoagulants. After blood sampling, the tubes were stored for 1 h at 2-8 °C to allow blood clotting and centrifuged for 30 min at 4 °C and 1000 x g. Following steps were performed on ice under a clean bench. The supernatant of each vial was collected by using a 5 mL serological pipette and was pooled in a 50 mL conical tube. Subsequently, the serum was again centrifuged for 15 min at 4 °C and 2570 x g. The supernatant was transferred to a new 50 mL conical tube, distributed in 1.5 mL safe-lock tubes and stored at -80 °C.

### 4.3.3. CH50 test

The CH50 test determines the activity of the classical complement pathway in plasma or serum. For the following *in vitro* assays, NHS, antibody-depleted serum or EDTA-plasma was used as complement source. Their activity was pre-analytically confirmed, because the complement system in general is very heat-sensitive as well as vulnerable to degradation at room temperature and requires appropriate storage conditions[188]. The analysis of NHS (in-house preparation), EDTA-plasma (in-house preparation) as well as IgM-/IgG-depleted serum (Pel-Freez) was performed by the Institute for Immunology (University Hospital Heidelberg) and heat-inactivated (hi) serum or plasma was used as control. The test is based on the lysis of antibody-sensitized sheep erythrocytes at 37 °C (Figure 5) and the results are calculated by plotting the dilution factor of the sample against the degree of haemolysis measured in a spectralphotometer (at 415 nm). CH50 determines the dilution of the sample to obtain 50% lysis of the erythrocytes.

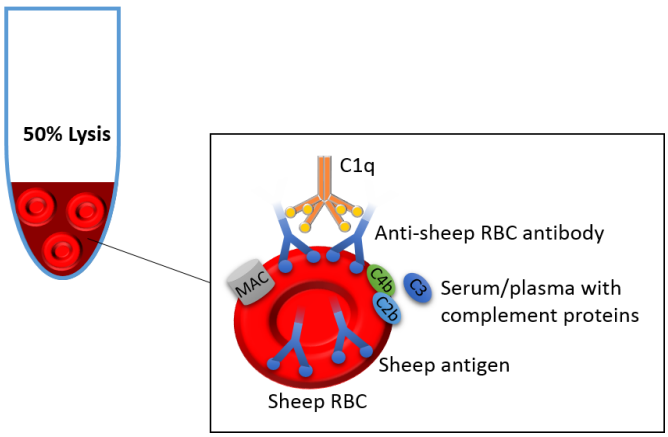


**Figure 5** Overview of the CH50 test. Sheep RBCs coated with anti-sheep RBC antibodies are incubated with the diluted serum or plasma samples at 37 °C. The classical pathway is triggered by binding of C1q to the anti-sheep RBC antibodies and the generation of the MAC leads to the lysis of the target cells in samples with active complement. After measuring free hemoglobin in the supernatant, the dilution of the sample to obtain 50% lysis of the sheep RBCs is calculated.

## 4.4. Complement targeting assays

To investigate whether trimodulin can interact with the complement system, thereby inhibiting activated complement factors and reduce complement-mediated cytotoxicity, the following *in vitro* assays were developed.

### 4.4.1. Opsonin ELISA

To analyze, if trimodulin is able to bind the opsonins C3b and C4b, an ELISA assay was established. The ELISA was adjusted to the protocol described by Rieben *et al.*[99]. For activation of the complement system, aggregated IgG (Intratect) was generated by incubation at 63 °C for 1 h and subsequent centrifugation at 3000 x g for 10 min to remove insoluble aggregates. The aggregated IgG was coated to the wells of a 96 well plate. Trimodulin and Intratect (used as IVIg control) in different dilutions as well as EDTA-plasma were added to the plate. Exclusively the remaining opsonins are detected (Figure 6). For this purpose, a secondary anti-IgG antibody, conjugated to a peroxidase, was used. The peroxidase in turn is able to cleave the added TMB substrate and sulfuric acid stops the reaction, thereby generating a color change. After that, the plate is measured at 450/690 nm in a spectralphotometer.

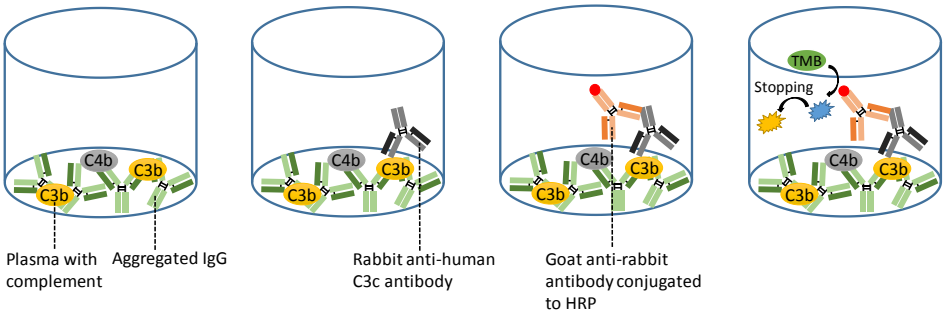


**Figure 6** Detection of remaining C3b or C4b after trimodulin addition. A 96 well flat (F) bottom plate is coated with aggregated IgG and incubated overnight at 2-8 °C. After washing, different dilutions of trimodulin and Intratect (used as IVIg control) are mixed with EDTA-plasma, distributed to the wells and the residual opsonins are detected with a goat anti-rabbit antibody, conjugated to a HRP. The ELISA was adjusted to the protocol described by Rieben *et al.* [99].

Each well of a 96 well F-bottom plate was coated with 100 µL of 0.1 µg/mL aggregated IgG in carbonate bicarbonate buffer (pH 9.4) and incubated overnight at 2-8 °C. After that, the plate was washed three times with 300 µL/well tris-buffered saline with tween 20 (TBS-T) washing buffer in an automated plate washer. The following steps were performed on wet ice. EDTA-plasma was 100-fold diluted in Gelatin Veronal Buffer with $Mg^{2+}$ and $Ca^{2+}$ containing 0.05% Tween 20 ($GVB^{++}$) and different concentrations of trimodulin and Intratect were prepared in their appropriate formulation buffer (FB) using cluster tubes (Table 1).

**Table 1** Dilutions of trimodulin and Intratect used in the Opsonin ELISA.

| Dilution | Concentration | Dilution Factor |
|---|---|---|
| 1 | 25 mg/mL | 2 |
| 2 | 20 mg/mL | 2.5 |
| 3 | 15 mg/mL | 3.33 |
| 4 | 10 mg/mL | 5 |
| 5 | 5 mg/mL | 10 |
| 6 | 1 mg/mL | 50 |
| 7 | 0.5 mg/mL | 100 |
| 8 | 0.1 mg/mL | 500 |

50 $\mu$L of the prepared EDTA-plasma was mixed with 50 $\mu$L of trimodulin (B588036) or Intratect (B791256) dilutions and distributed to the 96 well plate according to the plate layout in Table 2. As negative control for C3b and C4b detection, 50 $\mu$L trimodulin as well as Intratect were added to column 1 and 2 and mixed with 50 $\mu$L GVB$^{++}$. As positive control (column 3) served 50 $\mu$L EDTA-plasma mixed with 50 $\mu$L GVB$^{++}$. 50 $\mu$L of the pre-diluted trimodulin batches (B588016, B588026 and B588036) and Intratect were distributed to columns 4-11 in duplicates and mixed with 50 $\mu$L EDTA-plasma.

**Table 2** Plate layout of the Opsonin ELISA, indicating the distribution of the controls and samples.

| | 1 | 2 | 3 | 4 | 5 | 6 | 7 | 8 | 9 | 10 | 11 | 12 |
|---|---|---|---|---|---|---|---|---|---|---|---|---|
| A | Dil. 1 | Dil. 1 | 1 | Dil. 1 | Dil. 1 | Dil. 1 | Dil. 1 | Dil. 1 | Dil. 1 | Dil. 1 | Dil. 1 | |
| B | Dil. 2 | Dil. 2 | 2 | Dil. 2 | Dil. 2 | Dil. 2 | Dil. 2 | Dil. 2 | Dil. 2 | Dil. 2 | Dil. 2 | |
| C | Dil. 3 | Dil. 3 | 3 | Dil. 3 | Dil. 3 | Dil. 3 | Dil. 3 | Dil. 3 | Dil. 3 | Dil. 3 | Dil. 3 | |
| D | Dil. 4 | Dil. 4 | 4 | Dil. 4 | Dil. 4 | Dil. 4 | Dil. 4 | Dil. 4 | Dil. 4 | Dil. 4 | Dil. 4 | |
| E | Dil. 5 | Dil. 5 | 5 | Dil. 5 | Dil. 5 | Dil. 5 | Dil. 5 | Dil. 5 | Dil. 5 | Dil. 5 | Dil. 5 | |
| F | Dil. 6 | Dil. 6 | 6 | Dil. 6 | Dil. 6 | Dil. 6 | Dil. 6 | Dil. 6 | Dil. 6 | Dil. 6 | Dil. 6 | |
| G | Dil. 7 | Dil. 7 | 7 | Dil. 7 | Dil. 7 | Dil. 7 | Dil. 7 | Dil. 7 | Dil. 7 | Dil. 7 | Dil. 7 | |
| H | Dil. 8 | Dil. 8 | 8 | Dil. 8 | Dil. 8 | Dil. 8 | Dil. 8 | Dil. 8 | Dil. 8 | Dil. 8 | Dil. 8 | |
| | Neg. Ctr. trim. | Neg. Ctr. Intra. | Pos. Ctr. | trimodulin (B588016) + EDTA-Plasma | | trimodulin (B588026) + EDTA-Plasma | | trimodulin (B588036) + EDTA-Plasma | | Intratect (B791256) + EDTA-Plasma | | |

Ctr. = control; Dil. = dilution; Neg. = negative; Pos. = positive

Subsequently, the plate was covered with a sealing tape and was incubated for 1 h at 37 °C. After that, the supernatant was transferred to a U-bottom 96 well plate and was stored at -20 °C for additional Western Blot analysis. The F-bottom plate was washed three times with 300 $\mu$L/well TBS-T washing buffer in an automated plate washer and the primary antibody was prepared. A rabbit anti-human C3c or C4c antibody that can also detect C3b/C4b and iC3b/iC4b was used and diluted 3000-fold in GVB$^{++}$. 100 $\mu$L were added to each well and the plate was incubated for 1 h at room temperature (RT). After incubation, the secondary goat anti-rabbit antibody, conjugated to a horseradish peroxidase (HRP), was 2000-fold diluted and was distributed to the 96 well plate. It was incubated for 1 h at RT, following washing with 300 $\mu$L/well TBS-T washing buffer. For detection of the remaining C3b or C4b, 3,3',5,5'-tetramethylbenzidine (TMB) substrate was 20-fold diluted in TMB substrate buffer and 50 $\mu$L added to each well. After incubation for 20 min at RT, 50 $\mu$L of TMB stopping solution, containing sulfuric acid, was distributed to the plate and the absorbance subsequently measured in a spectralphotometer at 450/690 nm.

### 4.4.2. Fluid phase ELISA

In order to analyze if IgM of trimodulin can bind to the opsonins C3b or C4b, a fluid phase ELISA was developed. The ELISA was adjusted to the protocol described by Rieben *et al.*[99]. One 96 well F-bottom plate was coated with 100 $\mu$L/well of 0.1 $\mu$g/mL aggregated IgG in carbonate bicarbonate buffer (pH 9.4) (plate 1) and a second 96 well F-bottom plate was coated with 100 $\mu$L/well of 0.1 $\mu$g/mL rabbit anti-human C3c or C4b antibody (plate 2). Both plates were incubated at 2-8 °C overnight. Subsequently, plate 1 was washed three times with 300 $\mu$L/well TBS-T washing buffer in an automated plate washer. After that, the same plate layout and concentrations as described in the opsonin ELISA were used for the control as well as for sample preparation. Plate 1 was incubated at 37 °C for 1 h and plate 2 was washed with TBS-T washing buffer. 90 $\mu$L of PBS, containing 0,3% BSA and 0,05% Tween20 were distributed to

the wells, the supernatant of plate 1 was transferred to plate 2, mixed and incubated for additional 1 h at 37 °C. Plate 2 was washed three times with 300 $\mu$L/well TBS-T washing buffer in an automated plate washer and the primary antibody was prepared. A mouse anti-human IgM antibody was used and diluted 3000-fold in GVB$^{++}$. 100 $\mu$L were added to each well and the plate was incubated for 1 h at RT. After incubation, the secondary rabbit anti-mouse antibody, conjugated to a HRP, was 5000-fold diluted and was distributed to the 96 well plate. It was incubated for 1 h at RT, following washing with 300 $\mu$L/well TBS-T washing buffer. For detection of the IgM, TMB substrate was 20-fold diluted in TMB substrate buffer and 50 $\mu$L added to each well. After incubation for 20 min at RT, 50 $\mu$L of TMB stopping solution containing sulfuric acid was distributed to the plate and the absorbance subsequently measured in a spectralphotometer at 450/690 nm.

### 4.4.3. Anaphylatoxin ELISA

To investigate if trimodulin can bind the anaphylatoxins C3a and C5a and therefore reduce the complement-mediated cytotoxicity, an anaphylatoxin ELISA was developed. Two setups were established, one with zymosan-activated EDTA-plasma and the other with purified C5a.

#### 4.4.3.1. Coating of the 96 well plate with trimodulin

Trimodulin (B588036) was 500-fold pre-diluted in FB, then 10-fold serially diluted in carbonate bicarbonate buffer and 100 $\mu$L/well were coated to a 96 well F-bottom plate. As negative control for anaphylatoxin binding, carbonate bicarbonate buffer instead of trimodulin was added to the wells. After incubation overnight at 2-8 °C, the plate was washed three times with 300 $\mu$L/well TBS-T washing buffer in an automated plate washer and free binding-sites were blocked for 1 h at 37 °C by the addition of 100 $\mu$L PBS containing 5% BSA and 0.1% Tween 20. The plate was again washed with TBS-T washing buffer and 50 $\mu$L of 350 ng/mL purified C5a diluted in GVB$^{++}$ was distributed to each well. To control unspecific binding of the primary antibody, GVB$^{++}$ instead of purified C5a was added. The plate was incubated at 37 °C for 1 h. After that, the plate was washed with TBS-T washing buffer and a primary rabbit anti-human C5a antibody as well as a secondary goat anti-rabbit antibody, conjugated to HRP, were used to detect the bound C5a (Figure 7). 100 $\mu$L of 5000-fold diluted primary antibody in GVB$^{++}$ was distributed to the wells and the plate incubated for 1 h at RT. Following washing with TBS-T washing buffer, the secondary antibody was diluted 2000-fold in GVB$^{++}$ and was added to the wells. The plate was again incubated for 1 h at RT. By the addition of 20-fold diluted TMB substrate, in TMB substrate buffer and the stopping of the reaction after 20 min with TMB stopping solution, the absorbance was measured in a spectralphotometer at 450/690 nm.

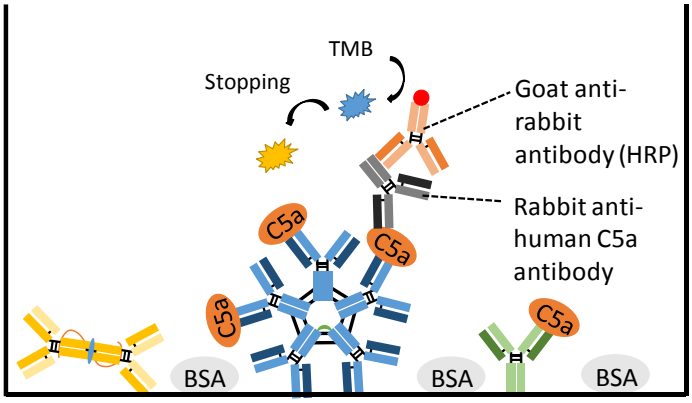


**Figure 7** Detection of C5a bound to trimodulin. A 96 well F-bottom plate was coated with different dilutions of trimodulin in carbonate bicarbonate buffer, blocked with BSA and incubated with 350 ng/mL purified C5a. After washing with TBS-T, bound C5a was detected with a primary rabbit anti-human C5a antibody and a secondary goat anti-rabbit antibody, conjugated to HRP.

#### 4.4.3.2. Coating of the 96 well plate with zymosan

This ELISA was performed by using two in-house coated plates and an anti-human C5a or C3a ELISA kit from BD (Figure 8). A 96 well F-bottom plate was coated with 100 $\mu$L of 20 $\mu$g/mL zymosan in carbonate bicarbonate buffer and was incubated overnight at 2-8 °C (plate 1). Zymosan is a carbohydrate complex derived from yeast cell walls and can activate the complement system in the absence of antibodies via the alternative pathway[189,190]. Furthermore, a second plate was coated with 5 $\mu$g/mL of a goat anti-human IgG+IgA+IgM antibody mix in carbonate bicarbonate buffer (plate 2) for the immobilization of trimodulin as well as Intratect on plate 2 and was incubated overnight at 2-8 °C. After that, the plates were washed three times with 300 $\mu$L TBS-T washing buffer in an automated plate washer. EDTA-plasma was 50-fold diluted in $GVB^{++}$ and 60 $\mu$L of this dilution was added to the wells of plate 1. It was incubated at 37 °C for 1 h. Subsequently, 50 $\mu$L of this supernatant containing activated complement factors was transferred to plate 2. For C3a detection, trimodulin (B588036) as well as Intratect were 20-fold pre-diluted, before a 2-fold serial dilution was performed in their appropriate FB. For C5a detection, trimodulin (B588036) and Intratect were 1250-fold pre-diluted and then 1.8-fold serially diluted in FB. After that, 50 $\mu$L of the respective dilutions were distributed to plate 2 As negative controls, trimodulin and Intratect without EDTA-plasma as well as EDTA-plasma without the products, as positive control for C3a or C5a detection, were added to the plate (see plate layout, Table 3). After mixture, the plate was incubated for 1 h at 37 °C. Subsequently, the supernatant of plate 2, containing the unbound C3a and C5a molecules, was transferred to the anti-human C3a or C5a coated microplate (plate 3) of the ELISA kit and the anaphylatoxins were detected after the manufacturers' instruction in a spectralphotometer at 450/690 nm.

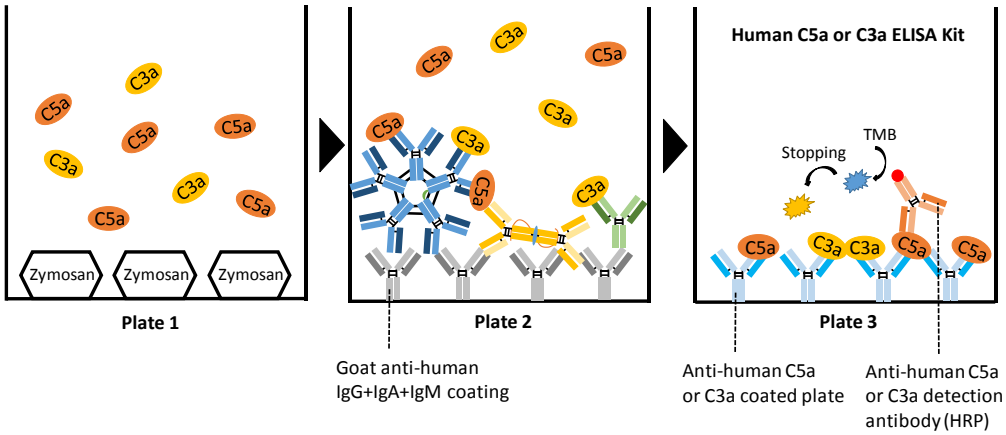


**Figure 8** Schematic overview of the anaphylatoxin ELISA, using a zymosan-coated microplate. A 96 well F-bottom plate was coated with 20 µg/mL zymosan in carbonate bicarbonate buffer (plate 1). EDTA-plasma was incubated on plate 1 to activate the complement system and generate the anaphylatoxins. The activated supernatant was transferred to a second plate coated with an anti-human IgG+IgA+IgM antibody and mixed with different dilutions of trimodulin or Intratect (plate 2). After that, an anti-human C3a or C5a coated plate of a C3a or C5a ELISA kit was used to detect the unbound anaphylatoxins with specific antibodies (plate 3) in a spectralphotometer.

**Table 3** Plate layout of the anaphylatoxin ELISA, indicating the distribution of the controls and samples.

| | 1 | 2 | 3 | 4 | 5 | 6 | 7 | 8 | 9 | 10 | 11 | 12 |
|---|---|---|---|---|---|---|---|---|---|---|---|---|
| A | Dil. 1 | Dil. 1 | Dil. 1 | Dil. 1 | 1 | Dil. 1 | Dil. 1 | Dil. 1 | Dil. 1 | | | |
| B | Dil. 2 | Dil. 2 | Dil. 2 | Dil. 2 | 2 | Dil. 2 | Dil. 2 | Dil. 2 | Dil. 2 | | | |
| C | Dil. 3 | Dil. 3 | Dil. 3 | Dil. 3 | 3 | Dil. 3 | Dil. 3 | Dil. 3 | Dil. 3 | | | |
| D | Dil. 4 | Dil. 4 | Dil. 4 | Dil. 4 | 4 | Dil. 4 | Dil. 4 | Dil. 4 | Dil. 4 | | | |
| E | Dil. 5 | Dil. 5 | Dil. 5 | Dil. 5 | 5 | Dil. 5 | Dil. 5 | Dil. 5 | Dil. 5 | | | |
| F | Dil. 6 | Dil. 6 | Dil. 6 | Dil. 6 | 6 | Dil. 6 | Dil. 6 | Dil. 6 | Dil. 6 | | | |
| G | Dil. 7 | Dil. 7 | Dil. 7 | Dil. 7 | 7 | Dil. 7 | Dil. 7 | Dil. 7 | Dil. 7 | | | |
| H | Dil. 8 | Dil. 8 | Dil. 8 | Dil. 8 | 8 | Dil. 8 | Dil. 8 | Dil. 8 | Dil. 8 | | | |
| | Negative Control trimodulin | | Negative Control Intratect | | Pos. Ctr. | trimodulin (B588036) + EDTA-Plasma | | Intratect (B791256) + EDTA-Plasma | | | | |

### 4.4.4. Complement-dependent cytotoxicity (CDC) assay

CDC can be initiated by binding of the complement protein C1q to the Fc domain of an antibody opsonizing a target cell. The binding of C1q triggers the activation of the complement cascade and leads to the formation of the MAC, which forms pores into the membrane causing the lysis of target cells (Figure 9).

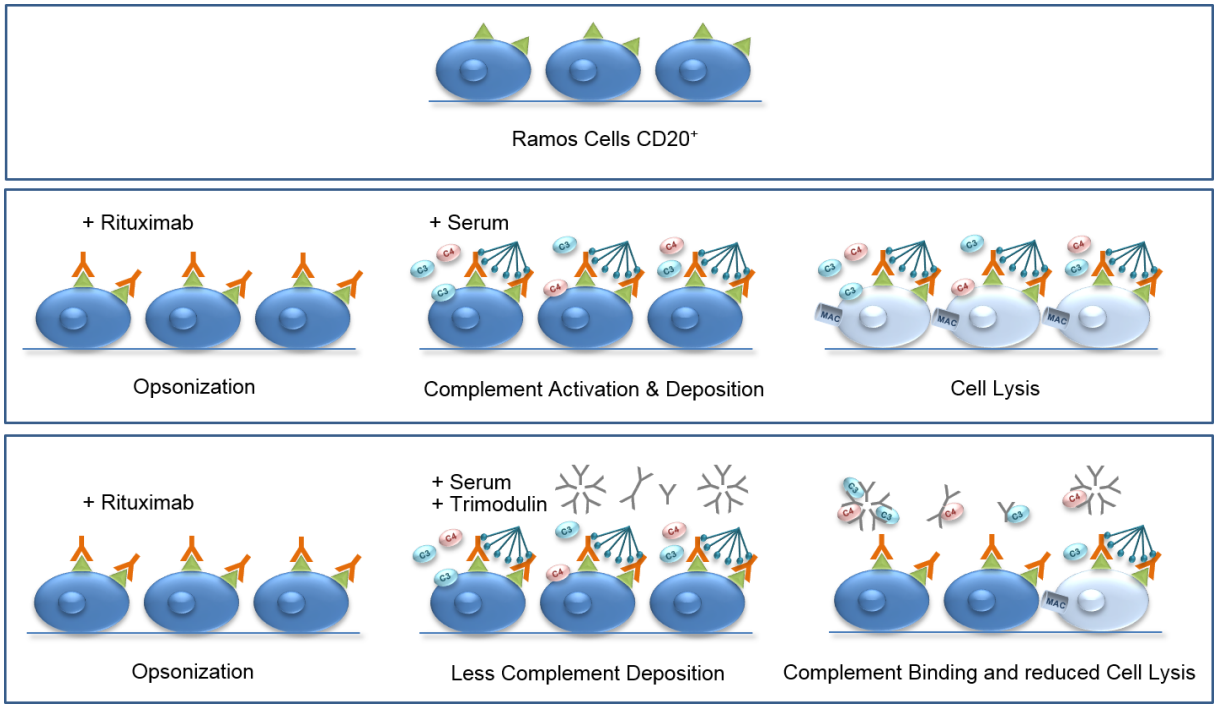


**Figure 9** Schematic overview of a CDC assay. (a) Ramos cells that express CD20 on their surface can be used as target cells in the CDC assay. (b) The chimeric monoclonal antibody Rituximab binds CD20 and the subsequent incubation with normal human serum (NHS) leads to the activation of the complement cascade by binding of C1q to the Fc domain of Rituximab. This triggers the formation of the MAC, which forms pores into the membrane and causes the lysis of the Ramos cells. (c) By the addition of trimodulin, activated complement components could be inhibited, leading to a reduced complement deposition and cell lysis.

#### 4.4.4.1. Rituximab

Rituximab is a CD20 specific chimeric monoclonal antibody used for the treatment of non-Hodgkin's lymphoma. By binding human complement component C1q, it activates the classical complement pathway and thereby induces B-cell death through CDC. Additionally, it can mediate ADCC with human effector cells as well as apoptosis [191,192].

In the CDC assay, Rituximab is used to initiate the CDC by binding of the complement protein C1q to its Fc domain, opsonizing the Ramos cells.

#### 4.4.4.2. Assay procedure

To investigate whether trimodulin can reduce CDC of Ramos cells through the interaction with activated complement factors (the complement cascade was activated by the binding of complement protein C1q to Rituximab), a flow cytometer-based assay was implemented. Intratect was used as IVIg control (see Figure 9).

Ramos cells were washed twice and adjusted to $5 \cdot 10^6$ cells/mL in CDC assay buffer, composed of serum-free RPMI-1640 medium and 10 mM HEPES. 50 $\mu$L of the cells/well were seeded to a V-bottom 96 well plate (plate 1) (Table 4) and stored at 37 °C and 5% $CO_2$. For the preparation of different dilutions of trimodulin (B588036), Intratect and Rituximab, a 96 well round (U) bottom plate was used (plate 2) (Table 5). Rituximab was pre-diluted to 1600 $\mu$g/mL in assay buffer and a 10-fold serial dilution was performed. In addition, six wells with 150 $\mu$L of 160 $\mu$g/mL Rituximab in assay buffer were distributed. Trimodulin and Intratect were 2-fold serially diluted in their appropriate FB. In another 96 well U-bottom plate (plate 3) (Table 6), 30 $\mu$L of 80% NHS in assay buffer were distributed. The wells of plate 3 with only assay buffer are the 100%-killing control.

**Table 4** Distribution of the Ramos cells on plate 1.

| | 1 | 2 | 3 | 4 | 5 | 6 | 7 | 8 | 9 | 10 | 11 | 12 |
|---|---|---|---|---|---|---|---|---|---|---|---|---|
| A | 50 $\mu$L Ramos cells | 50 $\mu$L Ramos cells | | | | | 50 $\mu$L Ramos cells | 50 $\mu$L Ramos cells | 50 $\mu$L Ramos cells | 50 $\mu$L Ramos cells | 50 $\mu$L Ramos cells | 50 $\mu$L Ramos cells |
| B | | | | | | | 50 $\mu$L Ramos cells | 50 $\mu$L Ramos cells | 50 $\mu$L Ramos cells | 50 $\mu$L Ramos cells | 50 $\mu$L Ramos cells | 50 $\mu$L Ramos cells |
| C | 50 $\mu$L Ramos cells | 50 $\mu$L Ramos cells | 50 $\mu$L Ramos cells | 50 $\mu$L Ramos cells | | | | | | | | |
| D | | | | | | | 50 $\mu$L Ramos cells | 50 $\mu$L Ramos cells | 50 $\mu$L Ramos cells | 50 $\mu$L Ramos cells | 50 $\mu$L Ramos cells | 50 $\mu$L Ramos cells |
| E | 50 $\mu$L Ramos cells | 50 $\mu$L Ramos cells | 50 $\mu$L Ramos cells | 50 $\mu$L Ramos cells | 50 $\mu$L Ramos cells | | 50 $\mu$L Ramos cells | 50 $\mu$L Ramos cells | 50 $\mu$L Ramos cells | 50 $\mu$L Ramos cells | 50 $\mu$L Ramos cells | 50 $\mu$L Ramos cells |
| F | 50 $\mu$L Ramos cells | 50 $\mu$L Ramos cells | 50 $\mu$L Ramos cells | 50 $\mu$L Ramos cells | 50 $\mu$L Ramos cells | | | | | | | |
| G | | | | | | | | | | | | |
| H | | | | | | | | | | | | |

**Table 5** Prepared dilutions of Ig preparations and Rituximab on plate 2.

| | 1 | 2 | 3 | 4 | 5 | 6 | 7 | 8 | 9 | 10 | 11 | 12 |
|---|---|---|---|---|---|---|---|---|---|---|---|---|
| A | Assay buffer | Assay buffer | | | | | 50 mg/mL trim. | 25 mg/mL trim. | 12.5 mg/mL trim. | 6.25 mg/mL trim. | 3.125 mg/mL trim. | 1.5625 mg/mL trim. |
| B | | | | | | | | | | | | |
| C | Assay buffer | Assay buffer | Assay buffer | Assay buffer | | | | | | | | |
| D | | | | | | | 50 mg/mL Intra. | 25 mg/mL Intra. | 12.5 mg/mL Intra. | 6.25 mg/mL Intra. | 3.125 mg/mL Intra. | 1.5625 mg/mL Intra. |
| E | 1600 μg/mL Ritux. | 160 μg/mL Ritux. | 16 μg/mL Ritux. | 1.6 μg/mL Ritux. | 0.16 μg/mL Ritux. | | | | | | | |
| F | | | | | | | | | | | | |
| G | 160 μg/mL Ritux. | 160 μg/mL Ritux. | 160 μg/mL Ritux. | 160 μg/mL Ritux. | 160 μg/mL Ritux. | 160 μg/mL Ritux. | | | | | | |
| H | | | | | | | | | | | | |

Intra. = Intratect; Ritux. = Rituximab; trim. = trimodulin.

**Table 6** Distribution of 80% NHS and assay buffer (as 100% killing control) on plate 3.

| | 1 | 2 | 3 | 4 | 5 | 6 | 7 | 8 | 9 | 10 | 11 | 12 |
|---|---|---|---|---|---|---|---|---|---|---|---|---|
| A | Assay buffer | Assay buffer | | | | | 80% NHS | 80% NHS | 80% NHS | 80% NHS | 80% NHS | 80% NHS |
| B | | | | | | | 80% NHS | 80% NHS | 80% NHS | 80% NHS | 80% NHS | 80% NHS |
| C | Assay buffer | Assay buffer | Assay buffer | Assay buffer | | | | | | | | |
| D | | | | | | | 80% NHS | 80% NHS | 80% NHS | 80% NHS | 80% NHS | 80% NHS |
| E | 80% NHS | 80% NHS | 80% NHS | 80% NHS | 80% NHS | | 80% NHS | 80% NHS | 80% NHS | 80% NHS | 80% NHS | 80% NHS |
| F | 80% NHS | 80% NHS | 80% NHS | 80% NHS | 80% NHS | | | | | | | |
| G | | | | | | | | | | | | |
| H | | | | | | | | | | | | |

After preparation, the assay components were mixed and incubated in different sequences on their appropriate plates:

(1) Pre-incubation of Ig preparations and NHS:

To investigate the effect of trimodulin on complement factors, 15 µL of the diluted Ig preparations (trimodulin or Intratect as IVIg control) of plate 2 was mixed with 30 µL of 80% NHS on plate 3. The plate was incubated for 1 h at 37 °C and 5% $CO_2$. Afterwards, 15 µL of 160 µg/mL Rituximab (plate 2) was mixed with the pre-incubated Ig preparations and NHS. In addition, 15 µL of serially diluted Rituximab was mixed with the appropriate wells on plate 3 and 15 µL assay buffer was added. 50 µL/well of these dilutions was then transferred to the prepared Ramos cells on plate 1 and incubated for 65 min at 37°C and 5% $CO_2$. As 100%-killing control, 10 µL of 8% Triton-X 100 was added to the wells containing Ramos cells only and was incubated for additional 15 min at 37 °C and 5% $CO_2$.

(2) Pre-incubation of Ig preparations and NHS and simultaneous pre-incubation of Rituximab and Ramos cells:

An additional pre-incubation step was added, in order to evaluate potential effects on CDC of the Ramos cells through Rituximab binding to CD20 before the addition of trimodulin. 30 µL of the diluted Ig preparations was mixed with the same amount of assay buffer and 60 µL of these dilutions was transferred to plate 3. Additionally, 16.5 µL of 160 µg/mL Rituximab was mixed with the Ramos cells on plate 1. Both plates were incubated for 1 h at 37 °C and 5% $CO_2$. Subsequently, 66.5 µL of plate 3 was mixed with the appropriate wells on plate 1 and was incubated for 65 min at 37°C and 5% $CO_2$. As 100%-killing control, 10 µL of 8% Triton-X 100 was added to the wells containing Ramos cells only and was incubated for additional 15 min at 37 °C and 5% $CO_2$.

(3) Incubation of Ig preparations, Rituximab, NHS and Ramos cells at the same time:

To investigate whether the order of the incubation of each component influences the effect of trimodulin on CDC, 60 µL of 160 µg/mL Rituximab was mixed with the serially diluted Ig preparations on plate 2. In addition, 60 µL of serially diluted Rituximab was mixed with the same amount of assay buffer. After that, 30 µL of these dilutions was transferred to plate 3 and was added to the appropriate wells. 50 µL/well of these dilutions was added to the prepared Ramos cells on plate 1 and incubated for 65 min at 37 °C and 5% $CO_2$. As control, 10 µL of 8% Triton-X 100 was added to the wells containing Ramos cells only and was incubated for additional 15 min at 37 °C and 5% $CO_2$.

(4) Pre-incubation of Rituximab and Ig preparations:

To analyze, if trimodulin has an impact on the binding of Rituximab to CD20 on the Ramos cells, the two components were pre-incubated. Therefore, 60 µL of the wells with 160 µg/mL Rituximab was mixed with the serially diluted Ig preparations on plate 2 before the plate was pre-incubated for 1 h at 37 °C and 5% $CO_2$. The following steps were the same as described in (3).

(5) Incubation of Ig preparations, NHS and Ramos cells, without Rituximab:

To analyze, if trimodulin is able to interact with CD20 on the Ramos cells and thereby inhibits the binding of Rituximab to this surface antigen, the same steps as described in (3) were performed. Different to the mentioned procedure in (3) was the addition of assay buffer to the Ig preparations, instead of Rituximab.

(6) Incubation of Ig preparations, Rituximab, Ramos cells and hi NHS:

To examine the effect of Rituximab in the absence of active complement factors, NHS was heat-inactivated for 30 min in a 56 °C water bath. 30 µL was distributed to the appropriate wells on plate 3. After that, the procedure followed the steps described in (3).

After the incubation as described in detail in 1,2,3,4,5 or 6, the plates were analyzed in a flow cytometer. To monitor the CD20 expression, the cells were stained with an anti-CD20 antibody, conjugated with APC. The antibody was 6-fold pre-diluted in PBS, 10 µL was distributed to the wells and the plate was incubated for 30 min at 2-8 °C. To exclude live from dead cells, the plates were centrifuged at 1000 x g for 5 min and resuspended in 100 µL propidiumiodid (PI), diluted 500-fold in assay buffer. This dye is able to detect dead cells in a population by specific binding the DNA and is not permeant to live cells. After incubation for 15 min at RT, the plate was measured in the flow cytometer and CDC was indicated as percentage [%-parent] of dead cells within all applied cells per well. The FB of each product was used as base level for CDC triggered by Rituximab and given in cell viability [%]. Based on this, the change in cell viability caused by trimodulin or Intratect was determined.

## 4.5. Opsonophagocytosis assay

Opsonophagocytosis is initiated by the opsonization of target cells by antibodies or opsonins, which bind to specific receptors on the phagocyte and lead to the killing as well as clearance of the pathogen. This opsonophagocytic killing assay was used to determine the antimicrobial ability of trimodulin to phagocyte bacteria, like *S. aureus* and *E. coli*. Moreover, the influence of the strong ability of IgM in trimodulin to activate the complement system compared to Intratect was examined regarding opsonization and phagocytosis. Differentiated HL-60 cells were used as effector cells and IgG-/IgM-depleted serum (NHS minus) as complement source.

### 4.5.1. Differentiation of HL-60 cells

In order to differentiate HL-60 cells to mature neutrophil-like granulocytes, the cells were counted in a Neubauer chamber, centrifuged at 350 x g for 5 min in a 50 mL conical tube and the supernatant discarded. After that, they were gently resuspended to $6 \cdot 10^5$ cells/mL in IMDM medium containing 20% FBS, 1% penicillin-streptomycin and 1.3% DMSO or 0.8% dimethylformamide (DMF). The suspension was transferred to a T-175 cell culture flask and was incubated at 37 °C and 5% $CO_2$ for 3-4 days. After that, the differentiated HL-60 cells were tested for their phenotype in a FACS Canto II.

### 4.5.2. Assay procedure (*E. coli*)

The OPA was performed in 96 well U-bottom plates and was adjusted to the OPA protocol described by Burton and Nahm[193]. Initially, the opsonization buffer (OB) was prepared by mixing 40 mL of distilled $H_2O$ ($dH_2O$) with 5 mL of 10x Hanks' Balanced Salt Solution (HBSS) containing $Mg^{2+}$ and $Ca^{2+}$ and 5 mL of 1% gelatin. 20 µL of the OB was transferred to the wells H1-H9, G4-G9, C1-C9 and B4-B9 (plate layout, see Table 7). After that, trimodulin and Intratect as IVIg control were 10-fold serially diluted in cluster-tubes and 3 µL of the pre-diluted products added to the wells H4-H9, G4-G9, C4-C9 and B4-B9. Subsequently, the differentiated as well as undifferentiated HL-60 cells (as control) were counted in a Neubauer chamber with 0.2% trypan blue solution, centrifuged at 350 x g for 5 min and washed with 10 mL OB. A requirement for using the HL-60 cells in the OPA was a cell viability of at least 90%. For the preparation of the cells, they were again centrifuged at 350 x g for 5 min and resuspended to $1 \cdot 10^7$ cells/mL in OB. After that, a vial from the frozen assay stock of the *E. colis* was rapidly thawed in a 37 °C water bath and centrifuged at 12000 x g for 2 min. The supernatant was carefully removed and discarded. For washing, 1 mL OB was added, mixed and the vial was centrifuged again at 12000 x g for 2 min. The bacterial pellet was resuspended in the original volume (0.5 mL) and was 4000-fold diluted in 10 mL OB to a concentration of approximately 10000 colony-forming units per mL (CFU/mL).

10 $\mu$l of this dilution was distributed to the samples and controls, indicated in Table 7 as well Table 8 and the plate was incubated at RT on a mini orbital shaker (700 rpm) for 30 min. Moreover, NHS minus was removed from the freezer and was thawed at RT. To prepare hi NHS minus as control, one vial was incubated for 30 min at 56 °C. Afterwards, hi and active NHS minus were diluted to 0.8% in the prepared HL-60 cells and 50 $\mu$L added to the appropriate wells. The plate was incubated for 45 min at 37 °C and 5% $CO_2$ on a mini orbital shaker (700 rpm). A required amount of LB agar-plates was dried by removing the lid under a clean bench for 30-60 min. After incubation, the 96 well plate was put on ice for 20 min to stop the phagocytic process and 5 $\mu$L of each well applied in triplets on the LB agar plates as 5 $\mu$L spots. The plate was immediately tilted until the spots were shaped into small fluid strips of about 2-3 cm and left for 10 min at RT to let the excess fluid seek into the agar. Subsequently, the plates were incubated upside-down at 37 °C and 5% $CO_2$ for 16-18 h. On the next day, the plates were removed from the incubator and the colonies manually counted. The data were analyzed with GraphPad Prism, after determination of CFU/mL by the following formula:

$$\text{CFU/mL} = \frac{\text{Colonies counted} \cdot \text{Dilution factor of the bacteria}}{\text{Amount plated [mL]}}$$

**Table 7** Overview of the 96 well plate, indicating the controls and samples used in the OPA (*E. coli*).

| | 1 | 2 | 3 | 4 | 5 | 6 | 7 | 8 | 9 | 10 | 11 | 12 |
|---|---|---|---|---|---|---|---|---|---|---|---|---|
| A | | | | | | | | | | | | |
| B | | | | Intra. 1 | Intra. 2 | Intra. 3 | Intra. 4 | Intra. 5 | Intra. 6 | | | |
| C | Ctr. A | Ctr. B | Ctr. C | Ctr. D1 | Ctr. D2 | Ctr. D3 | Ctr. D4 | Ctr. D5 | Ctr. D6 | | | |
| D | | | | | | | | | | | | |
| E | | | | | | | | | | | | |
| F | | | | | | | | | | | | |
| G | | | | trim. 1 | trim. 2 | trim. 3 | trim. 4 | trim. 5 | trim. 6 | | | |
| H | Ctr. A | Ctr. B | Ctr. C | Ctr. D1 | Ctr. D2 | Ctr. D3 | Ctr. D4 | Ctr. D5 | Ctr. D6 | | | |

Ctr. = control; Intra. = Intratect; trim. = trimodulin.

**Table 8** Composition of the controls and samples used in the OPA (*E. coli*).

| Sample | Composition |
|---|---|
| Ctr. A | Bacteria + hi NHS minus + undifferentiated HL-60 cells + FB |
| Ctr. B | Bacteria + hi NHS minus + differentiated HL-60 cells + FB |
| Ctr. C | Bacteria + NHS minus + differentiated HL-60 cells + FB |
| Ctr. D | Bacteria + hi NHS minus + differentiated HL-60 cells + Ig preparation |
| Sample | Bacteria + NHS minus + differentiated HL-60 cells + Ig preparation |

### 4.5.3. Assay procedure (*S. aureus*)

The OPA, described in 4.5.2 was performed with living *E. coli* (K12) bacteria that were non-pathogenic. Here, an additional OPA was performed with Alexa Fluor 488 labeled *S. aureus* bioparticles. The particles are devitalized and could therefore be used in a biosafety level 1 laboratory. The test was adjusted to a FACS-based method (based on the protocol of Fabian Bohländer; PhD thesis), to determine the fluorescence of differentiated HL-60 cells after the phagocytosis of the labeled bacteria. The composition of the controls and samples was the same as described in Table 8. Initially, one vial containing the lyophilized *S. aureus* pellet was resuspended with 500 $\mu$L Dulbecco's PBS (D-PBS) to obtain approximately $5 \cdot 10^7$ particles/mL and sonicated for 1 min. After that, the differentiated and undifferentiated HL-60 cells were centrifuged at 350 x g for 5 min, the supernatant removed and resuspended to $1.25 \cdot 10^6$ cells/mL. 1 mL of the cells was distributed per well to 24 well F-bottom plates. Subsequently, 10 $\mu$L of the *S. aureus* bioparticles and 20 $\mu$L of NHS minus as well as hi NHS minus were added to the cells and mixed. Different dilutions of trimodulin and Intratect were prepared by distributing the appropriate volume of the products to the wells and filling up with FB to obtain the same end-volume (1700 $\mu$L) in every well (Table 9). Moreover, Intratect was 1.8-fold pre-diluted in FB to the same IgG amount like trimodulin (≈ 56% IgG) and was afterwards added to the plate. The plates were incubated for 45 min at 37 °C. After incubation, the content of the 24 well plate was transferred to a 96 well deep well plate and centrifuged for 5 min at 350 x g. The supernatant was removed and the pellet was resuspended with 250 $\mu$L D-PBS. After an additionally centrifugation step at 350 x g for 5 min and resuspension with 250 $\mu$L D-PBS, 125 $\mu$L per well were transferred to a 96 well V bottom plate in doublets (Table 10). To ensure the measurement of just phagocytosed bioparticles by the differentiated HL-60 cells and to reduce the background fluorescence produced by bacteria that bound unspecifically to the surface of the cells, 30 $\mu$L of trypan blue solution was added for quenching. The plate was incubated for 5-10 min at 2-8 °C and centrifuged at 350 x g for 5 min. Subsequently, the pellet was resuspended with 100 $\mu$L D-PBS and the plate measured in the flow cytometer. To monitor the opsonophagocytosis of the Alexa Fluor 488 labeled *S. aureus* bioparticles initiated by trimodulin, the phagocytic index of the HL-60 cells was analyzed by using Excel and GraphPad Prism. It depicts the uptake of the labeled bacteria by the effector cells and was calculated by multiplying the median fluorescence intensity of the bacteria per positive cell with the percentage of the HL-60 cells containing at least one bacterium.

**Table 9** Dilutions of trimodulin and Intratect used in the OPA (*S. aureus*)

| Dilution | Concentration | Dilution Factor |
|---|---|---|
| 1 | 20 mg/mL | 2.5 |
| 2 | 15 mg/mL | 3.33 |
| 3 | 10 mg/mL | 5 |
| 4 | 5 mg/mL | 10 |
| 5 | 1 mg/mL | 50 |
| 6 | 0.5 mg/mL | 100 |
| 7 | 0.1 mg/mL | 500 |
| 8 | 0.05 mg/mL | 1000 |
| 9 | 0.01 mg/mL | 5000 |

**Table 10** Overview of the 96 well plate, indicating the controls and samples used in the OPA (*S. aureus*)

| | 1 | 2 | 3 | 4 | 5 | 6 | 7 | 8 | 9 | 10 | 11 | 12 |
|---|---|---|---|---|---|---|---|---|---|---|---|---|
| A | | | | Intra. 1 | Intra. 2 | Intra. 3 | Intra. 4 | Intra. 5 | Intra. 6 | Intra. 7 | Intra. 8 | Intra. 9 |
| B | | | | Intra. 1 | Intra. 2 | Intra. 3 | Intra. 4 | Intra. 5 | Intra. 6 | Intra. 7 | Intra. 8 | Intra. 9 |
| C | Ctr. A | Ctr. B | Ctr. C | Ctr. D1 | Ctr. D2 | Ctr. D3 | Ctr. D4 | Ctr. D5 | Ctr. D6 | Ctr. D7 | Ctr. D8 | Ctr. D9 |
| D | Ctr. A | Ctr. B | Ctr. C | Ctr. D1 | Ctr. D2 | Ctr. D3 | Ctr. D4 | Ctr. D5 | Ctr. D6 | Ctr. D7 | Ctr. D8 | Ctr. D9 |
| E | | | | trim. 1 | trim. 2 | trim. 3 | trim. 4 | trim. 5 | trim. 6 | trim. 7 | trim. 8 | trim. 9 |
| F | | | | trim. 1 | trim. 2 | trim. 3 | trim. 4 | trim. 5 | trim. 6 | trim. 7 | trim. 8 | trim. 9 |
| G | Ctr. A | Ctr. B | Ctr. C | Ctr. D1 | Ctr. D2 | Ctr. D3 | Ctr. D4 | Ctr. D5 | Ctr. D6 | Ctr. D7 | Ctr. D8 | Ctr. D9 |
| H | Ctr. A | Ctr. B | Ctr. C | Ctr. D1 | Ctr. D2 | Ctr. D3 | Ctr. D4 | Ctr. D5 | Ctr. D6 | Ctr. D7 | Ctr. D8 | Ctr. D9 |

Ctr. = control; Intra. = Intratect; trim. = trimodulin.

### 4.5.4. Flow cytometric analysis

In order to determine the phagocytosis of *S. aureus* bioparticles by HL-60 cells, a flow cytometer was used. This instrument allows the analysis of separated cells and particles one by one. The fluorescence-labeled samples are diluted inside the instrument to single-cells and therefore pass uniformly through the center of laser beams. This leads to the excitation of the fluorophores, thereby emitting fluorescence that is guided through optical filters as well as mirrors to specific detectors. The detectors are wavelength-sensors in terms of photomultiplier tubes (PMTs), which amplify electric signals and convert them to a voltage pulse. It is displayed in the software as event and shows detailed information as well as characteristics of a cell population. Moreover, two detectors of a flow cytometer measure the light scattering. The forward scatter (FSC) defines the size and the sideward scatter (SSC) the granularity of a cell.

The used FACS Canto II is a flow cytometer that offers a blue (488 nm), a red (633 nm) and a violet (405 nm) laser. The 8 fluorescence channels can define up to 8 cellular parameters.

In the OPA (*S. aureus*) the HL-60 cells were initially tested for their phenotype and their differentiation status, before the phagocytosis of the bioparticles could be determined. Therefore, the antibodies were added to 100 $\mu$L of $1{\cdot}10^6$ cells/mL:

**Table 11** Antibodies and volumes required for HL-60 cell stain.

| Excitation Laser | Fluorescence channel | Antibody | Required Volume |
|---|---|---|---|
| 488 nm | PE | Anti-human CD32 | 20 $\mu$L |
| | FITC | Anti-human CD35 | 20 $\mu$L |
| 633 nm | APC | Anti-human CD71 | 20 $\mu$L |
| | Alexa Fluor 700 | Anti-human CD64 | 5 $\mu$L |
| 405 nm | V500 | Anti-human CD16 | 5 $\mu$L |
| | Pacific Blue | Anti-human CD11b | 20 $\mu$L |

The anti-human CD16, CD32 and CD64 antibodies bind to the IgG Fc receptors FcγRIII, FcγRII and FcγRI, respectively. They are among others expressed on neutrophil granulocytes and play a role in mediating phagocytosis. CD35 is known as complement receptor 1 (CR1) or C3b/C4b receptor and enhances the clearance of complement opsonized immune complexes through phagocytosis by neutrophils. Undifferentiated HL-60 cells show a decreased expression of CD35, whereas the expression increases with the differentiation status of the cells. In comparison to CD35, transferrin receptor 1 (CD71) expression is downregulated in differentiated HL-60 cells. The anti-human CD11b antibody binds to one subunit of the complement receptor 3 (CR3), which consists of CD11b as well as CD18 and can be found on neutrophil granulocytes, where it is a specific receptor for iC3b and additionally mediates phagocytosis.

To monitor the expression of these receptors on differentiated HL-60 cells, they were centrifuged at 350 xg for 5 min, the supernatant discarded and resuspended to $1 \cdot 10^6$ cells/mL in D-PBS. 100 $\mu$L/well was distributed on a V-bottom 96 well plate and the required volume of each antibody was added (Table 11). When performing multicolor fluorescence, spectral overlap between the fluorophores is possible. Therefore it is important to apply a mathematically correction, called compensation. For this purpose, single stained cells were distributed to the plate. Moreover, background fluorescence through unspecific binding of the antibodies was measured by the addition of the appropriate isotype controls. Subsequently, the plate was incubated for 30 min at 2-8 °C. After that, it was centrifuged at 350 x g for 5 min and resuspended in 100 $\mu$L D-PBS. The cell suspension was analyzed using the FACS Canto II and the software BD FACSDiva. A template for each stain was designed and the appropriate PMT voltages, strategies and the automatic compensation applied. After that, the data were analyzed by using the software FlowJo X.

## 4.6. Protein analyses

In order to determine, if trimodulin is able to inhibit complement activation by scavenging the activated factors C3b and C4b in the fluid phase or if this is due to a covering of the deposited opsonins, the supernatant of the ELISA described in 4.4.1 was analyzed in a sodium dodecyl sulfate polyacrylamide gel electrophoresis (SDS-PAGE) and a subsequent Western Blot.

### 4.6.1. SDS-PAGE

SDS-PAGE is a method to separate proteins in an electric field depending on their size. It is performed by using a discontinuous polyacrylamide gel and a reducing agent that destroys the disulfide bonds of the proteins. Moreover, SDS is used to cover the intrinsic charge of the proteins to obtain continuous negatively charged, denatured samples. After the prepared samples are applied to the gel, an electric field is generated upon voltage application. The negatively charged proteins migrate towards the anode and are separated depending on their size, which is proportional to their molecular mass. The specific protein bands that develop through the separation emerge by the migration of smaller and larger proteins. The smaller ones move faster and the larger proteins are stronger retained in the gel. These bands can be visualized by using a Coomassie solution or by blotting it to a membrane and labeling the proteins with specific antibodies.

The SDS-PAGEs were performed by using a NuPage system and 8% bis-tris gels. Initially, the samples were diluted 2-fold in loading buffer, consisting of 1x LDS-sample buffer, 1x TCEP solution (reducing agent) and distilled water. In order to denature the samples, they were incubated for 10 min at 70 °C in a heating block. After that, the bis-tris gels were installed to the XCell SureLock Mini-Cell electrophoresis chamber and filled with 1x MOPS SDS running buffer. Additionally, 500 $\mu$L Antioxidant was added to the inner chamber. 10 $\mu$L of the prepared samples was distributed to the slots of the gel and 10 $\mu$L of the ready-to-use All Blue Prestained Protein Standard was added to the outer two slots. The electrophoresis chamber was connected to a power supply and run at 200 V for approximately 45 min. Subsequently, the gel was removed from the plastic cover and was transferred to a membrane for Western Blotting.

### 4.6.2. Western Blot

During a Western Blot, proteins that were separated by SDS-Page (4.6.1) are transferred to a nitrocellulose membrane and detected via specific antibodies. The transfer is achieved by an electric field, in which the negatively charged proteins move towards the anode. The proteins migrate from the gel to the membrane, thereby remain in place and bind. After that, the membrane is blocked to prevent unspecific binding of the detection antibody. The antibodies are added, incubated and bind to the specific proteins of interest. Moreover, the secondary antibody that is labeled with a fluorophore, binds to the primary antibody and the proteins are detected by an imager.

The Western Blots were performed by using an X Cell II Blot Module. Initially, a nitrocellulose membrane was equilibrated in 1x Western Blot Buffer for 10 min, containing Transfer Buffer (Thermo Scientific), 10% methanol, 0.1% Antioxidant and distilled water. Meanwhile, sponge pads and filter papers were also soaked in 1x Western Blot Buffer and transferred to the Blot Module. Three sponge pads were placed at the bottom of the module, followed by a filter paper, the gel, the membrane, a second filter paper and again three sponge pads. The Blot Module was transferred to the X Cell Sure Lock electrophoresis chamber and filled up with 1x Western Blot Buffer, whereas distilled water was added to the outer chamber. After that, the chamber was connected to the power supply and run at 100 V as well as 60 mA for 85-95 min. Subsequently, the membrane was transferred to Blocking Buffer and was incubated for 1 h on an orbital shaking platform at RT. The buffer was discarded and the primary antibody mix, diluted in Blocking Buffer containing 0.005% Tween 20 was added to the membrane (see Table 12). It was incubated for 1 h on an orbital shaking platform at RT. Afterwards, the membrane was washed in PBS containing 1x Tween 20 and incubated for 5 min on an orbital shaking platform. The washing solution was decanted and the washing procedure was repeated 4-5 times. The secondary antibody mix, diluted in Blocking Buffer containing 0.005% Tween 20 was added to the membrane and was incubated overnight on the orbital shaker at RT (see Table 12). On the next day, the antibody solution was discarded and washed in PBS containing 1x Tween 20 for 4-5 times as before. After that, two additional washing steps with 1x D-PBS were applied for 5 min each and finally the membrane was rinsed in distilled water, dried between filter paper and was scanned with the Typhoon Imager.

**Table 12** Primary and secondary antibodies used in the Western Blot.

| Primary antibody mix | Dilution | | Secondary antibody mix | Dilution |
|---|---|---|---|---|
| Mouse anti-human IgM | 1000-fold | In 25 mL Blocking Buffer | Donkey anti-mouse | 26666-fold |
| Rabbit anti-human IgG | 20000-fold | | Donkey anti-rabbit | 26666-fold |
| Goat anti-human C3c | 1000-fold | | Donkey anti-goat | 26666-fold |
| Tween 20 | 20000-fold | | Tween 20 | 20000-fold |

## 4.7. Statistical analyses

All statistical analyses were performed with the software GraphPad Prism. The data were depicted as mean with SD or standard error of the mean (SEM). To verify normal distribution of the data, a Kolmogorov-Smirnov or a Shapiro-Wilk test was used. Moreover, the significance for normally distributed data was calculated using a one-way ANOVA and a Bonferroni correction to compare more than two different groups. In order to compare more than two groups that are not normally distributed, the Kruskal-Wallis test was used. In addition, the Mann-Whitney test or Wilcoxon test was used for non-parametric calculations of two groups or pairs. The significance was shown as p-values and quantified with asterisks: * $p \leq 0.05$, ** $p \leq 0.01$, *** $p \leq 0.001$, **** $p \leq 0.0001$.

# 5. Results

Trimodulin exhibits various antimicrobial as well as immunomodulatory functions, which were shown in the past in many *in vitro* assays (see chapter 1.9.2)[165,166]. Nevertheless, the complex interactions caused by the mixture of IgG, IgM and IgA in trimodulin are not fully understood and have to be further evaluated in pre-clinical as well as clinical studies. The aim of this thesis was to further characterize the effects of trimodulin on the human complement system. Therefore, different *in vitro* assays were developed, to analyze if trimodulin is able to activate, but also to inhibit the complement cascades concentration-dependently. An opsonin, a fluid phase as well as an anaphylatoxin ELISA were used to monitor the binding and inhibition of various complement factors by trimodulin. Moreover, a CDC assay was established to evaluate the functional effect of trimodulin regarding complement inhibition. Finally, different OPA assays were used to detect complement activation and the associated opsonophagocytosis of bacteria.

## 5.1. Analysis of the hemolytic activity of different complement sources for the use in this thesis

In order to use different complement sources in the following assays, their hemolytic activity was previously determined by using the CH50 test. EDTA-plasma was used as complement source in the complement targeting assays, whereas NHS and hi NHS (used as control) were suitable complement sources for the CDC assay. Moreover, NHS IgG/IgM depleted as well as hi NHS IgG/IgM depleted (used as control) were applied in the OPA. For this purpose, active as well as hi plasma and serum were incubated with antibody-sensitized sheep erythrocytes. The more hemolysis was induced, the higher was the activity of the tested complement sources. Sera that were heat-inactivated and served as negative controls for complement activity did not show hemolytic activity in the CH50 test and were considered as suitable for the use in the assays as controls. NHS and EDTA-plasma were also appropriate complement sources for the different assays, because the values were within the reference range, with activities of 97% and 90%. IgG/IgM depleted NHS exhibited an activity of 51% in the CH50 test. Although, this was beneath the lower limit of the reference range, it was still used, because the absence IgM and IgG was an important requirement for the use in the OPA. Other depleted serum sources, tested in the CH50 showed even no activity due to their treatment by which the Igs were removed (data not shown).

**Table 13** Activity of different complement sources in the CH50 test.

| Complement Source | CH50 Activity | Reference Range |
|---|---|---|
| EDTA-plasma | 90% | 74-151% |
| NHS | 97% | |
| Hi NHS | No activity | |
| NHS IgG/IgM depleted | 51% | |
| Hi NHS IgG/IgM depleted | No activity | |

## 5.2. Immunomodulatory effects of trimodulin on the complement system

The activation of the complement cascade is an important function of the body's immune system to react against invading pathogens and to fight infections. Nevertheless, complement activation is not always beneficial and can also lead to inflammatory reactions due to an over-stimulated immune system. Hence, the ability of trimodulin to interact with activated complement factors and to reduce complement-mediated cytotoxicity was determined.

### 5.2.1. Trimodulin reduces the detection of the complement factors C3b and C4b concentration-dependently in the ELISA setting

In order to analyze, if trimodulin is able to interact with the opsonins C3b and C4b, an ELISA was performed. Initially, C3b was detected, after the addition of different concentrations of trimodulin. Moreover, three batches (B588016, B588026 and B588036) were compared in their ability to reduce the C3b detection (Figure 10). Intratect was used as IVIg control, because the differences between IgM and IgA in binding complement factors compared to pure IgG should be evaluated. Figure 10 shows the detection of C3b deposition on aggregated IgG. Trimodulin induced a concentration-dependent decrease in C3b detection. In addition, all three batches were highly comparable (Figure 10a). The optical density (OD) of the 100% C3b control (without trimodulin) was approximately 3.3 and was continually reduced to approximately 0.9 after addition of 12.5 mg/mL, which was the highest used trimodulin concentration. Compared to this, Intratect initially induced a slight increase in C3b detection in the lowest used concentration (0.05 mg/mL) and only after the addition of 0.5 mg/mL a slight decrease was seen. To compare the abilities of trimodulin and Intratect to reduce the C3b detection concentration-dependently, a statistical analysis was performed (Figure 10b). A significant decrease was seen after the addition of 12.5 mg/mL trimodulin compared to the addition of only trimodulin FB. Moreover, the difference between the highest used trimodulin and Intratect concentration (12.5 mg/mL) to compare the ability of both products was statistically significant. The difference between 12.5 mg/mL Intratect and the addition of only Intratect FB (w/o Intratect), was not significant. These data suggests that trimodulin inhibits the detection of C3b stronger than Intratect.

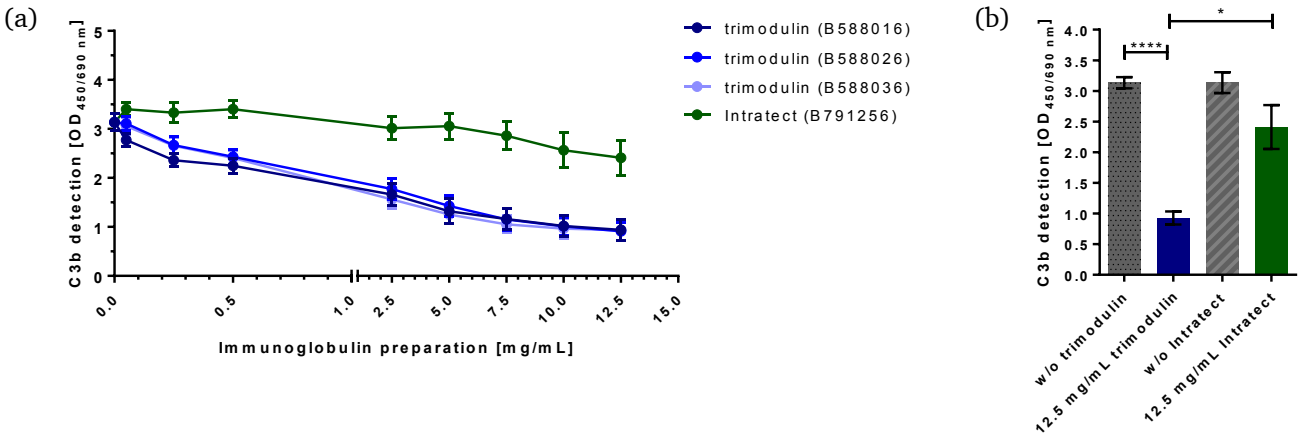


**Figure 10** Trimodulin inhibits the detection of C3b concentration-dependently. (a) A 96 well F bottom plate was coated with 0.1 µg/mL aggregated IgG (Intratect). After washing with TBS-T washing buffer, different dilutions of three batches trimodulin (blue) and Intratect (green; used as IVIg control) were distributed to the plate and mixed with 100-fold pre-diluted EDTA-plasma. After incubation for 1 h at 37 °C, an anti-human C3c antibody that is able to detect C3b and iC3b as well as a secondary goat anti-rabbit antibody (conjugated to HRP) were added. Finally, the plate was measured in an ELISA reader. Error bars indicate the standard error of the mean (SEM). Data represent results from six independent experiments performed in duplicates. (b) The highest used trimodulin and Intratect concentrations were compared with each other as well as with FB only (without (w/o) the products). Error bars indicate the SEM. Data represent results from six independent experiments performed in duplicates. The statistical analyses were performed using a Kruskal-Wallis test. Significance is shown as p-value: * $p \leq 0.05$ and **** $p \leq 0.0001$.

In order to analyze, if trimodulin is also able to reduce the C4b detection, an additional ELISA was performed. Figure 11 shows the detection of C4b on aggregated IgG after different concentrations of trimodulin and Intratect were added. Three batches of trimodulin (B588016, B588026 and B588036) were again compared in their ability to reduce the C4b detection. The detection of C4b was concentration-dependently decreased after the addition of trimodulin and all three used batches were highly comparable. The OD was reduced from 1.8 (w/o trimodulin) to approximately 0.4. In comparison to this, Intratect induced a strong increase in C4b detection in the lowest used concentration

(0.05 mg/mL) and the decrease started after the addition of 5 mg/mL Intratect. In order to compare the abilities of 12.5 mg/mL trimodulin to 12.5 mg/mL Intratect and to the appropriate FBs, a statistical analysis was performed (Figure 11). The difference between 12.5 mg/mL and trimodulin FB (w/o trimodulin) to reduce the C4b detection, was statistically significant. Moreover, the comparison of 12.5 mg/mL trimodulin and 12.5 mg/mL Intratect showed that the products were significantly different in their ability to decrease the C4b detection. Trimodulin can inhibit the detection of C4b stronger compared to Intratect.

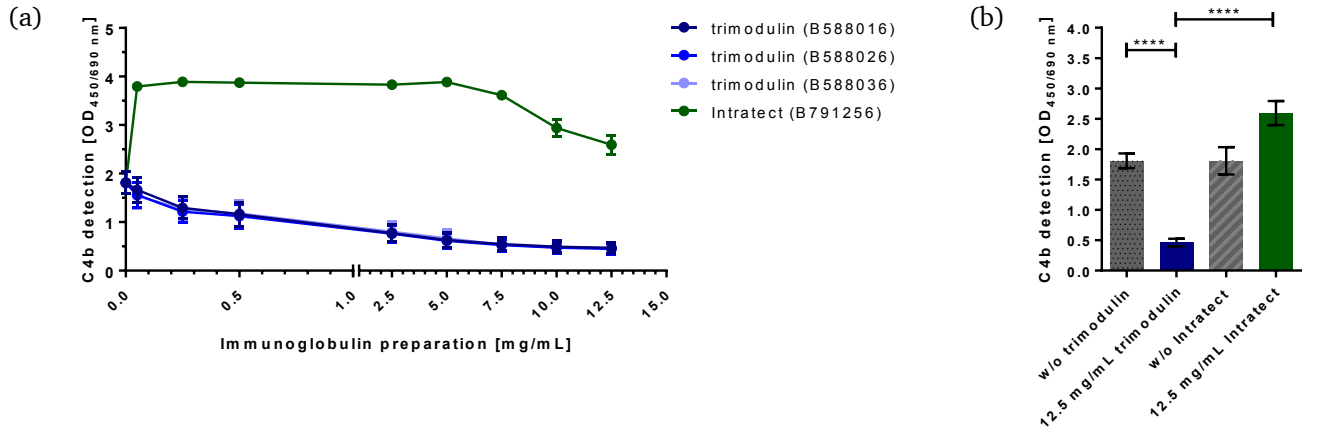


**Figure 11** Trimodulin inhibits the detection of C4b concentration-dependently. (a) A 96 well F bottom plate was coated with 0.1 µg/mL aggregated IgG (Intratect). After washing with TBS-T washing buffer, different dilutions of three batches trimodulin (blue) and Intratect (green; used as IVIg control) were distributed to the plate and were mixed with 100-fold pre-diluted EDTA-plasma. After incubation for 1 h at 37 °C, an anti-human C4c antibody that is able to detect C4b and iC4b as well as a secondary goat anti-rabbit antibody (conjugated to HRP) were added. Finally, the plate was measured in an ELISA reader. Error bars indicate the standard error of the mean (SEM). Data represent results from six independent experiments performed in duplicates. (b) The highest used trimodulin and Intratect concentrations were compared with each other as well as with FB only (without (w/o) the products). Error bars indicate the SEM. Data represent results from six independent experiments performed in duplicates. The statistical analyses were performed using a Kruskal-Wallis test. Significance is shown as p-value: **** $p \leq 0.0001$.

### 5.2.2. Analysis of the influence of IgM on C3b deposition

In order to determine, if the IgM fraction of trimodulin was responsible for the reduced C3b detection in the opsonin ELISA (see section 5.2.1), a fluid phase ELISA was performed. For this purpose, the supernatant of the opsonin ELISA was transferred to a second plate, coated with an anti-human C3c antibody (that is also able to bind C3b as well as iC3b) and the binding of IgM to C3b was detected with a mouse anti-human IgM antibody (Figure 12). The data revealed, the more trimodulin was added to the opsonin ELISA plate, the more IgM was able to bind to the C3b fragments in the supernatant, which was transferred to the fluid phase ELISA plate. Nevertheless, trimodulin incubated with $GVB^{++}$ instead of EDTA-plasma showed the same concentration-dependent increase in IgM detection as incubated with EDTA-plasma. It was suggested that the effect, seen after addition of the control (without EDTA-plasma), was due to an unspecific binding of trimodulin to the C3c coating in the absence of plasma. For this reason, it could not be assumed that the IgM fraction of trimodulin was mainly responsible for the binding of C3b in the fluid phase on the opsonin ELISA plate, which resulted in the reduced detection of C3b (see Figure 10).

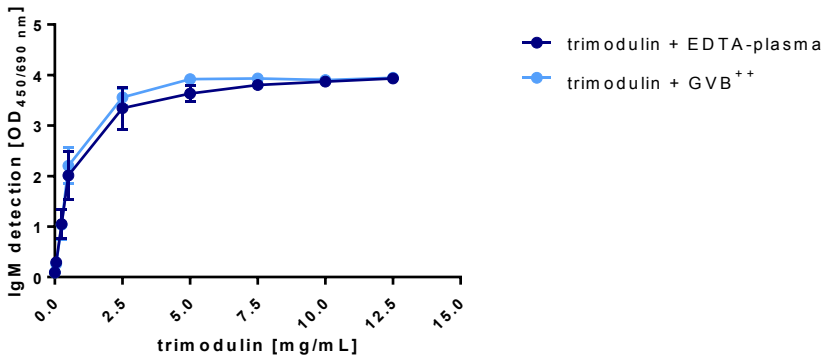


**Figure 12** Analysis of the IgM-C3b interaction using a fluid phase ELISA. The supernatant of the opsonin ELISA (see chapter 4.4.1) was transferred to a second plate coated with an anti-human C3c antibody and the binding of IgM to C3b was detected with a primary mouse anti-human IgM antibody and a secondary rabbit anti-mouse IgG antibody conjugated to HRP. In order to exclude unspecific binding of trimodulin (B588036) to the anti-C3c coating, trimodulin was incubated with $GVB^{++}$ instead of EDTA-plasma. After incubation of the plate for 1 h at 37 °C and the addition of the specific antibodies, the plate was measured in an ELISA reader. Error bars indicate the SEM. Data represents results from three independent experiments performed in duplicates.

### 5.2.3. Trimodulin covers activated complement factors in the ELISA setting

The opsonin ELISA revealed a concentration-dependent decrease in C3b and C4b detection after trimodulin addition. In order to analyze, if this was due to scavenging of the opsonins or to an overlay of trimodulin on the deposited complement factors, a SDS-PAGE and a subsequent Western blot analysis of the ELISA supernatants were performed (Figure 13). C3b (blue) as well as IgM (green) and IgG (red) were detected in the Western Blot analysis. The All Blue Prestained Protein Standard served as molecular weight marker (MW Marker) and was distributed to lane 1 and 12. It was used as standard for the determination of the sample size. In general, the IgG heavy chain was detected at ≈ 50 kDa and the light chain at ≈ 25 kDa. The bands in between were analyzed using mass spectrometry (PhD Thesis Fabian Bohländer) and show fragments of IgG. Bands at ≈ 80 kDa represent IgG heavy and light chains that were non-separated. Moreover, bands at ≈ 125 kDa show IgG molecules that were not reduced in the SDS-PAGE. The heavy chain of IgM was clearly detected at ≈ 75 kDa, whereas the bands at ≈ 60 kDa depict IgM fragments. Moreover, the alpha-chain of C3b is visible at ≈ 105 kDa, the iC3b alpha-chain at ≈ 65 kDa and in addition the C3b as well as iC3b beta-chain slightly at ≈ 75 kDa. Lane 2 was used as negative control for C3b detection consisting of 12.5 mg/mL trimodulin and $GVB^{++}$ without serum. The positive control for C3b detection (lane 3), containing serum and $GVB^{++}$, was used as 100% control for C3b detection and exhibits a band for the iC3b alpha-chain at ≈ 65 kDa. Lane 4 and 5 were also used as controls for pure C3b. The bands in lane 6-8 represent the EDTA-plasma samples from the opsonin ELISA (see 5.2.1), treated with 12.5 mg/mL (lane 6), 5 mg/mL (lane 7) and 0.05 mg/mL (lane 8) trimodulin. In the highest and the medium used trimodulin concentrations, the iC3b alpha-chain was not detectable. Just after addition of the lowest used trimodulin concentration a band became visible. This was also the case for lane 9-11, where Intratect-treated EDTA-plasma samples are displayed. No bands for the iC3b alpha-chain could be detected after the addition of 12.5 mg/mL (lane 9) as well as 5 mg/mL Intratect (lane 10). Just after the treatment with 0.05 mg/mL Intratect (lane 11), a band for iC3b was revealed.

These data were used to analyse, if a scavenging or the covering of C3b by trimodulin leads to its reduced detection in the ELISA assay. It is suggested that trimodulin rather covers and binds C3b deposited on aggregated IgG, because the supernatant contained no C3b in the highest as well as medium used trimodulin concentration (lane 6 and 7). For confirmation of the scavenging theory, which means the binding and removal of C3b in the fluid phase, the tested supernatant should have contained a high amount of C3b, when treated with a high amount of trimodulin. In the lowest used trimodulin concentration (0.05 mg/mL), a band for iC3b alpha-chain became visible. This leads to the assumption that the less trimodulin is available, the less C3b is pushed down to the aggregates and therefore a high amount of C3b is still in the supernatant, which is subsequently detected in the Western Blot analysis.

| Lane | Sample |
|---|---|
| 1 | MW Marker |
| 2 | Trimodulin 12.5 mg/mL + GVB$^{++}$ |
| 3 | EDTA-plasma + GVB$^{++}$ |
| 4 | Pure C3b 0.4 mg/mL |
| 5 | Pure C3b 0.2 mg/mL |
| 6 | Trimodulin 12.5 mg/mL + EDTA-plasma |
| 7 | Trimodulin 5 mg/mL + EDTA-plasma |
| 8 | Trimodulin 0.05 mg/mL + EDTA-plasma |
| 9 | Intratect 12.5 mg/mL + EDTA-plasma |
| 10 | Intratect 5 mg/mL + EDTA-plasma |
| 11 | Intratect 0.05 mg/mL + EDTA-plasma |
| 12 | MW Marker |

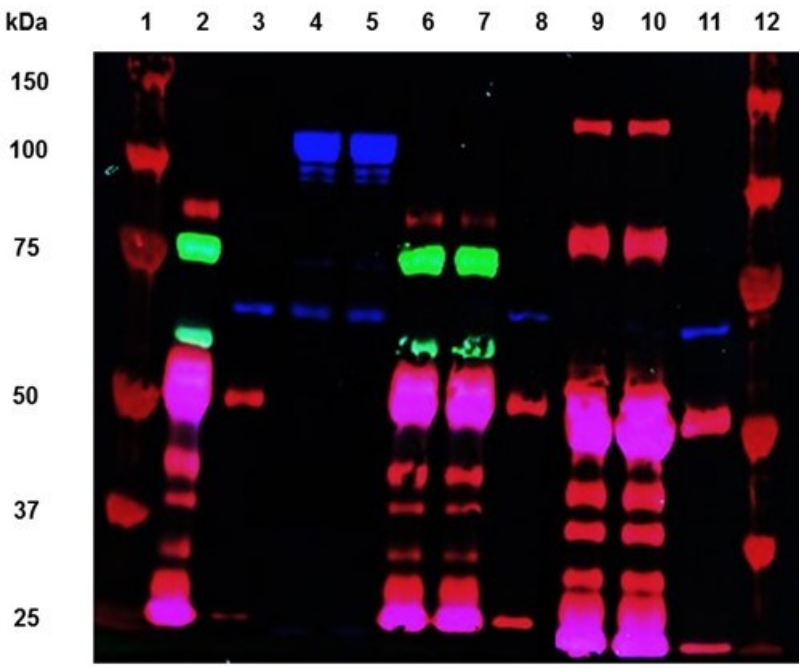


**Figure 13** SDS-PAGE and Western blot of the opsonin ELISA supernatant. An opsonin ELISA was performed as described in 4.4.1 and the supernatant was used for a subsequent SDS-PAGE and Western Blot analysis. As molecular weight (MW) marker the All Blue Prestained Protein Standard was added to lane 1 and 12. Lane 2 contained the negative control for C3b detection (12.5 mg/mL trimodulin + GVB$^{++}$). The positive controls for C3b detection (EDTA-plasma + GVB$^{++}$ as well as purified C3b) were distributed to lane 3-5. Lane 6-8 contained the plasma samples from the opsonin ELISA (described in 5.2.1) with low, medium and high trimodulin (B588036) concentrations and lane 9-11 the serum samples with low, medium and high Intratect concentrations (used as IVIg control). The Western Blot was scanned in a Typhoon imager and was analyzed with the software Image Quant TL. The green band at ≈ 75 kDa represents the heavy chain of IgM, whereas the green band at ≈ 60 kDa is an IgM fragment. The blue bands show the C3b alpha-chain at ≈ 105 kDa and the iC3b alpha-chain at ≈ 65 kDa. The C3b and iC3b beta-chains are weakly visible at ≈ 75 kDa. IgG is depicted in red with the heavy chain at ≈ 50 kDa and the light chain at ≈ 25 kDa. Between 50 kDa and 25 kDa fragments of IgG are detected. Moreover, non-reduced IgG is depicted at ≈ 125 kDa and non-separated heavy and light chains of IgG at ≈ 80 kDa. Data represent results from three independent experiments.

## 5.2.4. Interaction of trimodulin and anaphylatoxins

Besides the generation of opsonins after activation of the complement cascade, it is also important to control the amount of generated anaphylatoxins, to prevent complement-mediated cytotoxicity and inflammation. The opsonin ELISA showed a significant decrease of C3b and C4b detection after the addition of trimodulin (see 5.2.1). In order to determine, if trimodulin is also able to interact with C3a and C5a, an anaphylatoxin ELISA was established.

### 5.2.4.1. Detection of C5a using a trimodulin-coated plate

After trimodulin was coated to the plate in different dilutions, purified C5a was added, incubated and the plate was measured in an ELISA reader (Figure 14). In general, the detection of C5a was rather low, nevertheless a concentration-dependent decrease after the addition of trimodulin was observed. However, the incubation of trimodulin with only GVB$^{++}$ revealed the same detection and concentration-dependent decrease as with purified C5a. These results suggest that the used primary or secondary detection antibody bound unspecifically to trimodulin, which was coated to the plate. For this reason, it could not be distinguished, if the detected decrease of C5a was caused by the binding of trimodulin to this anaphylatoxin or if just the trimodulin coating was detected.

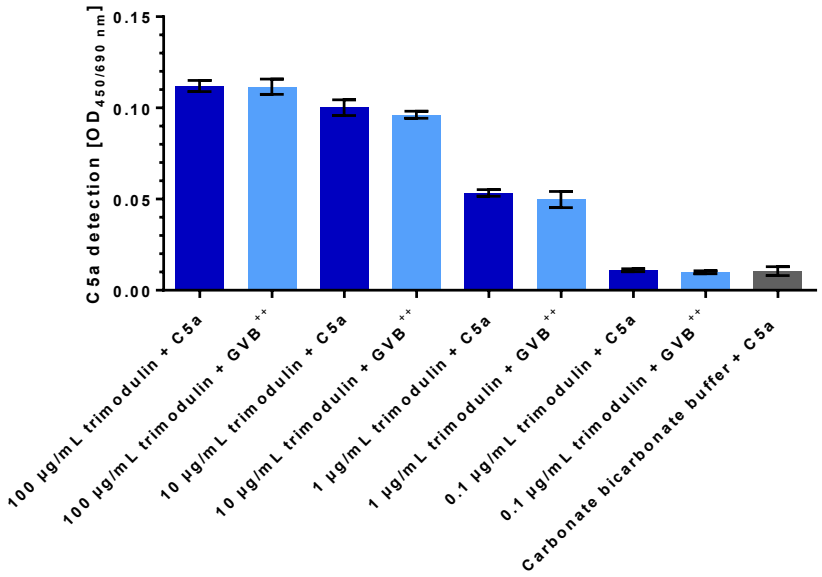


**Figure 14** Results of the anaphylatoxin ELISA using a trimodulin-coated plate. A 96 well F bottom plate was coated with 100 µL serially diluted trimodulin (B588036) and was incubated overnight at 2-8 °C. Carbonate bicarbonate buffer served as control for the specific binding of C5a to trimodulin. After washing, the plate was blocked with PBS containing 5% BSA as well as 0.1% Tween 20 and 50 µL of 350 ng/mL purified C5a was added to the wells. Additionally, $GVB^{++}$ instead of C5a was used as control for the unspecific binding of the primary anti-C5a antibody to trimodulin. The plate was incubated for 1 h at 37 °C, washed and after addition of the primary as well as secondary goat antibodies measured in an ELISA reader. Error bars indicate the SD. Data represent results from two independent experiments performed in duplicates.

#### 5.2.4.2. Detection of C5a and C3a after trimodulin addition using a zymosan-coated plate

Since the trimodulin-coated ELISA plate was unsuitable for the analysis of the trimodulin-anaphylatoxin interaction due to unspecific binding of the detection antibody to the coating, another setup was chosen. A zymosan-coated plate was used for the activation of the complement cascade and the generation of C3a as well as C5a in human EDTA-plasma. After transferring the supernatant containing the activated anaphylatoxins to a second plate coated with an anti-IgG, -IgA and -IgM antibody mix, trimodulin was added in different dilutions. Only the unbound C3a or C5a molecules were transferred to a third plate coated with specific anti-human C3a or C5a antibodies and detected in an ELISA reader (Figure 15). If trimodulin is able to bind and immobilize activated C3a or C5a on plate 2, then the anaphylatoxin detection on plate 3 would be reduced, compared to the control with trimodulin FB only. Figure 15a shows a high amount of generated C3a during the ELISA without the addition of trimodulin. The controls revealed that the detection antibody (anti-human C3a) did not bind to the anti-C3a coating unspecifically. Nevertheless, the addition of different dilutions of trimodulin as well as Intratect (used as IVIg control) did not induce a reduction of the C3a detection, which stayed high at ≈ OD 3.3.

Figure 15b shows the detection of C5a after the treatment with trimodulin and Intratect (used as IVIg control). In comparison to C3a, the generation of C5a was lower, but still well detectable without trimodulin (≈ OD 2.2). As described in Figure 15a for C3a, the C5a detection antibody did not bind to the anti-C5a coating unspecifically. After the addition of 0.65 $\mu$g/mL trimodulin, a slight decrease of C5a was visible. This decrease proceeded until a concentration of 22.22 $\mu$g/mL trimodulin. The difference between the OD of the 100% C5a control without trimodulin and the OD at 22.22 $\mu$g/mL trimodulin treatment was 0.85. Statistical analyses were performed using a Kruskal-Wallis test, because the data were not normally distributed, but revealed no significance. Moreover, in comparison to trimodulin, Intratect had no decreasing effects on the C5a detection.

These results suggests that trimodulin is able to slightly reduce activated C5a and can therefore influence the complement-mediated cytotoxicity triggered by this anaphylatoxin. The inhibition of C3a could not be detected in the described ELISA, which leads to the assumption that trimodulin can not bind to this anaphylatoxin and influences its activation.

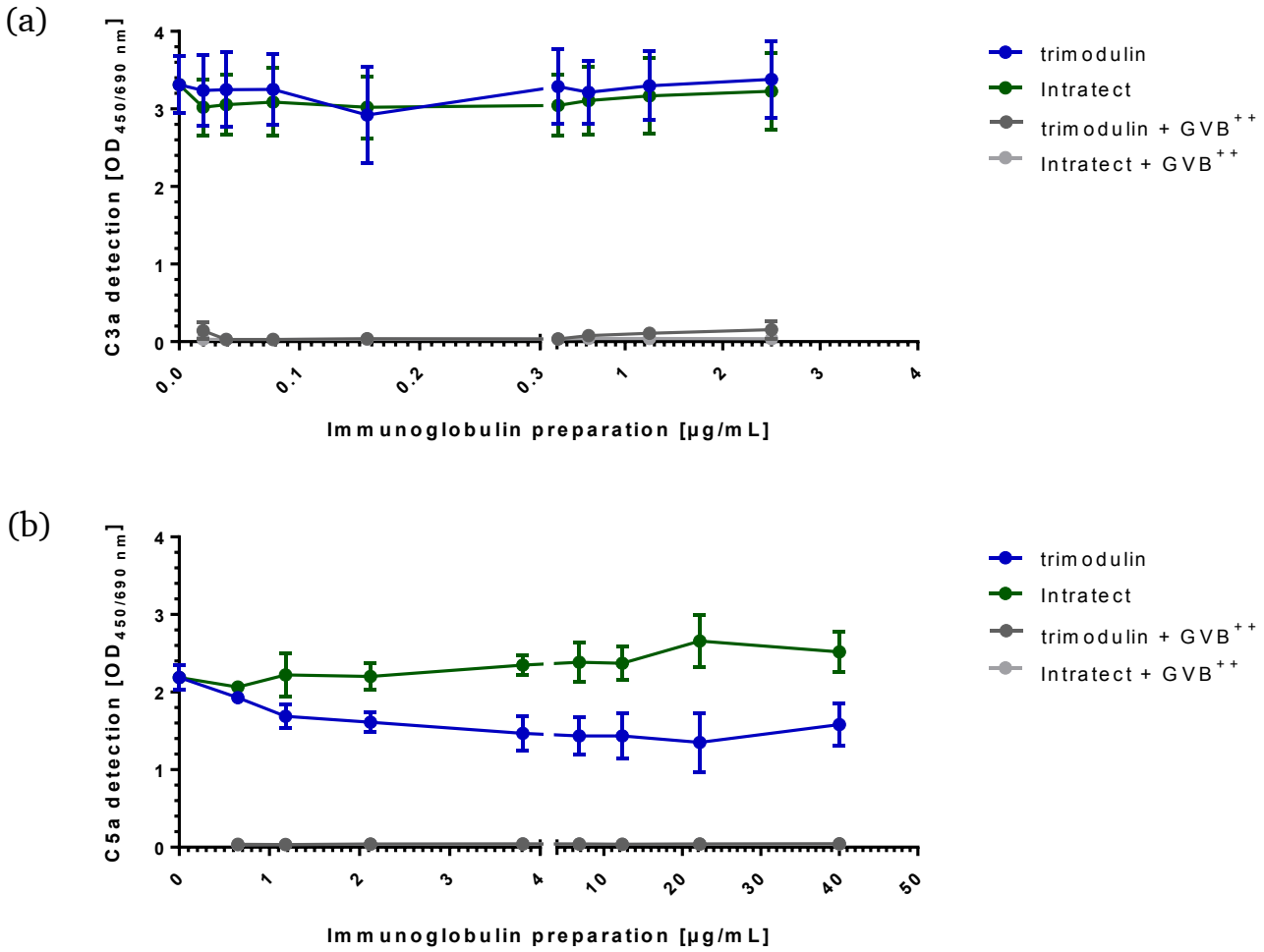


**Figure 15** Results of the anaphylatoxin ELISA using a zymosan-coated plate. One 96 well F bottom plate was coated with zymosan and another 96 well F bottom plate with an anti-human IgG/IgA/IgM antibody mix in carbonate bicarbonate buffer and incubated overnight at 2-8 °C. After washing, EDTA-plasma was added to the zymosan-coated plate for activation of the complement cascade and was incubated at 37 °C for 1 h. The supernatant was transferred to the anti-IgG/IgA/IgM-coated plate and was mixed with different dilutions of trimodulin (B588036). For immobilization and binding of C3a or C5a to trimodulin, the plate was again incubated for 1 h at 37 °C. Finally, the supernatant was transferred to a third plate, either coated with a specific anti-human C3a (a) or a specific anti-human C5a antibody (b) and measured in an ELISA reader at 450/690 nm. Error bars indicate the SEM. Data represent results from three independent experiments performed in duplicates.

## 5.2.5. Functional interaction of trimodulin with activated complement components

### 5.2.5.1. Trimodulin reduces the CDC of Ramos cells concentration-dependently

In order to confirm the previous results of the C3b/C4b ELISA in a biologically functional context and to investigate whether trimodulin can reduce CDC of Ramos cells through interaction with activated complement factors, a flow-cytometer-based CDC assay was used.

Initially, control experiments were performed, to determine the CD20 expression and the viability of the Ramos cells with and without the addition of Rituximab. Figure 16a shows the CD20 expression on Ramos cells (red line) in comparison to the unstained (filled grey area) and the isotype control

(dotted black line). After treatment with serial dilutions of Rituximab (Figure 16b) and 80% NHS, the CD20 expression obviously decreased from 98% to 19% and the viability from 92% to 22%. The previous results confirmed the suitability of the Ramos cells for the CDC assay.

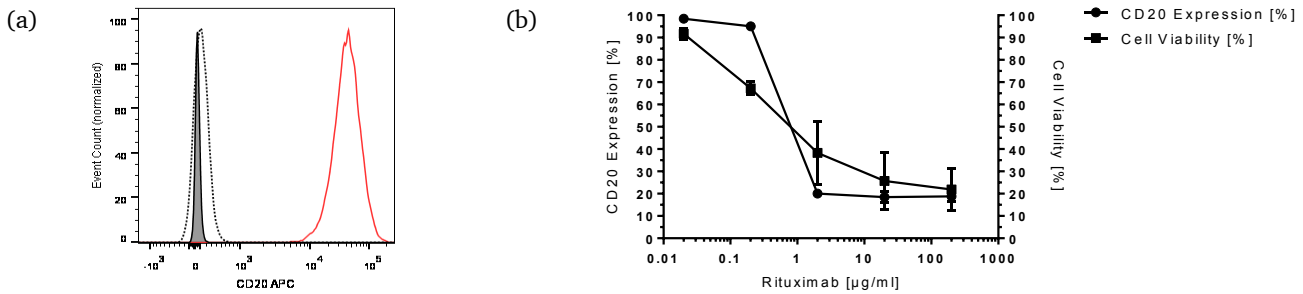


**Figure 16** CD20 expression on human Ramos cells. (a) Ramos cells ($5 \cdot 10^6$ cells/mL) were seeded to a V-bottom 96 well plate, diluted in assay buffer and stained with an anti-CD20 antibody and the appropriate isotype control. The expression of CD20 was measured in a flow cytometer. The filled grey area indicates the unstained Ramos cells, the dotted black line the isotype control and the red line the CD20 expression of the untreated cells. The data are representative for three independent experiments performed in duplicates. (b) Rituximab was serially diluted and incubated with 80% NHS and 50 µL Ramos cells ($5 \cdot 10^6$ cells/mL). After incubation, the cells were stained with PI as well as anti-CD20 antibody and measured in a flow cytometer. Error bars indicate the SD. Data represent results from three independent experiments performed in duplicates.

In order to examine the influence of trimodulin on complement activation and CDC of the Ramos cells, NHS and trimodulin were pre-incubated. Figure 17a shows the impact of trimodulin on CDC of the Ramos cells after pre-incubation with 80% NHS and subsequent addition of 160 $\mu$g/mL Rituximab. By addition of the FB control (without trimodulin), just 30% of the cells survived. In comparison to this, trimodulin reduced the CDC of the cells significantly in high concentrations. The survival of the cells increased concentration-dependent and was approximately 36% enhanced after the addition of 3.125 mg/mL trimodulin. In Figure 17b, the influence of Intratect as IVIg control was analyzed. Compared to the FB control, just the highest used concentration (6.25 mg/mL) induced a slight viability increase of the Ramos cells of about 7.8%. In total, the survival of the cells was up to 28% enhanced after the addition of trimodulin compared to Intratect.

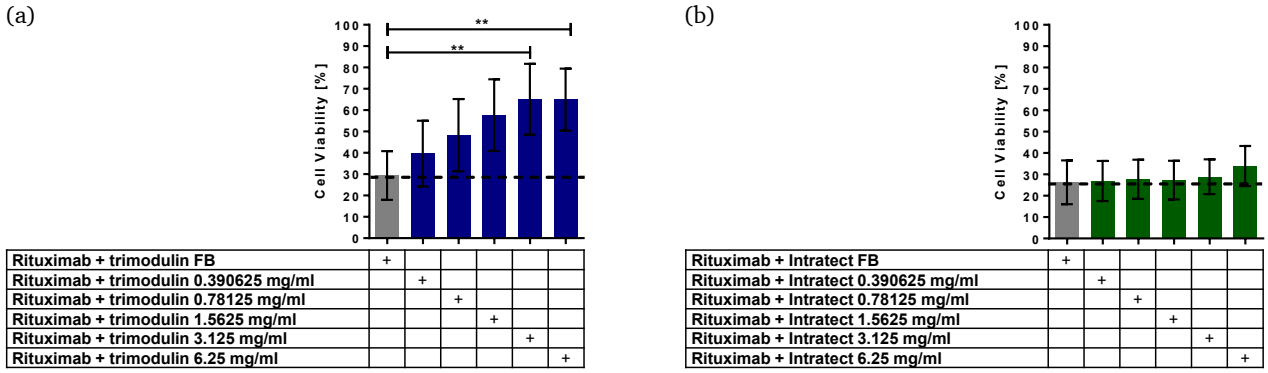


| | | | | | | |
|---|---|---|---|---|---|---|
| Rituximab + trimodulin FB | + | | | | | |
| Rituximab + trimodulin 0.390625 mg/ml | | + | | | | |
| Rituximab + trimodulin 0.78125 mg/ml | | | + | | | |
| Rituximab + trimodulin 1.5625 mg/ml | | | | + | | |
| Rituximab + trimodulin 3.125 mg/ml | | | | | + | |
| Rituximab + trimodulin 6.25 mg/ml | | | | | | + |

| | | | | | | |
|---|---|---|---|---|---|---|
| Rituximab + Intratect FB | + | | | | | |
| Rituximab + Intratect 0.390625 mg/ml | | + | | | | |
| Rituximab + Intratect 0.78125 mg/ml | | | + | | | |
| Rituximab + Intratect 1.5625 mg/ml | | | | + | | |
| Rituximab + Intratect 3.125 mg/ml | | | | | + | |
| Rituximab + Intratect 6.25 mg/ml | | | | | | + |

**Figure 17** Trimodulin reduces CDC of the Ramos cells after pre-incubation with NHS. (a) Trimodulin or (b) Intratect was pre-incubated with NHS and mixed with 20 µg/mL Rituximab as well as 50 µL Ramos cells ($5 \cdot 10^6$ cells/mL) on a 96 well plate. As control, the FB of the products was used to determine the base level of CDC. After incubation, the survival of the cells was measured by PI staining in a flow cytometer. Error bars indicate the SD. Data represent results from six independent experiments performed in duplicates. Statistical analyses were performed using a one-way ANOVA and a Bonferroni test. Significance is shown as p-value: ** $p \leq 0.01$. See Table 16 and Table 17 (appendix) for a detailed overview of the statistical analysis.

To analyze, if an additional pre-incubation step reduces or even inhibits the increasing effect of trimodulin regarding the cell viability of Ramos cells, Rituximab and the cells were pre-incubated simultaneously to the pre-incubation of trimodulin and NHS (see chapter 4.4.4.2, paragraph (2)). After that, both plates were pooled and the viability of the cells was monitored (Figure 18). As control, FB

without trimodulin was added and induced a survival of the cells of about 38% (Figure 18a). Compared to this, a concentration-dependent viability increase was induced by trimodulin addition. The highest used concentration (6.25 mg/mL) obviously enhanced the survival of the Ramos cells of about 22.7%. Figure 18b shows a small increasing effect on the cell viability of about 5.5% with the highest used Intratect concentration (6.25 mg/mL). In total, the survival was up to 17.2% enhanced after the addition of trimodulin compared to Intratect. In comparison to the results described in Figure 17, the increase in the cell viability was about 11% lower after the pre-incubation of Rituximab and the cells and the independent pre-incubation of trimodulin and NHS.

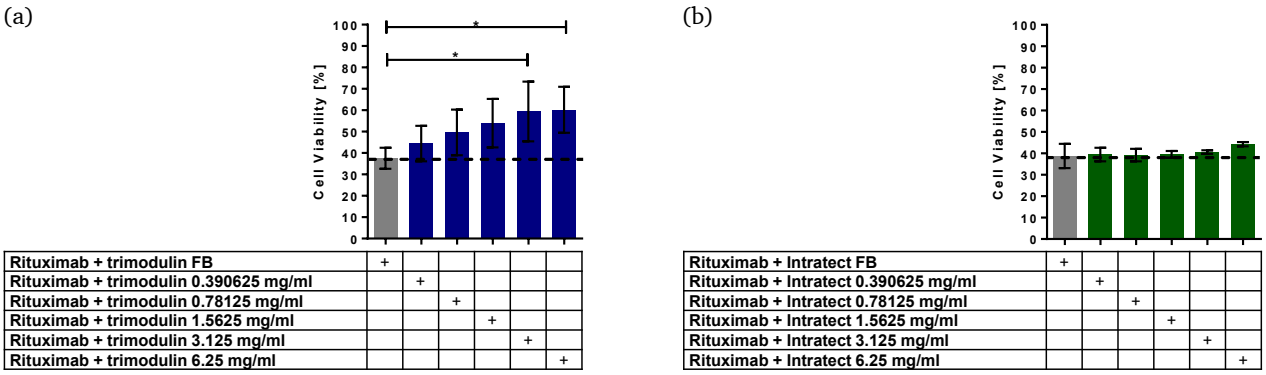


**Figure 18** Trimodulin still reduces the CDC of Ramos cells after an additional pre-incubation step. A pre-incubation step of trimodulin (a) or Intratect (b) with NHS and simultaneously of 20 µg/mL Rituximab and 50 µL Ramos cells/well ($5{\cdot}10^6$ cells/mL) was performed. After incubation, both plates were pooled, incubated and the survival of the cells was measured by PI staining in a flow cytometer. The FB of the products were used as control, to determine the base level of CDC. Error bars indicate the SD. Data represent results from five independent experiments performed in duplicates. Statistical analyses were performed using a one-way ANOVA and a Bonferroni test. Significance is shown as p-value: * $p \leq 0.05$. See Table 18 and Table 19 (appendix) for a detailed overview of the statistical analysis.

To analyze, weather the order of the incubation has an influence on the effect of trimodulin regarding CDC, all assay components were incubated simultaneously. Figure 19a shows a survival of 25% of the Ramos cells after treatment with the FB control. The viability increased concentration-dependently by the addition of serially diluted trimodulin until 40% in the highest used concentration (6.25 mg/mL). This was a significant change of about 15% in the CDC of the Ramos cells. The addition of Intratect FB induced 24.5% survival, whereas 6.25 mg/mL Intratect enhanced the viability of the Ramos cells about 13.3% (Figure 19b). The difference between the effect of trimodulin and Intratect in the highest used concentrations was 2.2%. Compared to the results described in Figure 17, trimodulin was not as effective in the inhibition of CDC after simultaneous incubation of the assay components. The highest viability increase in Figure 19a was 21% lower than the highest increase in Figure 17a.

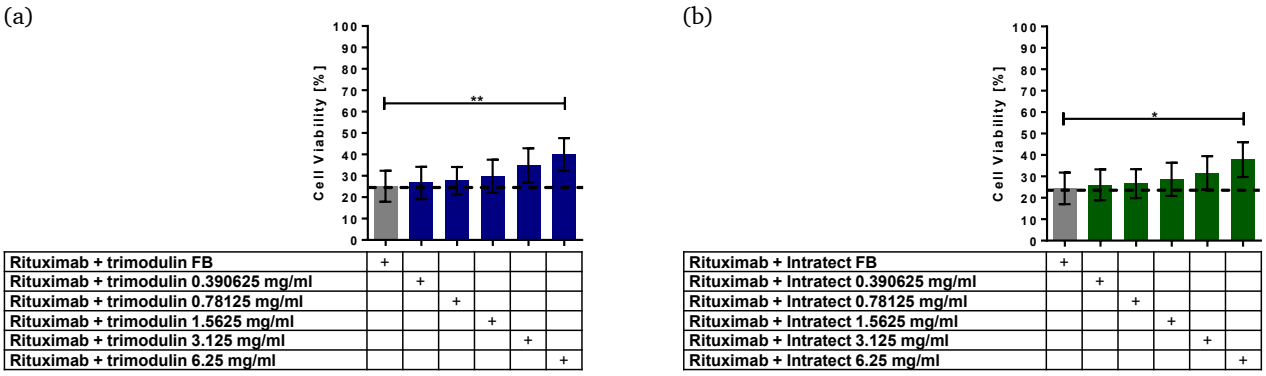


**Figure 19** The simultaneous incubation of all assay components reduces the influence of trimodulin on CDC of the Ramos cells. Trimodulin (a) or Intratect (b) was mixed with 20 µg/mL Rituximab, 80% NHS as well as 50 µL Ramos cells ($5{\cdot}10^6$ cells/mL) and incubated on a 96 well plate. The FB of the products were used to determine the base level of CDC. After incubation, the survival of the cells was measured by PI staining in a flow cytometer. Data represent results from six independent experiments performed

in duplicates. Statistical analyses were performed using a one-way ANOVA and a Bonferroni test. Significance is shown as p-value: ** $p \leq 0.01$ and * $p \leq 0.05$. See Table 20 and Table 21 (appendix) for a detailed overview of the statistical analysis.

In order to investigate, if trimodulin can interact with Rituximab and thereby inhibit the binding to CD20 which could lead to enhanced cell viability, both products were pre-incubated. There was no increasing effect regarding the Ramos cell viability compared to the other tested settings. The highest used trimodulin concentration (6.25 mg/mL) enhanced the survival of the cells significantly about 15% compared to the FB control (Figure 20a). The addition of 6.25 mg/mL Intratect (Figure 20b) increased the cell viability from 40.5% (FB control) to 50.3%. These results showed a 21% lower effect of 6.25 mg/mL trimodulin on CDC of the Ramos cells, compared to Figure 17a.

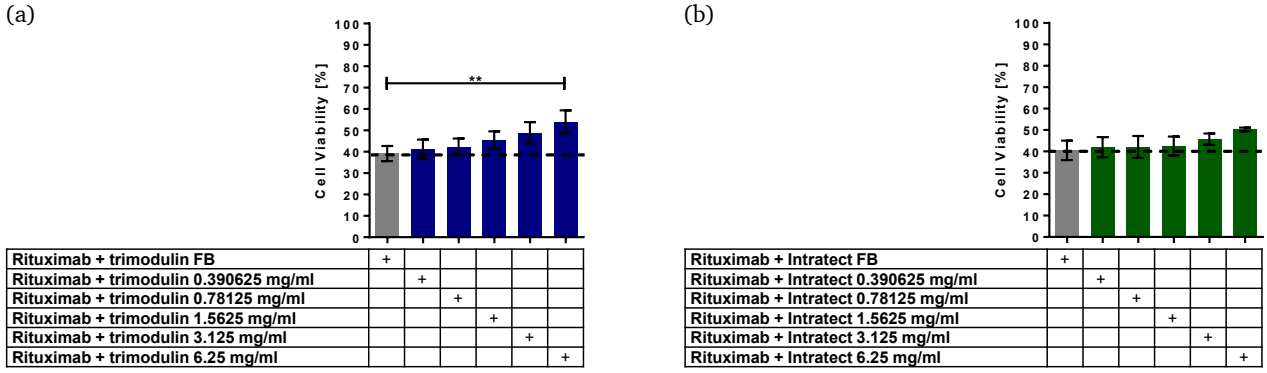


| | | | | | | |
|---|---|---|---|---|---|---|
| Rituximab + trimodulin FB | + | | | | | |
| Rituximab + trimodulin 0.390625 mg/ml | | + | | | | |
| Rituximab + trimodulin 0.78125 mg/ml | | | + | | | |
| Rituximab + trimodulin 1.5625 mg/ml | | | | + | | |
| Rituximab + trimodulin 3.125 mg/ml | | | | | + | |
| Rituximab + trimodulin 6.25 mg/ml | | | | | | + |

| | | | | | | |
|---|---|---|---|---|---|---|
| Rituximab + Intratect FB | + | | | | | |
| Rituximab + Intratect 0.390625 mg/ml | | + | | | | |
| Rituximab + Intratect 0.78125 mg/ml | | | + | | | |
| Rituximab + Intratect 1.5625 mg/ml | | | | + | | |
| Rituximab + Intratect 3.125 mg/ml | | | | | + | |
| Rituximab + Intratect 6.25 mg/ml | | | | | | + |

**Figure 20** Trimodulin does not influence the binding of Rituximab to CD20. Trimodulin (a) or Intratect (b) was pre-incubated with 20 µg/mL Rituximab on a 96 well plate. Subsequently, they were mixed with 80% NHS as well as 50 µL Ramos cells ($5 \cdot 10^6$cells/mL). The FB of the products were used as control, to determine the base level of CDC. After incubation, the survival of the cells was measured by PI staining in a flow cytometer. Error bars indicate the SD. Data represent results from three independent experiments performed in duplicates. Statistical analyses were performed using a one-way ANOVA and a Bonferroni test. Significance is shown as p-value: ** $p \leq 0.01$. See Table 22 and Table 23 (appendix) for a detailed overview of the statistical analysis.

To determine if the inhibition of CDC by trimodulin is due to a functional interaction with activated complement factors or due to a blocking of the complement cascade through an unspecific CD20 overlay by IgM, IgA or IgG, control experiments were performed. Figure 21 shows the viability and the CD20 expression of the Ramos cells after trimodulin (Figure 21a) and Intratect (Figure 21b) addition. The CD20 expression as well as the survival of the cells stayed high, about 98% and 94% for both products, and did not change concentration-dependently. Furthermore, the subsequent addition of Rituximab induced nearly the same CDC as shown in Figure 19, where all components were incubated simultaneously and did not lead to an increased cell viability of the Ramos cells (see appendix Figure 28). These results confirmed that trimodulin did not interact with CD20 and inhibited the binding of Rituximab to this surface antigen.

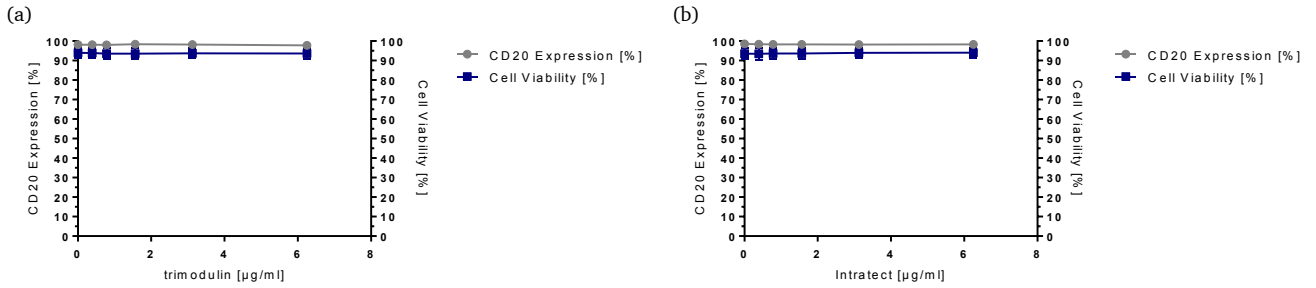


**Figure 21** Trimodulin does not interact with CD20 on Ramos cells. Trimodulin (a) or Intratect (b) was mixed with assay buffer, 80% NHS as well as 50 µL Ramos cells ($5 \cdot 10^6$ cells/mL) and incubated on a 96 well plate. The FB of the products were used as a control, to determine the base level of CDC. After incubation, the survival of the cells was measured by PI staining in a flow cytometer. Data represent results from three independent experiments performed in duplicates.

## 5.3. Concentration-dependent activation of the opsonophagocytosis of pathogens by trimodulin

The analyses described in 5.2 showed a concentration-dependent effect of trimodulin on the complement cascade that resulted in reduced CDC. It was suggested that this was caused by the binding as well as by the inhibition of complement factors in high trimodulin doses. In general, the control of the complement system is an important function to prevent the excessive activation of the immune system in an inflammatory environment, which can lead to tissue damage and multiple organ failure. Nevertheless, it is also necessary to protect the body against invading pathogens like bacteria, viruses and fungi, by mechanisms, like CDC or phagocytosis that require the activation of the complement cascade. In the following OPAs it was analyzed, if trimodulin is able to activate the complement system that opsonizes bacterial cells and to induce the subsequent phagocytosis of the pathogens. Initially, the phenotype of the differentiated HL-60 cells was characterized and the titration of IgG/IgM depleted NHS was performed prior to the use in the different OPAs.

### 5.3.1. Characterization of the HL-60 cell phenotype after differentiation for use in the OPA

Differentiated neutrophil-like HL-60 cells were used as effector cells in the OPA. Their differentiation status after three days as well as their Fcγ receptor expression for a successful induction of the opsonophagocytosis by Igs was monitored prior to use. Therefore, the expression of Fcγ as well as of the complement receptors was examined by screening the surface antigens in the FACS. For this purpose, differentiated HL-60 cells were incubated with antibodies that bind to the low (CD16), the medium (CD32) and the high (CD64) affinity receptors for IgG. Moreover, an anti-CD11b antibody was used to detect the CR3 on the differentiated cells. To control the differentiation status, an anti-CD35 antibody that binds to CR1, which is highly expressed on differentiated neutrophils, as well as an anti-CD71 antibody that is specific for neutrophilic progenitor cells, was incubated with the HL-60 cells (Figure 22). For using the HL-60 cells in the OPA, they should exhibit a high CD35 and a low CD71 expression. Unstained cells served as control and the specific isotype controls were added.

The detection of the Fcγ receptors showed an expression of 34.9% CD16 and 99.8% CD32, whereas CD64 expression was only slightly detected (7.9%). In addition, the complement receptors CD11b (CR3) as well as CD35 (CR1) were strongly expressed by differentiated HL-60 cells, whereas CD71 was not detected.

These data suggests that the differentiated HL-60 cells express Fcγ as well as the complement receptors, which are necessary to induce the phagocytosis of pathogenic cells after binding of IgG or opsonins. Furthermore, the high expression of CD35 as well as the absence of CD71 shows a successful differentiation. For that reason, the Ramos cells were assessed to be suitable for the OPA assay.

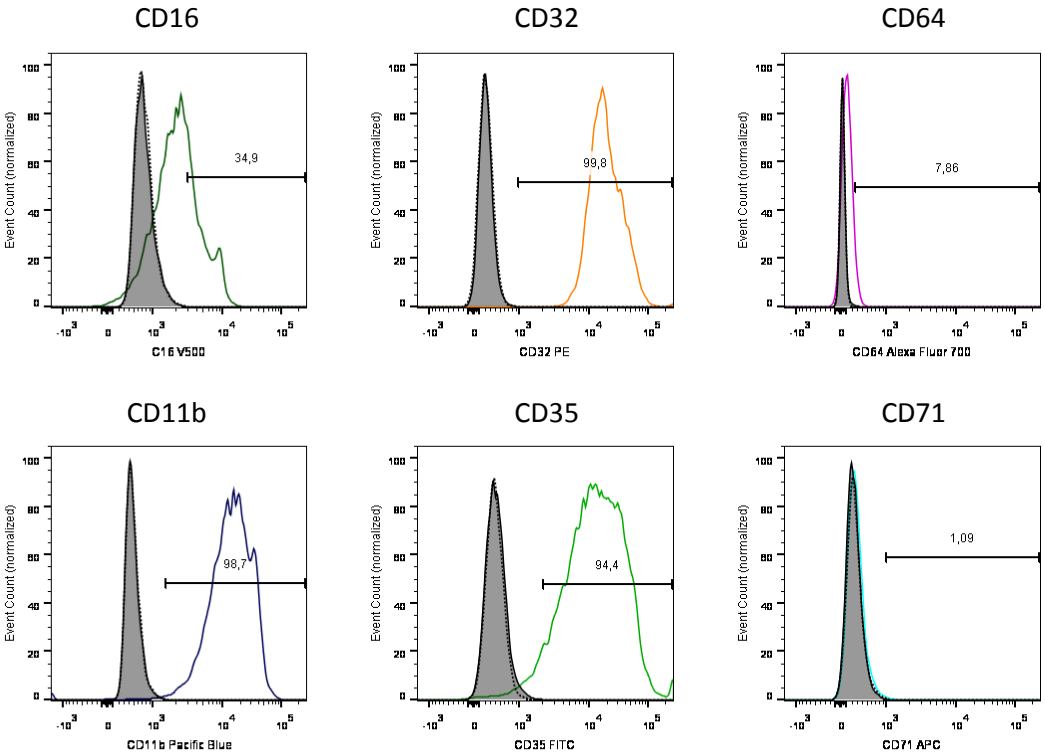


**Figure 22** Phenotype characterization of differentiated HL-60 cells. After differentiation, HL-60 cells were incubated with anti-CD16, anti-CD32, anti-CD64, anti-CD11b, anti-CD35 and anti-CD71 antibodies. As control, undifferentiated cells were used and the specific isotype controls were added to the wells. The expression of the surface receptors was measured in a flow cytometer. The filled grey area indicates the unstained HL-60 cells, the dotted black line the particular isotype control and the colored lines the individual receptor expressions of the differentiated cells. Dark green = CD16 expression, orange = CD32 expression, pink = CD64 expression, dark blue = CD11b expression, light green = CD35 expression and turquoise = CD71 expression. The data are representative for two experiments performed in duplicates.

### 5.3.2. Serum titration for use in the *E. coli* (K12) OPA

In order to analyze the effect of trimodulin in activating complement and induce the opsonophagocytosis of *E. coli* (K12), an OPA was developed. As complement source for the OPA, IgG/IgM depleted NHS (NHS minus) was used and analyzed in the CH50 test (see 5.1). Initially, the serum was titrated prior to use (Figure 23), to determine the appropriate concentration. Different concentrations of NHS minus were tested for their ability to induce the killing of *E. coli*. It was important to find a balance between a concentration of NHS minus that did not entirely kill the bacteria by itself (non-specific killing) and a concentration that was not as low as the Igs were not able to activate the complement system anymore. It was primarily in the focus, to examine if the addition of trimodulin could amplify the activation of the complement system and therefore the complement-mediated phagocytosis of *E. coli*, compared to Intratect (used as IVIg control). Figure 23 shows the bacterial survival [%] of *E. coli* after the addition of undifferentiated or differentiated HL-60 cells, active or inactive NHS minus and trimodulin FB. The data were normalized to control A comprised of bacteria, undifferentiated HL-60 cells, hi NHS minus as well as FB, which served as 100% control for bacterial survival. Approximately 25% less bacterial survival was seen compared to control A, after the addition of differentiated instead of undifferentiated cells. The addition of active serum in different concentrations induced 100% killing in the highest used concentrations (2%-10%), whereas 7% of the *E. coli* bacteria survived after 1% NHS minus addition. The lower the concentration of NHS minus was chosen, the higher was the survival of the bacterial cells. Moreover, it must paid attention that control C did not induce the same bacterial survival as control B without active complement, because otherwise the concentration of NHS was too low to be activated. 0.8% and 0.7% NHS minus were therefore tested

by addition of trimodulin or Intratect as IVIg control for their complement activity (see appendix Figure 29). After that, 0.8% NHS minus was found to be the optimal concentration for the OPA. Trimodulin did not further activate the complement system by addition of 0.7% NHS minus, whereas the killing of the bacteria was stronger compared to control C with 0.8% NHS minus when incubated together with low concentrations of trimodulin.

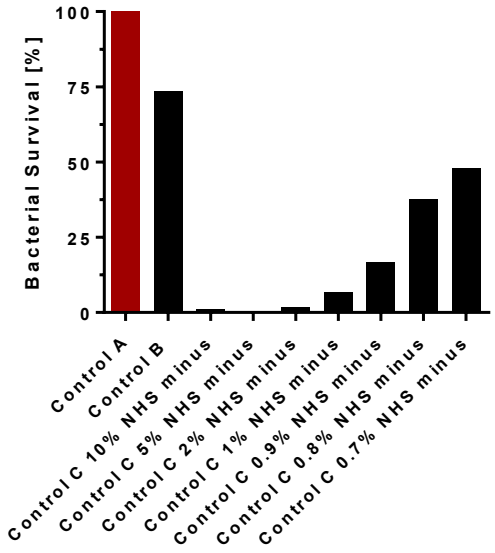


| Sample | Composition |
|---|---|
| Control A | Bacteria, undifferentiated HL-60 cells, hi NHS minus, FB |
| Control B | Bacteria, differentiated HL-60 cells, hi NHS minus, FB |
| Control C | Bacteria, differentiated HL-60 cells, NHS minus, FB |

**Figure 23** Titration of IgG/IgM depleted serum for use in the OPA. Initially, OB was prepared and 20 µL transferred to the appropriate wells of a 96 well U-bottom plate. 3 µL of trimodulin FB was added to the wells. Differentiated as well as undifferentiated HL-60 cells were counted and resuspended to $1 \cdot 10^7$ cells/mL. One vial of the cryopreserved *E. coli* assay stock was rapidly thawed in a water bath, centrifuged at 12000 x g for 2 min and washed with 1 mL OB. After additional centrifugation, the supernatant was removed and the pellet resuspended in 0.5 mL OB. The bacteria were 4000-fold diluted in 10 mL OB, 10 µL was added to the wells of the 96 well plate and the plate was incubated for 30 min at RT under shaking. In the meantime, the HL-60 cells were mixed with IgG/IgM depleted NHS (NHS minus) or hi IgG/IgM depleted NHS and OB for serum titration. After incubation, 50 µL of the HL-60 cell and NHS minus mix was distributed to the 96 well plate and was again incubated at 37 °C for 45 min. To stop the phagocytic process, the plate was placed on ice for 20 min, before 5 µL per well was distributed in triplets on a LB agar plate. The plates were incubated overnight in a 37 °C incubator and the CFU counted manually on the next day. The data were analyzed with GraphPad Prism, after determination of CFU/mL with Excel and the bacterial survival [%] was determined by normalization of the data. Control A served as 100% control for bacterial survival. Data represent results from two independent experiments performed in duplicates.

### 5.3.3. The *E. coli* (K12) OPA is suitable for investigating phagocytosis, but not for analyzing the opsonophagocytic activity induced by trimodulin

After the appropriate serum concentration for the *E. coli* OPA was determined in pre-experiments (see 5.3.2), the opsonophagocytosis of the bacteria induced by trimodulin (B588039) was analyzed. Therefore, the OPA was performed with all controls as well as the samples (trimodulin or Intratect) described in 4.5.2.. Initially, *E. coli* was pre-incubated with trimodulin (B588039) to enable the binding of the Igs before NHS minus as well as the HL-60 cells were added. After activation of the complement cascade, the covering of the bacterial surface by opsonins (opsonization) in general causes the enticement of effector cells and the subsequent opsonophagocytosis. As control, trimodulin was incubated with the components in the absence of NHS minus, to determine the ADCC, which is induced by antibodies and effector cells only. In addition, bacteria that were treated with hi NHS minus, as well as with undifferentiated HL-60 cells and trimodulin FB, were used as 100% control for the *E.coli* survival. The control, consisting of bacteria, hi NHS minus, differentiated HL-60 cells and trimodulin FB only, determined the direct killing of the *E. colis* by binding to TLRs on the neutrophils. Moreover, another control was used (bacteria, differentiated HL-60 cells, IgG/IgM depleted NHS and trimodulin FB) to

define the complement activity without Ig addition by the alternative pathway, which also leads to the opsonophagocytosis of pathogens and induces CDC.

Figure 24 shows the phagocytosis of *E. coli* bacteria by trimodulin. The growth of the bacteria is representatively seen in Figure 24a, where control D1-D6 (composed of the bacteria, hi NHS minus, differentiated HL-60 cells and the different used concentrations of trimodulin) was distributed to an LB agar plate. By counting the CFUs, a concentration-dependent increase in the bacterial survival was seen after trimodulin addition. The highest used trimodulin concentration (control D1 with 1810 $\mu$g/mL trimodulin) induced the slightest growth (11 CFUs), whereas 24 CFUs were counted after addition of 0.181 $\mu$g/mL trimodulin (control D5). In Figure 24b, the bacterial survival [CFU/mL] of the *E. colis* was calculated and analyzed after addition of all controls and the samples. Control A, which was used as 100% control, showed the highest viability of the bacteria with approximately $2.6 \cdot 10^8$ CFU/mL. Compared to this, the survival of the cells was slightly lower in control B (composed of the bacteria, hi NHS minus, differentiated HL-60 cells and FB), whereas control C (composed of the bacteria, NHS minus, differentiated HL-60 cells and FB) induced a survival of only $9 \cdot 10^7$ CFU/mL. A concentration-dependent increase of the viability was triggered after addition of trimodulin and incubation with hi NHS minus (light blue; control D1-D6) that was also seen in Figure 24a. Trimodulin was able to induce the phagocytosis without complement, triggered by the direct binding of Igs to the HL-60 cells. Moreover, the lowest viability was detected after 1810 $\mu$g/mL and the highest after 0.0181 $\mu$g/mL trimodulin addition. Trimodulin induced a different progression of the viability, when incubated together with active NHS depleted of IgG/IgM (dark blue). In the highest used concentration (1810 $\mu$g/mL) a high bacterial survival was detected, which correlates with low complement activity. The lower the concentration of trimodulin, the lower was the viability of the *E. coli* bacteria. In the lowest used concentration (0.0181 $\mu$g/mL), a slight increase in the survival was detected. Nevertheless, there was no significant difference between control C (w/o trimodulin) that showed high non-specific killing and the addition of 1.81 $\mu$g/mL trimodulin (dark blue), which induced the lowest bacterial survival. These data suggest that trimodulin is able to induce the phagocytosis of *E. coli*, but the opsonophagocytic capacity of trimodulin could not be detected. Moreover, it was shown that trimodulin inhibits the complement activation in high concentrations. However, the SD of the samples was too high to distinguish between assay variations and real effects induced by trimodulin.

(a)


(b)

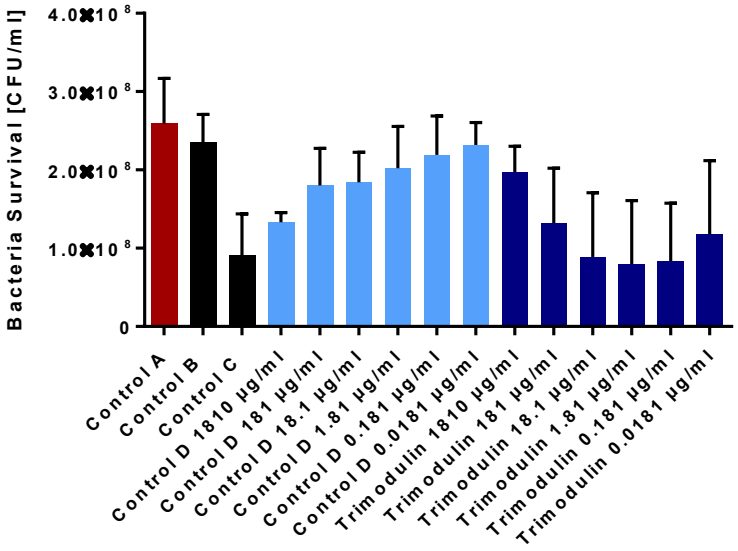


| Sample | Composition |
|---|---|
| Control A | Bacteria, undifferentiated HL-60 cells, hi NHS minus, FB |
| Control B | Bacteria, differentiated HL-60 cells, hi NHS minus, FB |
| Control C | Bacteria, differentiated HL-60 cells, NHS minus, FB |
| Control D | Bacteria, differentiated HL-60 cells, hi NHS minus, immunoglobulin preparation |
| Sample | Bacteria, differentiated HL-60 cells, NHS minus, immunoglobulin preparation |

**Figure 24** Trimodulin induces the phagocytosis of *E. coli* (K12) bacteria and is able to inhibit complement activation concentration-dependently. Trimodulin (B588039) and *E. coli* bacteria were pre-incubated on a 96 well U-bottom plate for 30 min at RT. After that, NHS depleted of IgG/IgM as well as HL-60 cells were added, mixed and were incubated for additional 45 min at 37 °C. (a) The plate was put on ice for 20 min and 5 µL of every well were distributed in triplets to LB agar plates for overnight incubation at 37 °C. The distribution of control D1-D6 (composed of the bacteria, hi NHS minus, differentiated HL-60 cells and the different used concentrations of the Ig preparations) is representative for the whole assay procedure and shows the growth of the bacterial cells. The CFUs were counted and the data was analyzed using GraphPad Prism. (b) Control A served as 100% control for bacterial survival [CFU/mL], control B determined the direct killing of the cells via binding of *E. coli* to the TLRs, control C was used to examine the activation of complement without Ig addition and control D showed the ADCC induced by trimodulin and HL-60 cells only. Trimodulin was 10-fold serially diluted (1810 µg/mL to 0.0181 µg/mL) to monitor concentration-dependent effects. Error bars indicate the SD. Data represent results from three independent experiments performed in triplicates. Statistical analyses were performed by using a Kruskal-Wallis test and are given in Table 26 and Table 27 (appendix).

To compare the effect of an IVIg and an IgM-/IgA-enriched preparation, Intratect was also tested in the OPA. The controls and the used concentrations of the samples were the same as described in 4.5.2. Figure 25 shows the opsonophagocytosis of *E. coli* induced by Intratect. The bacterial survival [CFU/mL] was calculated with Excel and was analyzed by the use of GraphPad Prism. Control A (the 100% survival control for *E. coli*) showed the highest viability with approximately $3.5 \cdot 10^8$ CFU/mL. Control B (composed of the bacteria, hi NHS minus, differentiated HL-60 cells and FB), which was used to monitor the direct killing of the bacteria by differentiated HL-60 cells without the addition of serum or the Ig preparations, a slight decrease of the bacterial survival was seen. Compared to this, control C (w/o trimodulin), which was used to determine the non-specific killing of the *E. colis* by NHS minus, induced a viability of only $8.6 \cdot 10^7$ CFU/mL. Moreover, Control D (Figure 25; light green; composed of the bacteria, hi NHS minus, differentiated HL-60 cells and the different used concentrations of Intratect) was compared to control D with different trimodulin concentrations (Figure 24). This comparison exhibited a higher total increase of approximately $2.5 \cdot 10^7$ CFU/mL in the survival of the cells by the addition of control D with Intratect (Figure 25), contrary to control D where trimodulin was added (approximately $1 \cdot 10^7$ CFU/mL; see Figure 24). The addition of active NHS minus (dark green) induced the same concentration-dependent progression of the bacterial viability as with hi NHS depleted of

IgG/IgM (light green). Nevertheless, the decrease of the survival was stronger with active, compared to inactive NHS minus. The highest used concentration of Intratect (1810 $\mu$g/mL) induced the lowest cell viability, which was due to high complement activity. Compared to control C that caused high non-specific killing, the difference was not significant. These data suggest that Intratect can also induce the phagocytosis as well as opsonophagocytosis of *E. coli* bacteria, but does not lead to a reduced complement activity in high concentrations. In addition, the SD of the samples treated with active NHS minus was again too high to distinguish between assay variations and real effects induced by Intratect.

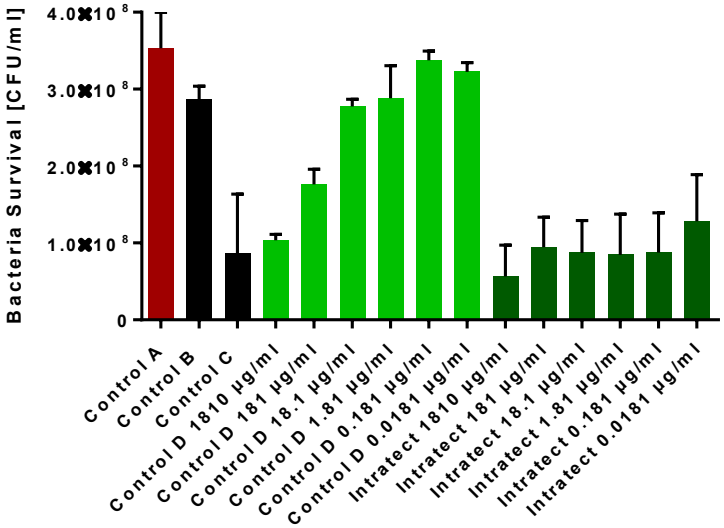


| Sample | Composition |
|---|---|
| Control A | Bacteria, undifferentiated HL-60 cells, hi NHS minus, FB |
| Control B | Bacteria, differentiated HL-60 cells, hi NHS minus, FB |
| Control C | Bacteria, differentiated HL-60 cells, NHS minus, FB |
| Control D | Bacteria, differentiated HL-60 cells, hi NHS minus, immunoglobulin preparation |
| Sample | Bacteria, differentiated HL-60 cells, NHS minus, immunoglobulin preparation |

**Figure 25** Intratect (used as IVIg control) induces the opsonophagocytosis of *E. coli* (K12), but does not inhibit complement activation concentration-dependently. Intratect and *E. coli* bacteria were pre-incubated on a 96 well U-bottom plate for 30 min at RT. After that, NHS depleted of IgG/IgM as well as HL-60 cells were added, mixed and were incubated for additional 45 min at 37 °C. The plate was put on ice for 20 min and 5 µL of every well were distributed in triplets to LB agar plates for overnight incubation at 37 °C. The CFUs were counted and the data was analyzed using GraphPad Prism. Control A served as 100% control for bacterial survival [CFU/mL], control B determined the direct killing of the cells via binding of *E. coli* to the TLRs, control C was used to examine the activation of complement without Ig addition and control D showed the ADCC induced by Intratect and HL-60 cells only. Intratect was 10-fold serially diluted (1810 µg/mL to 0.0181 µg/mL) to monitor concentration-dependent effects. Error bars indicate the SD. Data represent results from two independent experiments performed in triplicates. Statistical analyses were performed by using a Kruskal-Wallis test and are given in Table 28 and Table 29 (appendix).

### 5.3.4. Serum titration for use in the *S. aureus* bioparticles OPA

In the *E. coli* OPA, trimodulin induced an inhibition of the complement system, but the opsonophagocytic capacity regarding the bacteria could not be detected. This was caused by the high non-specific killing of the serum (control C) while trimodulin was not able to further activate the complement system. Moreover, the SD of the samples treated with active NHS was too high to distinguish between real effects and assay variations. Therefore, a FACS-based method was applied to reduce the high assay variations caused by the manually counting of the *E. colis* as well as to determine the non-specific killing of the serum in another setting. This additional OPA was could be evaluated in a flow cytometer, using *S. aureus* bioparticles conjugated to Alexa Fluor 488 instead of living *E. coli* bacteria. For this purpose, IgG/IgM depleted NHS was titrated prior to use in the assay, to find the appropriate concentrations. The HL-60 cell number and the concentration of the bioparticles were initially tested by

Fabian Bohländer (PhD thesis; data not shown) and were adopted in this OPA. Different serum concentrations were analyzed in preliminary experiments (0.6%, 1.2%, 1.5%) and 1.2% was regarded as best concentration (see appendix Figure 30). Trimodulin was able to activate the complement system by using 0.6% NHS minus. Nevertheless, a stronger activation was seen by using 1.2% NHS minus. 1.5% serum triggered a high complement-mediated phagocytosis of the bacteria, whereby only a slight increase in the opsonophagocytosis of *E. coli* was detected after trimodulin addition.

### 5.3.5. The *S. aureus* bioparticles OPA is suitable for analyzing the opsonophagocytosis induced by trimodulin

In order to analyze the ability of trimodulin to initiate the opsonophagocytosis of *S. aureus* bioparticles, an additional OPA was performed. Differentiated HL-60 cells were mixed with the bioparticles, NHS minus as well as trimodulin or Intratect (as IVIg control) was added and incubated for 45 min at 37 °C. The controls were the same as described in 5.3.3. In addition, untreated HL-60 cells were used to determine the background fluorescence without bacteria. After incubation, the cells were quenched with 0.2% trypan blue solution to delete the fluorescence of bacteria that were not phagocytosed and did unspecifically bind to the surface of the effector cells. Finally, the plate was measured in a flow cytometer and the phagocytic index was determined. Figure 26 shows the opsonophagocytosis of *S. aureus* bioparticles induced by trimodulin. The background fluorescence of the untreated HL-60 cells as well as of control A was negligible, because there was almost no fluorescence detectable. Control B (composed of the bioparticles, hi NHS minus, differentiated HL-60 cells and FB) showed a slight phagocytic index, which was due to the direct phagocytosis of the bacteria by the differentiated HL-60 cells. After the addition of the highest used trimodulin concentration (20 mg/mL) to hi NHS minus (control D composed of the bioparticles, hi NHS minus, differentiated HL-60 cells and 20 mg/mL trimodulin; light blue), which was used to determine the IgG-mediated phagocytosis of 20 mg/mL trimodulin, the phagocytic index was approximately $1.2 \cdot 10^7$. Compared to this, the values increased by the addition of lower trimodulin concentrations and reached the maximum at 1 mg/mL trimodulin. Furthermore, a strong decrease of the phagocytic index was detected by addition of lower trimodulin concentrations, with a minimum at 0.01 mg/mL. It was suggested that the values, detected in the high trimodulin concentrations (20-1 mg/mL), were caused by an inhibition of the phagocytosis. Moreover, control C (w/o trimodulin), which was used for the detection of the *S.aureus* phagocytosis induced by NHS minus only, showed a phagocytic index of approximately $1.5 \cdot 10^7$. After the addition of trimodulin and incubation with active NHS minus (dark blue), a strong increase of the phagocytic index was induced, with a maximum ($2.3 \cdot 10^7$) at 1 mg/mL trimodulin. The values of the phagocytic index decreased by addition of lower concentrations (0.5-0.01 mg/mL trimodulin). Finally, the statistical analysis revealed that the highest effect, caused by 1 mg/mL trimodulin, induced a significantly different phagocytic index, compared to control C (composed of the bioparticles, NHS minus, differentiated HL-60 cells and FB). In addition, the phagocytic index, induced by trimodulin without active NHS minus (control D 1mg/mL), was significantly lower in comparison to 1 mg/mL trimodulin with active NHS minus. It was assumed that the phagocytic indices that were detected in the range of 20-1 mg/mL, were caused by inhibitory effects of trimodulin regarding the opsonophagocytosis of *S. aureus* bioparticles. Table 14 as well as Table 15 give an overview of the differences between the trimodulin samples and controls in detail. The phagocytic indices of control D (w/o trimodulin) were subtracted from the phagocytic indices of the trimodulin samples and the significance shown as p-value (**** $p \leq 0.0001$) (Table 14). In Table 15, the differences of the phagocytic indices of the trimodulin samples and control C are depicted and the significances shown as p-value (* $p \leq 0.05$; *** $p \leq 0.001$; **** $p \leq 0.0001$). These data indicate that trimodulin is able to induce the phagocytosis and significantly increases the opsonophagocytosis of the bioparticles in the presence of active serum. Moreover, trimodulin can also inhibit the uptake of the bacteria in high concentrations.

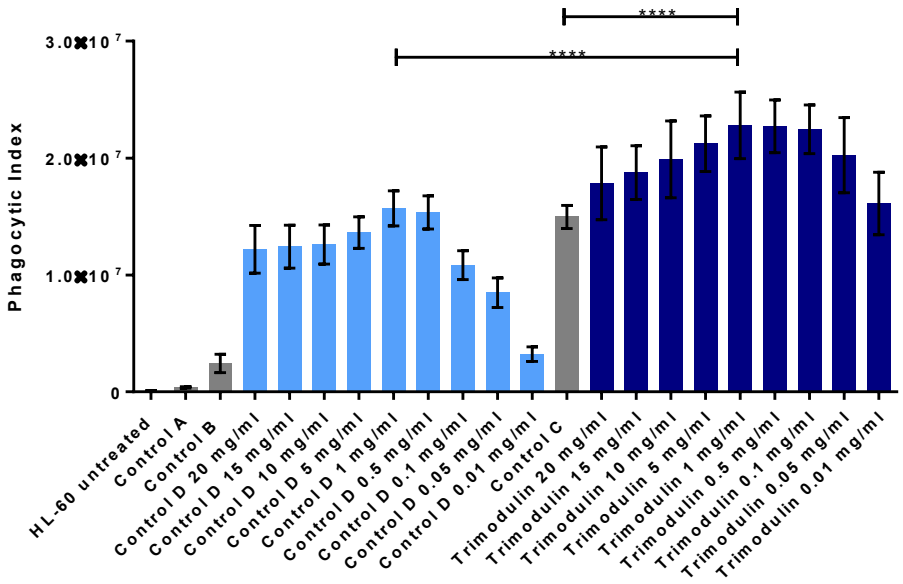


| Sample | Composition |
|---|---|
| Control A | Bacteria, undifferentiated HL-60 cells, hi NHS minus, FB |
| Control B | Bacteria, differentiated HL-60 cells, hi NHS minus, FB |
| Control C | Bacteria, differentiated HL-60 cells, NHS minus, FB |
| Control D | Bacteria, differentiated HL-60 cells, hi NHS minus, immunoglobulin preparation |
| Sample | Bacteria, differentiated HL-60 cells, NHS minus, immunoglobulin preparation |

**Figure 26** Trimodulin induces the concentration-dependent opsonophagocytosis of *S. aureus* bioparticles. Differentiated HL-60 cells, *S. aureus* bioparticles, NHS depleted of IgG/IgM as well as trimodulin (B588039) and the appropriate FB were mixed and incubated at 37 °C for 45 min. After that, the cells were quenched with 0.2% trypan blue solution and were subsequently analyzed by using a flow cytometer. The phagocytic index was calculated and the data depicted in a bar diagram using excel and GraphPad Prism. Control A served as 100% control for the bacteria, control B determined the direct phagocytosis of the cells via binding of *E. coli* to the TLRs, control C was used to examine the activation of complement without Ig addition and control D showed the ADCC induced by trimodulin and HL-60 cells only. Different dilutions of trimodulin were used to monitor concentration-dependent effects. Error bars indicate the SD. Data represent results from six independent experiments performed in duplicates. Statistical analyses were performed using a one-way ANOVA and a Bonferroni test. Significance is shown as p-value: **** $p \leq 0.0001$.

**Table 14** Comparison of the phagocytic index of trimodulin samples without active NHS minus (control D) with trimodulin samples after the addition of active NHS minus. Statistical analyses were performed using a one-way ANOVA and a Bonferroni test. Significance is shown as p-value: **** $p \leq 0.0001$.

| Trimodulin concentration | Phagocytic index control D | Phagocytic index trimodulin samples | Difference (trimodulin sample – control D) | Significance (p-value) |
|---|---|---|---|---|
| 20 mg/mL | $1.2 \cdot 10^7$ | $1.8 \cdot 10^7$ | $6 \cdot 10^6$ | **** |
| 15 mg/mL | $1.2 \cdot 10^7$ | $1.9 \cdot 10^7$ | $7 \cdot 10^6$ | **** |
| 10 mg/mL | $1.3 \cdot 10^7$ | $2.0 \cdot 10^7$ | $7 \cdot 10^6$ | **** |
| 5 mg/mL | $1.4 \cdot 10^7$ | $2.1 \cdot 10^7$ | $7 \cdot 10^6$ | **** |
| 1 mg/mL | $1.6 \cdot 10^7$ | $2.3 \cdot 10^7$ | $7 \cdot 10^6$ | **** |
| 0.5 mg/mL | $1.5 \cdot 10^7$ | $2.3 \cdot 10^7$ | $8 \cdot 10^6$ | **** |
| 0.1 mg/mL | $1.1 \cdot 10^7$ | $2.2 \cdot 10^7$ | $1.1 \cdot 10^7$ | **** |
| 0.05 mg/mL | $9.0 \cdot 10^6$ | $2.0 \cdot 10^7$ | $1.1 \cdot 10^7$ | **** |
| 0.01 mg/mL | $3.0 \cdot 10^6$ | $1.6 \cdot 10^7$ | $1.3 \cdot 10^7$ | **** |

**Table 15** Comparison of the phagocytic index of control C (without trimodulin) with the samples after trimodulin addition. Statistical analyses were performed using a one-way ANOVA and a Bonferroni test. Significance is shown as p-value: * $p \leq 0.05$, *** $p \leq 0.001$ and **** $p \leq 0.0001$.

| Phagocytic index control C | Trimodulin concentration | Phagocytic index trimodulin samples | Difference (trimodulin sample – control C) | Significance (p-value) |
|---|---|---|---|---|
| $1.5 \cdot 10^7$ | 20 mg/mL | $1.8 \cdot 10^7$ | $3 \cdot 10^6$ | * |
| | 15 mg/mL | $1.9 \cdot 10^7$ | $4 \cdot 10^6$ | *** |
| | 10 mg/mL | $2.0 \cdot 10^7$ | $5 \cdot 10^6$ | **** |
| | 5 mg/mL | $2.1 \cdot 10^7$ | $6 \cdot 10^6$ | **** |
| | 1 mg/mL | $2.3 \cdot 10^7$ | $8 \cdot 10^6$ | **** |
| | 0.5 mg/mL | $2.3 \cdot 10^7$ | $8 \cdot 10^6$ | **** |
| | 0.1 mg/mL | $2.2 \cdot 10^7$ | $7 \cdot 10^6$ | **** |
| | 0.05 mg/mL | $2.0 \cdot 10^7$ | $5 \cdot 10^6$ | **** |
| | 0.01 mg/mL | $1.6 \cdot 10^7$ | $1 \cdot 10^6$ | ns |

In order to compare the ability of an IgM-/IgA-enriched preparation to induce the opsonophagocytosis of *S. aureus* bioparticles with an IVIg, Intratect was used in the assay. The IgG preparation was initially pre-diluted in FB to the same IgG concentration as trimodulin (≈ 56%). After that, controls and samples were similarly diluted as described in 4.5.3. Figure 27 shows the opsonophagocytosis of the *S. aureus* bioparticles caused by Intratect. Compared to Figure 26, the background fluorescence was also negligible, as the untreated HL-60 cells as well as control A showed almost no fluorescence. In addition, control B (composed of the bioparticles, hi NHS minus, differentiated HL-60 cells and FB), which indicates the phagocytosis of the bacteria by the direct binding to TLRs of the HL-60 cells, was comparable to Figure 26. Control D (light green; composed of the bioparticles, hi NHS minus, differentiated HL-60 cells and Intratect) that was used to determine the effect of Intratect without active NHS minus, increased the phagocytic index to a maximum of $1.1 \cdot 10^7$ (0.056 mg/mL Intratect), whereas lower concentrations decreased the values concentration-dependently. Moreover, control C (composed of the bioparticles, NHS minus, differentiated HL-60 cells and FB)exhibited a phagocytic index of approximately $1.5 \cdot 10^7$, which was also comparable to Figure 26. The addition of Intratect (dark green) induced no increase in high concentrations (11.2-2.8 mg/mL), whereas a maximum phagocytic index ($2.3 \cdot 10^7$) was detected at 0.028 mg/mL Intratect that was again comparable to the effect of trimodulin (seen in Figure 26). By addition of the lowest used Intratect concentration (0.0056 mg/mL), the value of the phagocytic index decreased. Finally, the statistical analysis revealed that the highest effect, caused by 0.028 mg/mL Intratect induced a significantly different phagocytic index, compared to control C that was used to determine the phagocytosis triggered by NHS minus only. In addition, the phagocytic index, induced by Intratect without active NHS minus (control D 0.056 mg/mL), was significantly lower in comparison to 0.028 mg/mL trimodulin with active NHS minus. It was assumed that the phagocytic indices that were detected in the range of 11.2-0.56 mg/mL, were caused by an inhibition of the *S. aureus* opsonophagocytosis. The opsonophagocytic capacity of Intratect was comparable to the effects caused by trimodulin.

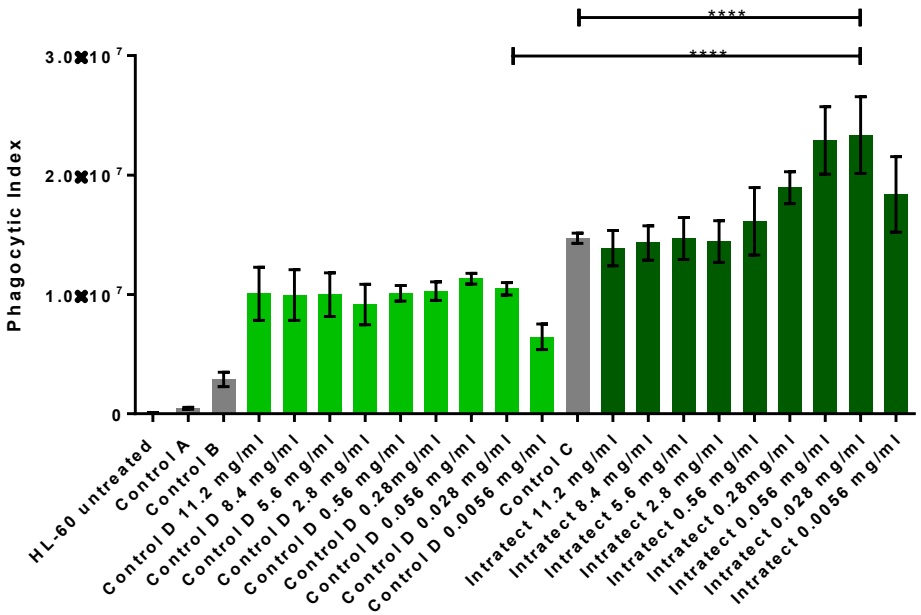


| Sample | Composition |
|---|---|
| Control A | Bacteria, undifferentiated HL-60 cells, hi NHS minus, FB |
| Control B | Bacteria, differentiated HL-60 cells, hi NHS minus, FB |
| Control C | Bacteria, differentiated HL-60 cells, NHS minus, FB |
| Control D | Bacteria, differentiated HL-60 cells, hi NHS minus, immunoglobulin preparation |
| Sample | Bacteria, differentiated HL-60 cells, NHS minus, immunoglobulin preparation |

**Figure 27** Intratect induces the concentration-dependent opsonophagocytosis of *S. aureus* bioparticles. Differentiated HL-60 cells, *S. aureus* bioparticles, NHS depleted of IgG/IgM as well as Intratect (as IVIg control) and the appropriate FB were mixed and were incubated at 37 °C for 45 min. After that, the cells were quenched with 0.2% trypan blue solution and were subsequently analyzed by using a flow cytometer. The phagocytic index was calculated and the data depicted in a bar diagram using excel and GraphPad Prism. Control A served as 100% control for the bacteria, control B determined the direct phagocytosis of the cells via binding of *E. coli* to the TLRs, control C was used to examine the activation of complement without Ig addition and control D showed the ADCC induced by Intratect and HL-60 cells only. Different dilutions of Intratect were used to monitor concentration-dependent effects. Error bars indicate the SD. Data represent results from five independent experiments performed in duplicates. Statistical analyses were performed using a one-way ANOVA and a Bonferroni test. Significance is shown as p-value: **** $p \leq 0.0001$. See Table 30 and Table 31 (appendix) for a detailed overview of the statistical analysis.

## 6. Discussion

In the 19th century, von Behring and Kitasato discovered for the first time antibody molecules in the serum of immunized rabbits that destroyed or neutralized virulent tetanus bacteria in mice, which obtained this immune serum[194]. These findings signed the beginning of the modern therapeutic Ig treatment[195]. Today it is known that antibodies exhibit a broad spectrum of functions, supporting the immune system to fight infections[44,74]. IVIg preparations, comprised of high amounts of polyvalent IgG molecules pooled from thousands of healthy donors, are primarily used as replacement therapy for patients with immunodeficiencies, but also for the treatment of autoimmune and inflammatory disorders[150–152,196]. Both, antimicrobial as well as immunomodulatory effects are of high relevance, to find a balance between activation and inhibition of the immune system. Especially the complement system has a dual role in health and disease. On the one hand, it is responsible for the protection of the host against pathogens by activating complement factors leading to the destruction of microorganisms, but on the other hand it triggers many inflammatory effects that can be harmful to the host by an uncontrolled activation[9,197]. Inflammation is mainly caused by anaphylatoxins, but also opsonins, like the fragments C3b, C4b and iC3b, can induce damage due to excessive and continuous activation of the complement system. Therefore, this system has to be tightly regulated. Basta *et al*. already reported that Igs have the ability to activate but also to inhibit the complement system concentration-dependently[11].

In this PhD thesis, the ambivalent effects of the IgM- and IgA-enriched Ig preparation trimodulin regarding complement activation and inhibition were evaluated. Initially, the ability of trimodulin to bind and inhibit the deposition of the activated opsonins C3b as well as C4b on aggregated IgG was characterized. For this purpose, an ELISA was established, which was based on the studies of Rieben *et al.*[99,166]. It was shown that trimodulin was responsible for the concentration-dependent decrease in the detection of the complement factors C3b and C4b. The highest used concentrations of trimodulin had the strongest effect in reducing the detection of the opsonins (see Figure 10). In comparison, the addition of Intratect, used as IVIg control, was not as effective as trimodulin in inhibiting the detection of deposited C3b and C4b. Only a slight decrease in the C3b detection occurred, whereas the amount of detected C4b even increased in low concentrations before a decrease was detectable in high concentrations. The interaction of the complement system with high-dose IVIg preparations was already seen in various studies of Basta *et al*. They reported the binding of C3b as well as C4b to IgG molecules and the prevention of opsonin deposition on target cells[94,95,198]. In addition, Rieben *et al*. determined the capacity of different Ig preparations (IVIg, IgM-enriched, IgA-enriched as well as IgM- and IgA-enriched preparations) regarding complement inhibition by using an ELISA and measuring the deposition of the complement factors C3, C4 and C1q on aggregated IgG. They also detected a reduced deposition of the factors after the addition of IVIg, IgM-enriched as well as IgM- and IgA-enriched preparations and reported that IgM-enriched Ig preparations were more efficient in the inhibition of complement than IVIgs, whereas IgA had no inhibitory capacity[99,166]. Moreover, Roos *et al.* demonstrated that IgM-enriched Ig preparations have an up to 10 times stronger complement inhibitory capacity than IVIg preparations, seen in experiments were the hyperacute rejection of pig xenografts in primates was prevented by complement inhibition through Ig preparations[98]. Trimodulin, which consists of approximately 56% IgG, 21% IgA and 23% IgM, was also more potent in the reduction of complement deposition in the opsonin ELISA than Intratect as IVIg control (see Figure 10 and Figure 11). The IgM molecules of trimodulin, are able to bind to activated complement components and therefore contribute to the strong inhibitory capacity seen after trimodulin addition[11]. Moreover, the main component of trimodulin is IgG that is also able to bind and inhibit activated complement factors. This composition makes trimodulin a more potent inhibitor compared to IVIgs like Intratect. Moreover, the pentameric structure of serum IgM in trimodulin is able to bind complement factors in a higher amount at the same time, compared to the monomeric IgG molecules[60]. It is suggested that the higher avidity of IgM also contributes to the stronger efficacy of trimodulin to complement factors compared to Intratect. It was seen that the decrease in the C3b level (≈ OD 2.4) was higher as compared to the decrease in the C4b level (≈ OD 1.4) after the addition of trimodulin. This might be due to the generally lower amount of factor C4 in serum (approximately 100-400 mg/mL), which is cleaved to C4b as well as C4a. C3, which is processed to C3b and C3a, has an

approximate serum concentration of about 900-1800 mg/mL[199]. The increase of C4b (≈ OD 2) in the low Intratect concentrations (compared to the serum control) could be due to an activation of the complement system by the Ig preparation. Compared to Intratect, no increase in C4b was detectable after the addition of trimodulin in low concentrations. Complement needs two or more IgG molecules in a specific distance to each other for the binding of C1q and activation of the classical pathway[45]. Compared to this, IgM molecules must change their confirmation for C1q binding from the planar secreted (= "star") to the "staple" form. This mechanism takes place when IgM binds to antigens on the surface of target cells[200]. It is suggested that in the opsonin ELISA IgM did not change its confirmation in the presence of only aggregated IgG molecules compared to the presence of target cells, therefore was not able to activate the complement system and only its inhibitory capacity was detected in the ELISA setting. Moreover, after the addition of Intratect to the EDTA-plasma on the 96 well plate, a high generation of C4b compared to C3b was detected. C4b is only produced during classical and lectin pathway activation, whereas C3b is also generated in the alternative pathway[12]. In general, it is known that aggregated IgG, IgA or IgM molecules activate the complement system via the alternative pathway[201]. In the ELISA setting, the alternative pathway is already activated when C3 binds to the aggregated IgG coating. Therefore, the generation of C3b was assumed to be completed before Intratect was added and no increase of C3b compared to C4b could be detected.

Rieben *et al.* demonstrated that the inhibition of the complement system by using Ig preparations is not caused by excessive complement activation and associated consumption of the complement factors[99]. It is rather discussed if the mechanism of complement inhibition is due to the scavenging (= binding and removal) of the activated complement factors from the site of inflammation[94,95,99,102,198,202]. To investigate, which Ig subclass was mainly responsible for the reduced C3b as well as C4b detection and to determine if this inhibition was due to a scavenging of the factors, a fluid phase ELISA was established. The analysis revealed the more trimodulin was added, the more IgM bound to C3b in the fluid phase and was detected on a second ELISA plate coated with an anti-human C3c antibody (that is also able to detect C3b as well as iC3b). However, the negative control (w/o EDTA-plasma) detected a non-specific binding of IgM to the coating or to the plate and therefore the assay was unsuitable for the determination of the mechanism as well as of the Ig subclass responsible for the inhibition of complement factors (see Figure 12). In general, problems with the specificity of an ELISA are well known challenges[203]. Non-specific binding of Igs causes false positive results, induced for example by Ig preparations that directly bind to the polystyrene surface of the plate due to non or inadequate blocking or to the blocking agent itself[204–206]. For this reason, a Western Blot analysis of the opsonin ELISA supernatant was performed, where IgG, IgM and C3b (as well as iC3b and C3c) were detected in order to determine whether scavenging of the opsonins by Ig preparations caused the reduced complement detection. It was clearly seen that just the treatment with 0.05 mg/mL trimodulin or Intratect revealed a band for the iC3b alpha chain, compared to higher (12.5 mg/mL as well as 5 mg/mL) trimodulin or Intratect concentrations (see Figure 13). The assumption for the scavenging theory, which means the binding and removal of the activated complement factors by Igs, was a detection of high C3b (iC3b/C3c) amounts and at the same time high amounts of the Ig preparation in the Western Blot analysis. The more trimodulin or Intratect was added, the more C3b (iC3b/C3c) should be detected. Since this was not the case (no C3b was detected in high Ig concentrations), it is suggested that the inhibitory effect, which was seen in the opsonin ELISA measured by reduced C3b concentrations, was not due to a scavenging of this opsonin. It is rather supposed to be caused by a binding and covering as well as an associated retention of the complement factors on the opsonin ELISA plate by the Ig preparations. In the opsonin ELISA setting, the molecular weight of the Ig molecules seems to play a role for the decreased detection of C3b as well as C4b. After the cleavage of the complement factors upon their activation, they may be directly bound by the Ig preparations and pushed down to the coating. Because IgM in its pentameric form has a molecular weight of 990 kDa compared to the IgG monomers with a molecular weight of 150 kDa, trimodulin was able to bind and cover the opsonins more efficiently than Intratect. Therefore, high amounts of the Ig preparations imply a more efficient covering as lower amounts of trimodulin or Intratect, where more C3b can be detected in the supernatant. Additionally, Basta *et al.* reported that IgG is able to covalently bind to C3b molecules[11].It is suggested that also in the ELISA setting the complement factors covalently bind to the coating (aggregated IgG) as well as to the Ig molecules and

are consequently retained on the opsonin ELISA plate. Therefore, they were not detectable after the addition of high trimodulin or Intratect concentrations in the supernatant, which was analyzed in the Western Blot.

The results of the opsonin ELISA and the subsequent Western Blot analysis did not show a scavenging of the activated complement components that was described in various studies[24,99,166]. Nevertheless, these data were the first evidences that trimodulin is able to interact with activated opsonins in high concentrations and may inhibit further activation of the complement system that is associated with inflammatory reactions.

Anaphylatoxins are small polypeptides that are released in the circulation after the cleavage of its precursors and mediate inflammation caused by various effector functions. They contribute to the pathogenesis of many autoimmune, neurodegenerative as well as infectious diseases[207]. It is important to regulate and control their activation to prevent harmful effects for the host triggered by an over-stimulation of the immune system. To analyze the capacity of trimodulin to bind the anaphylatoxins C5a and C3a an ELISA was developed. The test was performed by using a trimodulin-coated plate and purified C5a or C3a was added. After washing, it was analyzed if the complement factors were bound by trimodulin and could therefore be detected by specific antibodies. A concentration-dependent decrease of C5a was seen, but the negative control (w/o EDTA-plasma) revealed the non-specific binding of the detection antibodies to the coating (see Figure 14). The problem of such non-specific bindings is also described by Tate & Ward, where the interference of detection antibodies with specific ELISA systems is reported[208]. Since the problem of non-specific binding was also revealed in the anaphylatoxin ELISA, it was impossible to distinguish if the binding of trimodulin to C5a or just the non-specific interference of the detection antibodies with the trimodulin coating was detected. Therefore, a second ELISA was performed by using a zymosan-coated plate. It was suggested that this setting reduced the non-specific binding, which was seen in the ELISA using a trimodulin-coated plate. In this setting, the complement factors that were not bound after the incubation with trimodulin on a second plate, were detected by transferring the supernatant to an anti-C3a or anti-C5a coated third plate. The results showed no influence of trimodulin or Intratect (used as IVIg control) on C3a detection. Compared to this, the detection of C5a revealed a slight decrease of this complement factor after trimodulin addition, whereas Intratect did not reduce the detection of C5a concentration-dependently (see Figure 15). The first evidences that Igs are able to bind to activated C3a as well as C5a molecules is described by Nezlin *et al*. They reported that the binding sites for both anaphylatoxins are mainly found in the Fab region of the IgG molecule[209]. Basta *et al.* supported this theory with *in vitro* and *in vivo* assays, demonstrating that Fab containing IVIg fragments were able to reduce anaphylatoxin mediated effector functions and prevented lethal cardio respiratory distress induced by C5a in a porcine model. Moreover, they demonstrated a shift in the molecular weight of the anaphylatoxins after the incubation with Fab fragments in a Western Blot analysis, indicating the binding of the fragments to C3a as well as C5a[11]. In general, the studies support the results of the anaphylatoxin ELISA, where a slight decrease in the C5a amount due to trimodulin addition was detected and it was suggested that this decrease was caused by trimodulin binding to the anaphylatoxin. Nevertheless, trimodulin did not inhibit the detection of C3a. This effect could be beneficial in inflammatory conditions, because the C3a molecule exhibit also anti-inflammatory properties. Besides triggering inflammatory reactions, it is also able to operate as an antagonist for C5a and balances between pro- and anti-inflammatory mechanisms. Especially in an acute setting of inflammation, it prevents the mobilization as well as accumulation of neutrophils and is therefore important for the limitation of inflammatory reactions[30,38]. Moreover, Intratect did not exhibit any inhibitory capacity regarding C3a or C5a, which can be due to different binding affinities caused by another manufacturing process or due to the absence of IgM molecules compared to trimodulin.

In future studies, it is important to further evaluating the interaction of trimodulin and C5a, because only a trend of C5a inhibition by trimodulin was detectable and should be supported by additional analyses.

One important effector function, triggered by the activation of the complement system is the CDC of target cells. It is a substantial mechanism for the destruction of pathogens or infected cells, but if

dysregulated it contributes to a number of inflammatory pathologies or autoimmune diseases[48,83]. The control and inhibition of the complement system to prevent excessive CDC is therefore of high relevance. In the opsonin and anaphylatoxin ELISA it was observed that trimodulin is able to interact with the activated complement system by binding to the target molecules C3b, C4b and C5a. To determine, if the binding of these factors by the Igs of trimodulin has also functional impacts on complement-mediated effector functions, a CDC assay was developed. In general, CDC assays are used to test the ability of therapeutic monoclonal antibodies (e.g. Rituximab, anti CD20 mAb) to induce the CDC of target cells[83,210,211]. In this study, the assay was established to determine whether trimodulin is able to bind as well as functionally neutralize complement factors and therefore to inhibit CDC. Initially, the human B lymphocytic Ramos cell line, which was used as target for CDC, was characterized. The Ramos cells exhibited a high CD20 expression on their surface that confirmed the suitability of the cells for the use in the CDC assay. Moreover, they reacted highly sensitive to Rituximab addition and showed a concentration-dependent decrease in their cell viability. In addition, the CD20 detection decreased concentration-dependently after the addition of Rituximab (see Figure 16). Dorvignit *et al.* compared different B lymphocytic cell lines (Daudi, Raji and Ramos cells) in their CD20 expression as well as in their sensitivity to Rituximab and reported that Ramos cells showed the highest CD20 expression as well as the highest sensitivity to CDC activity[172]. A CD20-negative phenotypic change of Ramos cells after Rituximab treatment was also described in various studies[212–215]. It is reported that this is to some extent due to a masking of CD20, but mainly caused by the down-modulation of this transmembrane protein[212]. The complete mechanism of down-modulation is not fully understood, but it is suggested that an internalization of CD20 takes place after Rituximab binding. Additionally, mechanisms like protein folding, exportation, glycosylation or microRNA binding are discussed[213,216]. After characterization of the CD20 positive Ramos cells, the assay was performed by the pre-incubation of trimodulin with serum and subsequently addition to the cells in parallel with Rituximab. It was seen that trimodulin (compared to only FB) obviously increased the viability of the Ramos cells in all used concentrations, which suggests that it is able to inhibit activated complement factors concentration-dependently and therefore to prevent the CDC of Ramos cells (see Figure 17). It also confirmed the previous ELISA results, where the binding of C3b, C4b as well as C5a was confirmed. These results demonstrated for the first time that trimodulin can functionally inhibit CDC, which leads to a reduced inflammatory response. It is assumed that this is due to binding and inhibition of the activated complement factors by trimodulin. In comparison, Intratect showed only a slight increasing effect of the cell viability in the highest used concentration. This supports the assumption that IgM is more efficient in inhibiting complement activation than IgG and underlines the advantages of using trimodulin to reduce inflammation compared to IVIG preparations. The results were supported by the study of Rieben *et al.* that described the functional reduction of C3, C5b-9 as well as C6 deposition in an *in vivo* rat model by an IgM- and IgA-enriched preparation, whereas the effect of an IVIg was not as effective. In addition, Walpen *et al.* exposed the advantages of IgM in preventing hyperacute xenograft rejection by demonstrating a strong complement inhibitory effect in an *in vitro* xenotransplantation model with PK15 cells compared to IgG, where no inhibition was seen.

Nevertheless, control experiments were performed, to determine if the decrease in complement deposition was due to the binding of complement and not due to unspecific overlay (e.g. to CD20) by trimodulin. A pre-incubation of the Ramos cells and Rituximab simultaneously to the pre-incubation of trimodulin and serum was performed to ensure that Rituximab already bound to CD20 before trimodulin was added and that trimodulin was not able to inhibit the binding of Rituximab to its target. An obvious concentration-dependent increase in the viability of the Ramos cells was detected after trimodulin addition, which confirms the assumption that trimodulin inhibits activated complement factors and does not influence the binding of Rituximab to CD20 (see Figure 18). Anyhow, the increase was slightly less effective compared to the viability that was seen after the pre-incubation of only trimodulin and serum. This could be due to an interaction of trimodulin with Rituximab when added at the same time, which can prevent the binding of Rituximab to CD20. However, it could also be caused by a faster and more efficient complement activation when Rituximab already bound to CD20, compared to the situation in which Rituximab initially bind CD20 before it can interact with C1q. It is known that C1q binds monomeric IgG with very low affinity, but clustering of IgG allows multivalent C1q binding and promotes efficient complement activation[217–220]. Recently, it was also shown that the C1 molecule is strongly

activated by ordered IgG hexamers, formed on the surface of a target cell[221]. Rituximab, not pre-incubated with the Ramos cells and added together with pre-incubated trimodulin and serum (see Figure 17) could sterically be inhibited from forming hexamers through the immune complexes or C3b molecules, which are generated by the alternative complement pathway and bind subsequently to the cell surface. This is one possible mechanism to explain the higher cell viability after the pre-incubation of serum and trimodulin compared to the incubation order where also Rituximab was pre-incubated together with the Ramos cells. Moreover, to exclude that trimodulin covered CD20 and Rituximab was not able to bind to CD20 anymore, a pre-incubation of trimodulin with the Ramos cells and without addition of Rituximab was performed. The subsequent detection of CD20 revealed that the expression of the surface antigen was as high as without trimodulin. This implies that no steric hindrance of Rituximab through trimodulin was induced and furthermore that CD20 was not covered by trimodulin, which further supports the direct inhibition of the activated complement factors by trimodulin (see Figure 21). Moreover, the subsequent addition of Rituximab clearly triggered the lysis of the target cells and was not as much inhibited as seen after the pre-incubation with trimodulin and serum (see appendix Figure 28). These results finally supported the hypothesis that trimodulin is able to prevent CDC by binding to activated complement factors and that this inhibition was not due to a functionally covering of CD20 by trimodulin.

In addition, all assay components were also incubated at the same time to further characterize the mechanism by which trimodulin inhibited complement activity. A lower Ramos cell viability after trimodulin addition was detected (see Figure 19) as compared to the cell viability, which was seen after the pre-incubation of trimodulin and serum (see Figure 17). This result leads to the hypothesis that activated complement factors, like C3b or C4b are torn between the binding to the Ramos cells and to IgG as well as IgM molecules of trimodulin. For example, the binding of C1q to two IgG molecules of Rituximab (classical pathway) or the spontaneous induction of the alternative pathway, generate activated C3b as well as C4b molecules. These factors are on the one hand able to bind to the cell surface and further activate the complement cascade or on the other hand, to IgM and IgG molecules that inhibits the activation[11,222,223]. Therefore, it is suggested that a balance between activation and inhibition of the complement system takes place when all components were incubated at the same time and the cell viability is not as high as seen after pre-incubation of trimodulin and serum.

Finally, the pre-incubation of Rituximab and trimodulin was performed, to exclude that Ig molecules of trimodulin can interact with the murine variable regions of the chimeric Rituximab antibody, which could neutralize Rituximab and lead similarly to an increase in the cell viability. It is known that patients that received monoclonal anti-mouse antibodies developed human anti-murine antibodies (HAMA), which caused immunogenicity[224]. With the development of chimeric murine/human antibodies, the problem of HAMA should have been solved. Hosono *et al.* reported that chimeric murine/human antibodies show little to no reactivity to HAMA[225]. Nevertheless, it is reported that indeed the immunogenicity was reduced, human anti-chimeric antibodies (HACA) could still develop, because of the murine parts[226]. However, it was observed, that the increase in the viability of the Ramos cells was lower, as compared to the viability, which was detected after the pre-incubation of trimodulin and serum (see Figure 20). Therefore, it is suggested that trimodulin did not interact with Rituximab and did not prevent the binding to CD20, but rather supported a direct effect of trimodulin against the deposition of complement components on the surface of Ramos cells.

The CDC assay showed that trimodulin was able to directly interact with activated complement factors and thereby inhibiting the CDC of Ramos cells. In future studies it should evaluated which complement factors are inhibited by trimodulin. It is suggested that the first component of the classical pathway, C1q, is not bound and inhibited by trimodulin in the fluid phase. C1q needs the staple confirmation of the IgM pentamer to enable binding, which is only present when the Ig is bound to an antigen[200]. Moreover, there are no indications in the literature of C1q binding to circulating IgG or IgA molecules. It is assumed that the C3b and C4b molecules, generated by the classical and the alternative pathway in this setting, are bound by trimodulin in the fluid phase and therefore prevented from further activation. The strongest inhibition of CDC was detected after the pre-incubation of trimodulin and serum. In general, complement can also be activated upon binding to polymer surfaces, like polystyrene plates, triggered by the alternative pathway[227,228]. Therefore, trimodulin pre-incubated with serum on a

polystyrene plate was able to directly interact with the activated opsonins as well as to prevent them from binding to the surface of the Ramos cells in the next incubation step and inhibit further activation of the complement system.

The anti-inflammatory mechanisms of trimodulin are of high relevance in severe inflammatory diseases like sCAP. It is known that inflammation in sCAP is triggered by an over-stimulated immune response. Especially the complement system contributes to disease severity after uncontrolled activation[116,229]. This is caused e.g. by high bacterial load or metabolic products of the bacterial lysis, together with antibiotic resistant bacteria that cannot be cleared completely by the immune system and lead to the release of pro-inflammatory mediators, like cytokines. Therefore, it is important to additionally treat the overstimulated host response, besides administering antimicrobial therapeutics.

Trimodulin was shown to reduce CDC, which contributes to inflammation, by binding and inhibiting activated complement factors. This mechanism can also be helpful to reduce the hyper-activation of the complement cascade, triggered among others by pneumolysin and teichnoic acid of *S. pneumoniae*[119]. It is assumed that trimodulin can therefore reduce the systemic spread of inflammation and prevent pneumonia-induced sepsis, pulmonary damage as well as multi-organ failure in sCAP. The studies of Müller-Redetzky *et al.* support the theory by demonstrating that targeting activated complement components can improve the patient's outcome. They reported that the inhibition of C5a, which is considerably elevated in sCAP, could protect against lung and liver injury in mice, infected with pneumonia[120,123]. Trimodulin was also able to bind C5a seen in the anaphylatoxin ELISA (Figure 15). The early treatment of sCAP patients with trimodulin can therefore be a promising adjunctive therapy, next to the standard antimicrobial application, to prevent nonspecific complement activation and to improve the progress of disease. Moreover, the reduced mortality of sCAP patients with an elevated level of the inflammatory marker CRP in the CIGMA study, promotes the anti-inflammatory functions of trimodulin[163]. Nevertheless, the time by which a therapeutic is administered to the patients plays also a role for the outcome of disease severity. Calbo *et al.* report that patients with a prolonged time between the first symptoms of pneumonia and hospital admission exhibited higher levels of pro-inflammatory cytokines as well as a higher expression of acute phase proteins. They also underline that time is crucial for an optimal modulation of the inflammatory response, because the release of pneumococcal antigens, which cause inflammation, takes place over time. This indicates that it is important for future studies to determine the optimal time point at which trimodulin is administered to obtain the best outcome for the patients[230].

An over-stimulation of the immune system is also observed in severe COVID-19 patients. It is reported that this can lead to hyper-inflammation and implies acute organ failure as well as cardiac arrest, although an adequate oxygenation of the patients was performed[231–233]. There is evidence that the complement system contributes to the development of hyper-inflammatory conditions. Studies described the activation of the complement system in response to SARS-CoV infection and reported that mice were protected from pulmonary inflammation as well as respiratory failure with a deficiency of complement factor C3[138]. Severe COVID-19 patients show also an activation of the complement system in lung, skin as well as sera and positively respond to a treatment with complement inhibitors[141,234,235]. Exhibiting immunomodulatory properties as one relevant MoA it is assumed that trimodulin might be regarded as beneficial for the treatment of hyper-inflammatory conditions in severe COVID-19 patients. The results of the CDC assay (see section 5.2.5.1) supported this hypothesis and showed that trimodulin is able to interact and inhibit activated complement factors. Especially complement factor C5a seems to play a role in the development of inflammation, because its concentrations are elevated in severe COVID-19 cases above 10 nM in serum or plasma[139]. In the anaphylatoxin ELISA, a trend in inhibiting complement factor C5a by trimodulin was also detected. Multiple therapeutic agents are available that also target complement and being studied for COVID-19. They are mostly monoclonal antibodies (e.g. eculizumab, ravulizumab, IFX-1 and AMY-101) that inhibit specific complement components or the activation of the complement system per se and promote the recovery of the patients [139,147,236,237]. In comparison to monoclonal antibodies, trimodulin is not exclusively able to inhibit complement, but can modulate various effector functions. It was seen that trimodulin can for example reduce the release of

proinflammatory cytokines as well as influence the TLR expression on monocytes that contributes to a reduced stimulation of the immune system[165]. Therefore, the ability of trimodulin to modulate various effector functions at the same time could be an advantage for severe COVID-19 patients, which suffer from an over-stimulated immune system. Moreover, the application of IVIg therapy in severe and critically ill COVID-19 patients is recommended by the national diagnosis and treatment protocol for COVID-19 (Trial Version 7) in China and by the Peking Union Medical College Hospital[238,239]. It is reported that the early treatment with high-dose IVIgs can lead to a reduced need of mechanical ventilation, to a shortened duration of hospital stay and to an improved 28-day survival[239]. However, in future studies the potential of Ig preparations, as add-on therapy to the standard treatment of COVID-19 patients, should be evaluated to obtain a beneficial outcome.

As discussed in the previous paragraphs, it is an important function of Ig preparations to control and prevent excessive activation of the complement system and to protect the host against tissue damage as well as multiple organ failure. Nevertheless, the activation of the complement system is also a necessary and substantial effect of IgG and IgM molecules to eliminate intruding pathogens by effector functions like CDC or phagocytosis[45].

To determine the antimicrobial activity of trimodulin and to compare it with the complement inhibitory capacity, two OPAs were developed using *E. coli* bacteria (K12) and *S. aureus* bioparticles. Initially, the phenotype of the differentiated HL-60 cells was analyzed, to determine the differentiation status and to test if they are suitable for the use in the OPA. The analysis of the complement receptors 1 and 3 (CD35 and CD11b) and the FcγRs (CD16, CD32 and CD64) revealed that both complement receptors as well as CD32 were highly expressed, whereas a medium CD16 expression was shown and CD64 was only slightly detectable. Moreover, no expression of CD71 was visible on the differentiated HL-60 cells (see Figure 22). The results for the FcγR expression on differentiated HL-60 cells are in accordance with various studies. Worley *et al.* reported an upregulation of CD16 and CD32 after differentiation of the HL-60 cells with DMSO, whereas CD64 was only slightly detectable[240]. Moreover, Trayner *et al.* also showed a slight expression of CD64 after DMSO addition and Verbrugge *et al.* detected that CD64 expression was lost during differentiation[241,242]. The upregulation of the complement receptors CD11b and CD35 is also described and serves as marker for the successful differentiation of the HL-60 cells[243–245]. Additionally, it is reported that HL-60 cells exhibit a loss of CD71 upon differentiation with DMSO[241,246]. In comparison to HL-60 cells, freshly isolated neutrophils show also a high CD16 as well as CD32 expression, whereas CD64 is not detectable[240,247]. Furthermore, CD11b as well as CD35 are also upregulated on neutrophils during an infection[248]. Due to the results of the phenotypic characterization, the HL-60 cells were assessed as suitable for the application in the OPA assays. In general, the use of a cell line compared to primarily isolated neutrophils allows faster as well as high throughput analyses, because isolated neutrophils exhibit short half-lives and must be prepared freshly prior to an assay as cryopreservation can affect their functionality[249]. Nevertheless, differences between HL-60 cells and primarily isolated neutrophils, like a lower level of antimicrobial activity of the HL-60 cells or varieties in their surface receptor expression, have to be considered when analyzing their effector functions[240,250].

After the phenotypic characterization of the HL-60 cells, the IgM/IgG depleted NHS was titrated to determine the optimal concentration for the use in the *E. coli* OPA and 0.8% NHS minus was assessed as best concentration. Higher amounts of NHS minus caused high non-specific killing and lower amounts prevented further activation of the complement system by trimodulin. Non-specific killing of serum in the absence of antibodies and in the presence of pathogens is a known difficulty in opsonophagocytic assays[251]. A pre-adsorption step with the bacteria of interest prior to the assays should be effective to reduce non-specific killing in OPAs. Afterwards, the sera must be tested for their activity in a CH50 test[193]. Abbanat *et al.* described a reduction of more than 40% non-specific killing after addition of a pre-adsorption step with *E. coli* bacteria[252]. Moreover, Burton & Nahm reported a dramatically decrease of non-specific killing after the pre-adsorption of baby rabbit serum with an unencapsulated pneumococcal strain[253]. In this thesis, the pre-adsorption of *E. coli* bacteria with NHS minus was also evaluated, but did not significantly decrease the non-specific killing of the serum (data not shown). Therefore, the NHS minus was adjusted to use the concentration at which the lowest non-specific killing was detected, but trimodulin still was able to activate the complement system.

To analyze, if trimodulin is able to induce the opsonophagocytosis of *E. coli*, the OPA was performed with the appropriate NHS minus concentration. Different controls were used to determine the 100% survival of the bacteria (control A), the direct effect of the differentiated HL-60 cells on the *E. coli* growth (control B), the mechanisms induced by complement activation without antibody addition (control C) and the effector functions triggered by the Ig molecules of trimodulin without NHS minus addition (control D). It was detected that control B in comparison to control A showed a slight decrease in the survival of the *E. colis* (see Figure 24). Control B consisted of the bacteria, hi NHS minus, differentiated HL-60 cells as well as trimodulin FB. In general, differentiated HL-60 cells express TLRs on their surface that can recognize specific conserved patterns of microbial components (PAMPs)[254,255]. Moreover, TLRs can trigger antimicrobial host responses by phagocytosis, degranulation as well as NETosis[256,257]. *E. coli* K12 compromises lipopolysaccharide (LPS) in its outer membrane that in turn is able stimulate TLR4, which is present on differentiated HL-60 cells and this leads to the killing of the pathogens[258,259]. The analysis of control C composed of bacteria, NHS minus, differentiated HL-60 cells as well as trimodulin FB, showed a strong decrease in the survival of the *E. coli* bacteria. Complement can be activated via the classical, lectin and the alternative pathway[7,12]. The classical pathway is in this setting negligible, because no IgG and IgM molecules were available in NHS minus for C1q activation. It is also reported that the lectin pathway is only involved in opsonization and phagocytosis of yeast species trough binding of MBL to mannose residues on the pathogen, whereas the uptake of bacteria is mostly MBL independent[260]. Therefore, it was suggested that complement was activated by the spontaneous hydrolysis of C3 in the alternative pathway, upon the presence of microbial inflammatory mediators of *E. coli*. Activated complement factors can trigger various effector functions. They are able to lyse pathogens through CDC, by assembly of the terminal MAC into the membrane, can initiate complement-mediated phagocytosis by binding to CR1 and CR3 on the phagocyte and lead to NETosis as well as degranulation of neutrophils. Control C comprised differentiated HL-60 cells, which express CR1 and CR3 on their surface, leading to the assumption that the activated complement factors bound to the phagocytes and induced the killing of the pathogens. Moreover, it was detected that trimodulin concentration-dependently decreased the cell viability of the bacteria without the addition of NHS minus and in presence of differentiated HL-60 cells (control D). High trimodulin concentrations showed an obvious decreasing effect in the survival of the *E. coli* (see Figure 24). There are several effector functions, which might be responsible for the reduced viability of the bacteria. The binding of trimodulin opsonized the surface of the *E. coli* cells and attracted the phagocytes (differentiated HL-60 cells), which bound to the Ig molecules of trimodulin via their FcRs. After binding to antibody-opsonized bacteria, the effector cells are able to destroy the pathogens via ADCP, ADCC (degranulation) or NETosis in the absence of serum[48,70,261]. HL-60 cells only exhibit FcγRs (IgG) as well as the FcαR (IgA), whereas the Fc$\mu$R (IgM) is not expressed[63,262]. For this reason, the destruction of the bacteria that was seen in control D was mostly IgG and to some extent IgA triggered. Nevertheless, it is reported that IgA-mediated opsonization as well as phagocytosis induce NETosis and ROS production, which results in the subsequent cell death of the phagocyte[263]. Because the viability of the HL-60 cells was still high after assay incubation (data not shown), it is suggested that mainly IgG was responsible for the killing of the *E. coli* bacteria by phagocytosis or degranulation in control D. After incubation of the bacteria with NHS minus, differentiated HL-60 cells and trimodulin (sample), a dual effect regarding the bacterial survival was detected. In high concentrations, trimodulin exhibited an increasing effect on the *E. coli* viability compared to control C (without trimodulin) and compared to the same concentration of trimodulin in control D (without NHS minus). However, the viability decreased in lower concentrations, whereas a slight increase in the lowest trimodulin concentration was detected (see Figure 24). These data showed for the first time that trimodulin exhibits an ambivalent effect towards the complement system. On the one hand, high trimodulin doses triggered the inhibition of the opsonophagocytosis and on the other hand, an uptake of the bacteria was induced in low concentrations. It was suggested that the reduction in the opsonophagocytic capacity of the HL-60 cells was caused by an inhibition of complement activation after trimodulin addition. These findings are in accordance and support the results of the CDC assay, where an obvious inhibition of the complement system was also detected in high trimodulin doses (see Figure 17). Nevertheless, trimodulin did not stronger activate complement via the classical pathway in this setting and thereby did not amplify the opsonophagocytosis of *E. coli* compared to control C,

where complement activation was induced by the alternative pathway. It was already shown that high-dose Ig preparations can scavenge activated complement factors, whereas low doses are able to activate the complement system[17,95,198,264,265]. However, in the *E. coli* OPA only the phagocytosis of the bacteria could be detected, but the assay was not able to depict the opsonophagocytic effect of trimodulin. The use of Intratect (as IVIg control) showed that control A (100% control for the *E. coli* growth), control B (used to determine the direct effect of differentiated HL-60 cells on the viability of *E. coli*) as well as control C (used for evaluating the effects of NHS minus on *E. coli* growth without addition of the Ig preparation) were comparable to trimodulin. However, a stronger decrease of the cell viability was induced with high Intratect doses in control D. This was caused by the higher amount of IgG molecules in Intratect (≈ 96%) compared to trimodulin (≈ 56%), which were responsible for the induction of phagocytosis without the addition of NHS minus. Moreover, Intratect did not inhibit complement activation in high doses, but triggered the opsonophagocytosis of *E. coli* compared to control C. Roos *et al.* as well as Rieben *et al.* already described that IgM is a more potent complement inhibitor than IgG molecules[98,223]. It is suggested that trimodulin inhibits complement components stronger, because of the high avidity of IgM together with the ability of IgG to bind activated complement components as compared to Intratect, which exclusively contains IgG molecules. These data are additionally supported by the results generated in the opsonin ELISA, which showed a slight reduction in the detection of the C3b as well as C4b molecules, whereas a strong decrease of the complement factors was seen after trimodulin addition (see Figure 10 and Figure 11). Nevertheless, a high SD was detected in the *E. coli* OPA, which made it difficult to distinguish between assay variations and real effects induced by trimodulin. It was assumed that the high SD was caused by the evaluation method used in the OPA, because the bacteria were manually counted on LB agar pates, which was susceptible for variations. Therefore, another OPA was developed by using a FACS-based method to evaluate the opsonophagocytosis of Alexa Fluor 488 conjugated *S. aureus* bioparticles induced by trimodulin.

The *S. aureus* bioparticles OPA was performed by using the same controls and samples as in the *E. coli* OPA. Data were evaluated by calculating the phagocytic index, which depicts the median fluorescence intensity of living HL-60 cells that ingested the bioparticles after trimodulin addition. Hence, a discrimination between cells that ingested high amounts of bioparticles as well as cells with a lower phagocytic capacity was possible. Untreated HL-60 cells were used as additional control to determine the background fluorescence of the cells without the addition of Alexa Fluor 488 conjugated bioparticles. It was detected that untreated HL-60 cells as well as control A (bacteria, undifferentiated HL-60 cells, hi NHS minus and FB) showed nearly no phagocytic index, which implies a low background fluorescence of the bioparticles without differentiated HL-60 cells (see Figure 26). Control B that comprised bacteria, differentiated HL-60 cells, hi NHS minus and FB, induced a slight increase in the phagocytic index compared to control A. In general, *S. aureus* bioparticles are heat- or chemically inactivated pathogens, even though they are suitable for the use in phagocytic assays[266]. As gram-positive bacteria, they exhibit the counterpart to LPS, lipoteichoic acid (LTA) as well as peptidoglycan in their cell wall[267]. These PAMPs are able to stimulate the release of proinflammatory cytokines and activate leukocytes *in vitro*[268]. TLR2, which is present on differentiated HL-60 cells, is able to detect PAMPs like LTA or peptidoglycan and activates the phagocyte[254,269]. Therefore, an increase of the phagocytic index was seen in control B, because the HL-60 cells were activated by the interaction of *S. aureus* PAMPs with TLR2. Control C, which was used to determine the effect of NHS minus regarding opsonophagocytosis of the pathogens without the addition of trimodulin, showed a high phagocytic index, as compared to the other controls. This was already seen in the *E. coli* OPA and was suggested to be caused by the activation of complement via the alternative pathway by binding to CR1 as well as CR3 on the HL-60 cells and leading to CDC, degranulation, NETosis as well as opsonophagocytosis. The analysis of control D (bacteria, differentiated HL-60 cells, hi NHS minus and trimodulin) revealed a concentration-dependent increase in the phagocytic index from high to medium concentrations of trimodulin and a strong decrease after addition of low concentrations. It was assumed that in this setting high-dose trimodulin was able to inhibit the phagocytosis of *S. aureus* bioparticles by its anti-inflammatory functions. Besides their complement inhibitory capacity, high concentrations of Ig preparations are additionally able to block FcγRs and therefore to inhibit the binding of immune-complexes to these receptors. Moreover, it is described that high-dose Ig preparations can also upregulate the inhibitory

receptor FcγRIIb[91,157,270–274]. These mechanisms are important functions of Ig preparations and used for the therapy of autoimmune or inflammatory disorders. For this reason, it was suggested that trimodulin is able to activate the phagocytosis of *S. aureus* bacteria in lower doses by binding of IgG molecules to their specific FcγRs on the HL-60 cells, whereas high doses blocked this interaction. After incubation of trimodulin with bacteria, differentiated HL-60 cells as well as NHS minus (sample) a concentration-dependent increase of the phagocytic index from high to medium trimodulin concentrations and a decrease in lowest concentrations was seen. The increase in the opsonophagocytosis of *S. aureus* was significantly stronger compared to control D as well as to control C. This demonstrated for the first time that trimodulin is able to activate the complement system and to increase the opsonophagocytosis of the bacteria. Additionally, the ambivalent effect of trimodulin in activating and inhibiting the immune system was detected. On the one hand, it was suggested that high trimodulin doses could inhibit the complement system as well as lead to a blocking of FcγRs and to an upregulation of the inhibitory FcγRIIb. On the other hand, trimodulin was able to activate the complement system via the classical pathway and to induce the ingestion of the *S. aureus* bioparticles in the presence of NHS minus. Walpen *et al.* as well as Wagner *et al.* reported that high-dose Ig preparations are able to inhibit complement activation induced by the classical pathway, but not the anti-bacterial activity triggered by the alternative pathway[275,276]. This dual role of Ig preparations ensures the killing of intruding pathogens by mechanisms like opsonophagocytosis or CDC, but also prevents excessive complement activation. The alternative pathway, induced by NHS minus in the absence of trimodulin (control C), was also active after trimodulin treatment (samples), because the phagocytic index of the sample did not exhibit lower values than control C. Compared to this, the additional activation of complement via the classical pathway was prevented in high trimodulin doses.

These results show that trimodulin is able to activate the classical complement pathway in low concentrations and amplifies the clearance of *S. aureus* bioparticles. Additionally, the killing of the pathogens is ensured, despite the inhibition of the complement system in high trimodulin doses, because the alternative pathway was not inhibited by trimodulin.

For comparison, Intratect (as IVIg control) was diluted to the same IgG amount as trimodulin (≈ 56%) and was used in the *S. aureus* OPA. It was detected that Intratect without the addition of NHS minus (control D) also induced the concentration-dependent phagocytosis of *S. aureus* bioparticles (see Figure 27). High concentrations triggered the strongest phagocytosis of the bacteria, whereas the effect decreased in low Intratect concentrations. Nevertheless, the phagocytic index was lower as observed for trimodulin. It is suggested that the higher values generated after trimodulin treatment, were caused by the presence of IgA molecules in trimodulin compared to Intratect, which only consists of IgG molecules. IgA is able to initiate phagocytosis via the binding to its FcαR, which is also present on differentiated HL-60 cells[262]. Moreover, a blocking of the phagocytosis in high Intratect doses could not be detected. Compared to this, trimodulin induced the blocking of the phagocytosis (seen in control D), which was assumed to be caused by a higher amount of IgG-aggregates in trimodulin as compared to Intratect (master thesis Fabian Bohländer). In general, FcγRs exhibit low affinity for binding monomeric circulating IgG and are rather activated by immune complexes[92]. Therefore, the blocking of the FcγRs is also more likely due to an interaction with IgG-aggregates than to the binding of monomeric IgG molecules. However, in the Intratect sample an ambivalent effect of the IVIg preparation was detected regarding complement activation. High Intratect doses revealed an inhibition of the *S. aureus* opsonophagocytosis and low concentrations triggered the ingestion of the particles. This dual effect was already seen in the trimodulin sample with almost the same phagocytic indices. It is reported that generally IgM molecules are more potent complement inhibitors /activators than IgG[12,98,223]. One IgM molecule is able to bind and activate C1q, the first component of the classical pathway, whereas two or more IgG molecules in a specific distance to each other are needed for the same purpose. Moreover, IgM has a higher avidity as IgG to bind activated complement components due to its pentameric structure[60]. Therefore, it was assumed that trimodulin was able to induce a stronger opsonophagocytosis compared to Intratect. Nevertheless, the results of the *S. aureus* OPA showed that trimodulin and Intratect induced the same activation of the classical complement pathway as well as the same opsonophagocytosis. However, the OPA was performed by using *S. aureus* bioparticles instead of living bacteria. These particles are fragments of *S. aureus* and are not present in their native conformation as well as size.

Moreover, living *S. aureus* bacteria express a polysaccharide capsule, which masks their surface, impedes phagocytosis and therefore contributes to the pathogenesis of *S. aureus*[277,278]. It is assumed that the bioparticles did not exhibit an intact capsule, because of their treatment for inactivation, hence being less pathogenic. For this reason, it is suggested that less complement and Igs are necessary to induce the opsonophagocytosis of the bioparticles, compared to living bacteria. This in turn leads to the assumption that the IgG molecules of Intratect already induced the complete opsonophagocytosis of the bacteria cells in low concentrations and no further activation of the complement system through IgM was necessary. Therefore, no difference in the phagocytic capacity of trimodulin and Intratect was visible.

For an improved comparison of trimodulin and Intratect as well as for the evaluation of the differences between IgM and IgG molecules in inducing the opsonophagocytosis of pathogens, the OPA should be performed by using living *S. aureus* bacteria in future studies. Moreover, gram-positive *S. aureus* bacteria are, contrary to *E. coli* bacteria, one of the relevant pathogens in sCAP and cause excess mortality [279,280]. For this reason, it is important to analyze the opsonophagocytic capacity of trimodulin regarding living *S. aureus* bacteria, as sCAP relevant pathogens. Nevertheless, the results of the OPA provided the first evidence that trimodulin is able to induce the opsonophagocytosis of gram-positive bacteria and that it could therefore improve the outcome of patients with sCAP.

In general, trimodulin was developed for the treatment of patients with severe infections and is currently tested for the indications sCAP as well as COVID-19. It is known that patients with severe infections often suffer from antibody depletion. In the study of de la Torre *et al.,* they reported that sCAP patients, which require ICU treatment, showed a decreased level of IgG and IgA molecules in serum as compared to patients with milder progression of sCAP. Moreover, it was observed that the low Ig levels contribute to disease severity as well as mortality[281]. In addition, Bermejo-Martín *et al.* showed that the combined decrease of $IgG_1$, IgM as well as IgA is responsible for a higher mortality rate in patients with severe sepsis or septic shock[282]. Therefore, it could improve the patient's outcome when treated with an IgM- or IgA-enriched Ig preparation like trimodulin. The CIGMA study already demonstrated that sCAP patients, which exhibited a reduced IgM level, an elevated CRP level or both, showed a reduced 28-day mortality when treated with trimodulin as add-on therapy[163]. In the *S. aureus* OPA it was clearly demonstrated that trimodulin has an antimicrobial effect against sCAP relevant pathogens. Especially in patients with reduced Ig levels, the supplementation of exogenous Igs with trimodulin, next to the standard antibiotic therapy, is therefore an important tool to provide the patients with sufficient amounts of Igs to reduce disease severity as well as mortality.

The severity of infections, like sCAP or COVID-19, can also be increased by the simultaneous infection of the host with multiple pathogens. For example, bacterial co-infections are common in viral respiratory infections and contribute to disease severity[216,283]. It was already demonstrated that SARS- and MERS-CoV patients develop major complications due to bacterial co-infections[284,285]. Relating to COVID-19, various studies report bacterial co-infections in SARS-CoV-2 positive patients as well. Nevertheless, Landsbury *et al.* revealed that only 7% of hospitalized COVID-19 patients and 14% of ICU patients exhibit bacterial co-infections. This can be due to an unavailability of data, because most of the studies that are available until now, did not screen for co-infecting pathogens and could therefore be an underestimated problem. In general, the most commonly co-infecting bacteria identified in SARS-CoV-2 positive patients, are *M. pneumoniae, P. aeruginosa, H. influenzae* and *K. pneumoniae*[286]. Additionally, *C. pneumoniae*, *L. pneumoniae, S. aureus* and *S. pneumoniae* were also detected in COVID-19 patients[287–289]. It is also reported that bacterial co-infections contribute to ICU admission as well as mechanical ventilation of COVID-19 patients[287]. Furthermore, the alveoli in severe SARS-CoV-2 infections are often injured[290]. This in turn can lead to a facilitated influx of bacteria and viruses, which at worst can induce sepsis and septic shock[291]. Indeed, trimodulin does not exhibit antibodies directed against SARS-CoV-2, nevertheless it contains a broad spectrum of other anti-viral as well as anti-bacterial antibodies. Therefore, it is suggested that trimodulin is able to neutralize various pathogens, like co-infecting bacteria, by its antimicrobial mechanisms like CDC, ADCP, ADCC as well as opsonophagocytosis. In the *S. aureus* OPA it was detected that trimodulin is able to activate complement and leads to the opsonophagocytosis of the pathogens. Moreover, trimodulin comprises IgA and IgM molecules, which are the first line of defense at the lung epithelium[54,292]. All these characteristics support the assumption

that trimodulin can also help to neutralize co-infectious bacteria in severe viral infections like COVID-19, besides modulating the immune system and that this reduces disease severity as well as mortality.

The aim of this PhD thesis was the functional characterization of trimodulin to obtain new insights in the MoA of this IgM- and IgA-enriched Ig preparation. In summary, it was demonstrated that trimodulin exhibits an ambivalent effect regarding complement activity by activating but also by inhibiting the complement system concentration-dependently. Initially, the opsonin and anaphylatoxin ELISAs showed the interaction of trimodulin with the activated complement factors C3b, C4b as well as C5a. The detection was obviously reduced by the binding and an overlay of these factors on the 96 well plate. Moreover, trimodulin showed a stronger ability to decrease the detection of C3b as well as C4b compared to the IVIg control (Intratect). In order to functionally prove the complement inhibitory mechanisms of trimodulin, a CDC assay was developed. This assay showed for the first time that trimodulin was able to reduce the CDC of Ramos cells and therefore obviously inhibited activated complement factors, which was supported by various control experiments. Additionally, it was shown that Intratect did not exhibit complement inhibitory capacity. This clearly demonstrated the benefit of using trimodulin compared to a standard IVIg preparation for preventing the over-stimulation of the complement system. Therefore, it is assumed that trimodulin may help patients with a hyper-activation of the immune system that causes inflammation, seen in autoimmune or inflammatory disorders.

Moreover, an OPA was developed to additionally examine the antimicrobial mechanisms of trimodulin. The assay demonstrated that trimodulin activated the complement system in relatively low doses and therefore induced the opsonophagocytosis of *S. aureus* bioparticles. Simultaneously, it was detected that trimodulin still inhibited complement activation via the classical pathway in high doses. These results revealed that the OPA was able to depict the dual MoA of trimodulin regarding complement activity. Indeed, the complement system was inhibited in high trimodulin concentrations; however, the neutralization of the bacteria was still ensured by the addition of low trimodulin doses. These antimicrobial functions of trimodulin are relevant for the destruction of invading pathogens, which trigger severe infections, like sCAP. Nevertheless, the complement system can also be harmful to the host, when over-activated and induce tissue damage as well as multiple organ failure. Therefore, it is important that the complement system is balanced between activation and inhibition.

In this PhD thesis, trimodulin was functionally characterized regarding its ability to activate and to inhibit the complement system. The results gave new insights and improved the understanding of the complex MoA of this IgM- and IgA-enriched preparation. Moreover, the data support the hypothesis that trimodulin can be used for the treatment of inflammatory or autoimmune diseases, besides for the therapy of severe infections. Especially for COVID-19 patients, it would be beneficial to prevent the hyper-activation of the complement system, which makes trimodulin a promising agent for the treatment of this infection. Nevertheless, to further decipher the MoA of trimodulin regarding complement activation and inhibition, various functions should be addressed in future studies. It is important to evaluate the detailed mechanisms of the individual Ig subclasses in trimodulin and to analyze which subclass is mainly responsible for activation and for inhibition of the complement system. Moreover, it should be examined which complement factors and pathways are inhibited by trimodulin. Finally, it is also important to analyze the modulation of signaling pathways in effector cells after the inhibition of the complement system.

The findings of this PhD thesis gave substantial insights into the MoA of trimodulin, displaying the complex network and various interactions of the human immune system and can be regarded as valuable results for the future research on IgM- and IgA-enriched preparations.

# 7. Appendix

## 7.1. Additional Results

### 7.1.1. Complement-dependent cytotoxicity assay

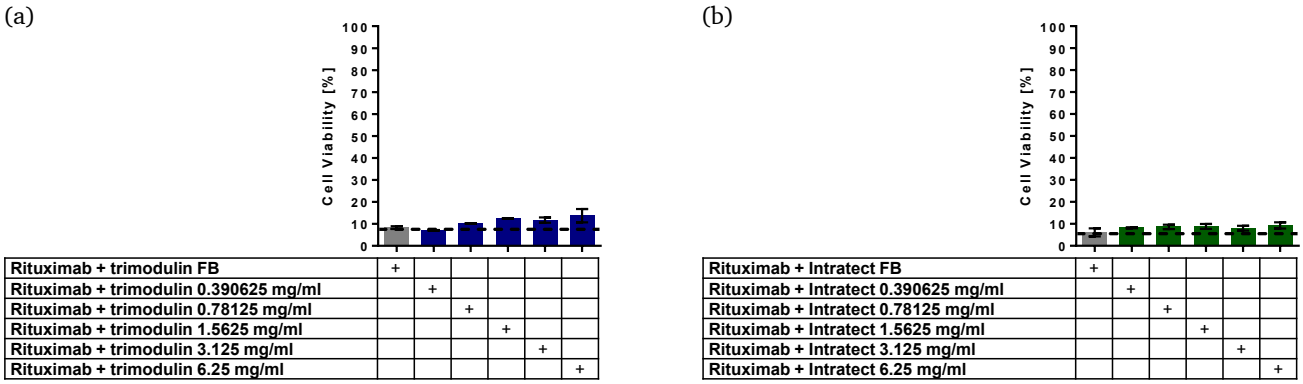


**Figure 28** Trimodulin does not inhibit CDC after pre-incubation with Ramos cells. Trimodulin (a) or Intratect (b) was mixed with assay buffer, 80% NHS as well as 50 µL Ramos cells ($5{\cdot}10^6$ cells/mL) and pre-incubated on a 96 well plate for 30 min at 37 °C. After that, 15 µL of 160 µg/mL Rituximab was added to the wells and the plate was incubated for additional 80 min at 37 °C. After incubation, the survival of the cells was measured by PI staining in a flow cytometer. Data represent results from two independent experiments performed in duplicates. See Table 24 and Table 25 for a detailed overview of the statistical analysis.

**Table 16** Statistical analysis of the pre-incubation of trimodulin with NHS (see Figure 17) by using a one-way ANOVA and a Bonferroni test. Significance is shown as p-value: * $p \leq 0.05$ and ** $p \leq 0.01$.

| Comparison | Significance (p-value) |
|---|---|
| Rituximab vs. trimodulin 0.390625 mg/mL | ns |
| Rituximab vs. trimodulin 0.78125 mg/mL | ns |
| Rituximab vs. trimodulin 1.5625 mg/mL | * |
| Rituximab vs. trimodulin 3.125 mg/mL | ** |
| Rituximab vs. trimodulin 6.25 mg/mL | ** |

**Table 17** Statistical analysis of the pre-incubation of Intratect (see Figure 17) with NHS by using a one-way ANOVA and a Bonferroni test.

| Comparison | Significance (p-value) |
|---|---|
| Rituximab vs. Intratect 0.390625 mg/mL | ns |
| Rituximab vs. Intratect 0.78125 mg/mL | ns |
| Rituximab vs. Intratect 1.5625 mg/mL | ns |
| Rituximab vs. Intratect 3.125 mg/mL | ns |
| Rituximab vs. Intratect 6.25 mg/mL | ns |

**Table 18** Statistical analysis of the pre-incubation of trimodulin with NHS and simultaneous of Rituximab and Ramos cells (see Figure 18) by using a one-way ANOVA and a Bonferroni test. Significance is shown as p-value: * $p \leq 0.05$.

| Comparison | Significance (p-value) |
|---|---|
| Rituximab vs. trimodulin 0.390625 mg/mL | ns |
| Rituximab vs. trimodulin 0.78125 mg/mL | ns |
| Rituximab vs. trimodulin 1.5625 mg/mL | ns |
| Rituximab vs. trimodulin 3.125 mg/mL | * |
| Rituximab vs. trimodulin 6.25 mg/mL | * |

**Table 19** Statistical analysis of the pre-incubation of Intratect with NHS and simultaneous of Rituximab and Ramos cells (see Figure 18) by using a one-way ANOVA and a Bonferroni test.

| Comparison | Significance (p-value) |
|---|---|
| Rituximab vs. Intratect 0.390625 mg/mL | ns |
| Rituximab vs. Intratect 0.78125 mg/mL | ns |
| Rituximab vs. Intratect 1.5625 mg/mL | ns |
| Rituximab vs. Intratect 3.125 mg/mL | ns |
| Rituximab vs. Intratect 6.25 mg/mL | ns |

**Table 20** Statistical analysis of the simultaneous incubation of all assay components with trimodulin (see Figure 19) by using a one-way ANOVA and a Bonferroni test. Significance is shown as p-value: ** $p \leq 0.01$.

| Comparison | Significance (p-value) |
|---|---|
| Rituximab vs. trimodulin 0.390625 mg/mL | ns |
| Rituximab vs. trimodulin 0.78125 mg/mL | ns |
| Rituximab vs. trimodulin 1.5625 mg/mL | ns |
| Rituximab vs. trimodulin 3.125 mg/mL | ns |
| Rituximab vs. trimodulin 6.25 mg/mL | ** |

**Table 21** Statistical analysis of the simultaneous incubation of all assay components with Intratect (see Figure 19) by using a one-way ANOVA and a Bonferroni test. Significance is shown as p-value: * $p \leq 0.05$.

| Comparison | Significance (p-value) |
|---|---|
| Rituximab vs. Intratect 0.390625 mg/mL | ns |
| Rituximab vs. Intratect 0.78125 mg/mL | ns |
| Rituximab vs. Intratect 1.5625 mg/mL | ns |
| Rituximab vs. Intratect 3.125 mg/mL | ns |
| Rituximab vs. Intratect 6.25 mg/mL | * |

**Table 22** Statistical analysis of the pre-incubation of trimodulin with Rituximab (see Figure 20) by using a one-way ANOVA and a Bonferroni test. Significance is shown as p-value: ** $p \leq 0.01$.

| Comparison | Significance (p-value) |
|---|---|
| Rituximab vs. trimodulin 0.390625 mg/mL | ns |
| Rituximab vs. trimodulin 0.78125 mg/mL | ns |
| Rituximab vs. trimodulin 1.5625 mg/mL | ns |
| Rituximab vs. trimodulin 3.125 mg/mL | ns |
| Rituximab vs. trimodulin 6.25 mg/mL | ** |

**Table 23** Statistical analysis of the pre-incubation of Intratect with Rituximab (see Figure 20) by using a one-way ANOVA and a Bonferroni test.

| Comparison | Significance (p-value) |
|---|---|
| Rituximab vs. Intratect 0.390625 mg/mL | ns |
| Rituximab vs. Intratect 0.78125 mg/mL | ns |
| Rituximab vs. Intratect 1.5625 mg/mL | ns |
| Rituximab vs. Intratect 3.125 mg/mL | ns |
| Rituximab vs. Intratect 6.25 mg/mL | ns |

**Table 24** Statistical analysis of the pre-incubation of trimodulin with Ramos cells (see Figure 21) by using a one-way ANOVA and a Bonferroni test.

| Comparison | Significance (p-value) |
|---|---|
| Rituximab vs. trimodulin 0.390625 mg/mL | ns |
| Rituximab vs. trimodulin 0.78125 mg/mL | ns |
| Rituximab vs. trimodulin 1.5625 mg/mL | ns |
| Rituximab vs. trimodulin 3.125 mg/mL | ns |
| Rituximab vs. trimodulin 6.25 mg/mL | ns |

**Table 25** Statistical analysis of the pre-incubation of Intratect with Ramos cells (see Figure 21) by using a one-way ANOVA and a Bonferroni test.

| Comparison | Significance (p-value) |
|---|---|
| Rituximab vs. Intratect 0.390625 mg/mL | ns |
| Rituximab vs. Intratect 0.78125 mg/mL | ns |
| Rituximab vs. Intratect 1.5625 mg/mL | ns |
| Rituximab vs. Intratect 3.125 mg/mL | ns |
| Rituximab vs. Intratect 6.25 mg/mL | ns |

## 7.1.2. *E. coli* opsonophagocytosis assay

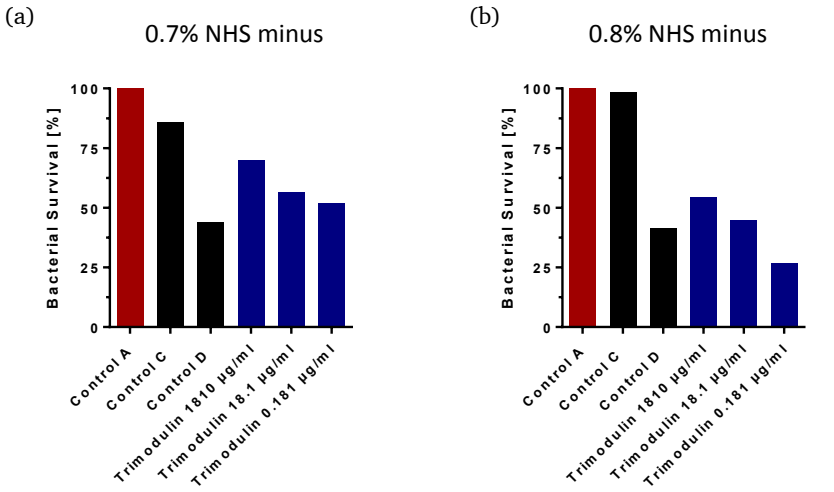


| Sample | Composition |
|---|---|
| Control A | Bacteria, undifferentiated HL-60 cells, hi NHS minus, FB |
| Control B | Bacteria, differentiated HL-60 cells, hi NHS minus, FB |
| Control C | Bacteria, differentiated HL-60 cells, NHS minus, FB |
| Sample | Bacteria, differentiated HL-60 cells, NHS minus, immunoglobulin preparation |

**Figure 29** Comparison of 0.7% and 0.8% NHS minus for use in the *E. coli* OPA. Trimodulin (B588039) and *E. coli* bacteria were pre-incubated on a 96 well U-bottom plate for 30 min at RT. After that, (a) 0.7% NHS minus or (b) 0.8% NHS minus as well as HL-60 cells were added, mixed and were incubated for additional 45 min at 37 °C. The plate was put on ice for 20 min and 5 µL of every well was distributed in triplets to LB agar plates for overnight incubation at 37 °C. The CFUs were counted and the data was analyzed using GraphPad Prism. Control A served as 100% control for bacterial survival [CFU/mL], control B determined the direct killing of the cells via binding of *E. coli* to the TLRs and control C was used to examine the activation of complement without Ig addition. Trimodulin was 100-fold serially diluted (1810 µg/mL to 0.181 µg/mL) to monitor concentration-dependent effects. Data represent results from two independent experiments performed in triplicates.

**Table 26** Statistical analysis of the *E. coli* OPA by comparing control C (bacteria, differentiated HL-60 cells, NHS minus and FB) with the trimodulin samples (see Figure 24). Statistical analyses were performed using a Kruskal-Wallis test.

| Comparison | Significance (p-value) |
|---|---|
| Control C vs. trimodulin 1810 $\mu$g/mL | ns |
| Control C vs. trimodulin 181 $\mu$g/mL | ns |
| Control C vs. trimodulin 18.1 $\mu$g/mL | ns |
| Control C vs. trimodulin 1.81 $\mu$g/mL | ns |
| Control C vs. trimodulin 0.181 $\mu$g/mL | ns |
| Control C vs. trimodulin 0.0181 $\mu$g/mL | ns |

**Table 27** Statistical analysis of the *E. coli* OPA by comparing control D (bacteria, differentiated HL-60 cells, hi NHS minus and different trimodulin concentrations) with the trimodulin samples (see Figure 24). Statistical analyses were performed using a Kruskal-Wallis test.

| Comparison | Significance (p-value) |
|---|---|
| Control D 1810 $\mu$g/mL vs. trimodulin 1810 $\mu$g/mL | ns |
| Control D 181 $\mu$g/mL vs. trimodulin 181 $\mu$g/mL | ns |
| Control D 18.1 $\mu$g/mL vs. trimodulin 18.1 $\mu$g/mL | ns |
| Control D 1.81 $\mu$g/mL vs. trimodulin 1.81 $\mu$g/mL | ns |
| Control D 0.181 $\mu$g/mL vs. trimodulin 0.181 $\mu$g/mL | ns |
| Control D 0.0181 $\mu$g/mL vs. trimodulin 0.0181 $\mu$g/mL | ns |

**Table 28** Statistical analysis of the *E. coli* OPA by comparing control C (bacteria, differentiated HL-60 cells, NHS minus and FB) with the Intratect samples (see Figure 25). Statistical analyses were performed using a Kruskal-Wallis test.

| Comparison | Significance (p-value) |
|---|---|
| Control C vs. Intratect 1810 $\mu$g/mL | ns |
| Control C vs. Intratect 181 $\mu$g/mL | ns |
| Control C vs. Intratect 18.1 $\mu$g/mL | ns |
| Control C vs. Intratect 1.81 $\mu$g/mL | ns |
| Control C vs. Intratect 0.181 $\mu$g/mL | ns |
| Control C vs. Intratect 0.0181 $\mu$g/mL | ns |

**Table 29** Statistical analysis of the *E. coli* OPA by comparing control D (bacteria, differentiated HL-60 cells, hi NHS minus and different Intratect concentrations) with the Intratect samples (see Figure 25). Statistical analyses were performed using a Kruskal-Wallis test.

| Comparison | Significance (p-value) |
|---|---|
| Control D 1810 $\mu$g/mL vs. Intratect 1810 $\mu$g/mL | ns |
| Control D 181 $\mu$g/mL vs. Intratect 181 $\mu$g/mL | ns |
| Control D 18.1 $\mu$g/mL vs. Intratect 18.1 $\mu$g/mL | ns |
| Control D 1.81 $\mu$g/mL vs. Intratect 1.81 $\mu$g/mL | ns |
| Control D 0.181 $\mu$g/mL vs. Intratect 0.181 $\mu$g/mL | ns |
| Control D 0.0181 $\mu$g/mL vs. Intratect 0.0181 $\mu$g/mL | ns |

### 7.1.3. *S. aureus* opsonophagocytosis assay

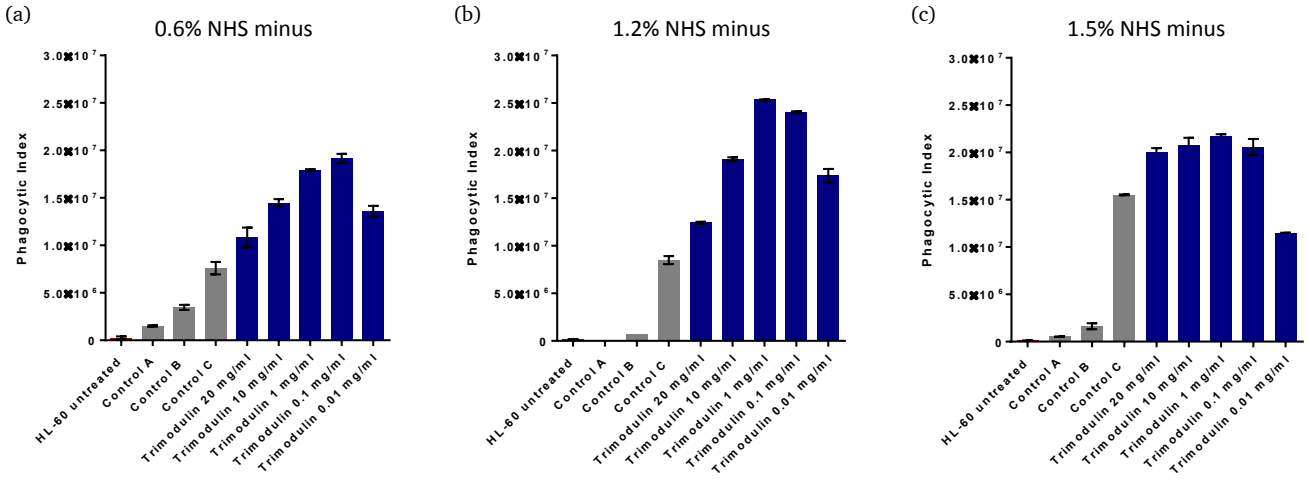


| Sample | Composition |
|---|---|
| Control A | Bacteria, undifferentiated HL-60 cells, hi NHS minus, FB |
| Control B | Bacteria, differentiated HL-60 cells, hi NHS minus, FB |
| Control C | Bacteria, differentiated HL-60 cells, NHS minus, FB |
| Sample | Bacteria, differentiated HL-60 cells, NHS minus, immunoglobulin preparation |

**Figure 30** Comparison of 0.6%, 1.2% and 1.5% NHS minus for the use in the *S. aureus* OPA. Differentiated HL-60 cells, *S. aureus* bioparticles, (a) 0.6% NHS minus or (b) 1.2% NHS minus or (c) 1.5% NHS minus as well as trimodulin (B588039) and the appropriate FB were mixed and incubated at 37 °C for 45 min. After that, the cells were quenched with 0.2% trypan blue solution and were subsequently analyzed by using a flow cytometer. The phagocytic index was calculated and the data depicted in a bar diagram using excel and GraphPad Prism. Control A served as 100% control for the bacteria, control B determined the direct phagocytosis of the cells via binding of *E. coli* to the TLRs and control C was used to examine the activation of complement without Ig addition. Different dilutions of trimodulin were used to monitor concentration-dependent effects. Error bars indicate the SD. Data represent results from two independent experiments performed in duplicates.

**Table 30** Comparison of the phagocytic index of Intratect samples without active NHS minus (control D) with Intratect samples after the addition of active NHS minus (see Figure 27). Statistical analyses were performed using a one-way ANOVA and a Bonferroni test. Significance is shown as p-value: *** $p \leq 0.001$ and **** $p \leq 0.0001$.

| Intratect concentration | Phagocytic index control D | Phagocytic index Intratect samples | Difference (Intratect sample – control D) | Significance (p-value) |
|---|---|---|---|---|
| 11.2 mg/mL | $1.0 \cdot 10^7$ | $1.4 \cdot 10^7$ | $4 \cdot 10^6$ | *** |
| 8.4 mg/mL | $9.9 \cdot 10^6$ | $1.4 \cdot 10^7$ | $4.1 \cdot 10^6$ | **** |
| 5.6 mg/mL | $9.9 \cdot 10^6$ | $1.5 \cdot 10^7$ | $5.1 \cdot 10^6$ | **** |
| 2.8 mg/mL | $9.2 \cdot 10^6$ | $1.4 \cdot 10^7$ | $4.8 \cdot 10^6$ | **** |
| 0.56 mg/mL | $1.0 \cdot 10^7$ | $1.6 \cdot 10^7$ | $6 \cdot 10^6$ | **** |
| 0.28 mg/mL | $1.0 \cdot 10^7$ | $1.9 \cdot 10^7$ | $9 \cdot 10^6$ | **** |
| 0.056 mg/mL | $1.1 \cdot 10^7$ | $2.3 \cdot 10^7$ | $1.2 \cdot 10^7$ | **** |
| 0.028 mg/mL | $1.0 \cdot 10^7$ | $2.3 \cdot 10^7$ | $1.3 \cdot 10^7$ | **** |
| 0.0056 mg/mL | $6.5 \cdot 10^6$ | $1.8 \cdot 10^7$ | $1.15 \cdot 10^7$ | **** |

**Table 31** Comparison of the phagocytic index of control C (without Intratect) with the samples after Intratect addition (see Figure 27). Statistical analyses were performed using a one-way ANOVA and a Bonferroni test. Significance is shown as p-value: *** $p \leq 0.001$ and **** $p \leq 0.0001$.

| Phagocytic index control C | Intratect concentration | Phagocytic index Intratect samples | Difference (Intratect sample – control C) | Significance (p-value) |
|---|---|---|---|---|
| $1.5 \cdot 10^7$ | 11.2 mg/mL | $1.4 \cdot 10^7$ | $1 \cdot 10^6$ | ns |
| | 8.4 mg/mL | $1.4 \cdot 10^7$ | $1 \cdot 10^6$ | ns |
| | 5.6 mg/mL | $1.5 \cdot 10^7$ | no difference | ns |
| | 2.8 mg/mL | $1.4 \cdot 10^7$ | $1 \cdot 10^6$ | ns |
| | 0.56 mg/mL | $1.6 \cdot 10^7$ | $1 \cdot 10^6$ | ns |
| | 0.28 mg/mL | $1.9 \cdot 10^7$ | $4 \cdot 10^6$ | **** |
| | 0.056 mg/mL | $2.3 \cdot 10^7$ | $8 \cdot 10^6$ | **** |
| | 0.028 mg/mL | $2.3 \cdot 10^7$ | $8 \cdot 10^6$ | **** |
| | 0.0056 mg/mL | $1.8 \cdot 10^7$ | $3 \cdot 10^6$ | *** |

## References


1. Chaplin, D. 1. Overview of the human immune response. *Journal of Allergy and Clinical Immunology* 117, 430–435 (2006).
2. Chaplin, D. Overview of the immune response. *Journal of Allergy and Clinical Immunology* 125, 3–23 (2010).
3. Thompson, A. E. The Immune System. *Jama* 313, 1686 (2015).
4. McComb, S., Thiriot, A., Krishnan, L. & Stark, F. Introduction to the Immune System. in *Immunoproteomics* (eds. Fulton, K. M. & Twine, S. M.) vol. 1061 1–20 (Humana Press, 2013).
5. Simon, A. K., Hollander, G. A. & McMichael, A. Evolution of the immune system in humans from infancy to old age. *Proc. R. Soc. B.* 282, 20143085 (2015).
6. Sarma, J. V. & Ward, P. A. The complement system. *Cell Tissue Res* 343, 227–235 (2011).
7. Walport, M. J. Advances in Immunology: Complement (First of Two Parts). *New England Journal of Medicine* 344, 1058–1066 (2001).
8. Szebeni, J. *The Complement System: Novel Roles in Health and Disease*. (Kluwer Academic Publishers, 2004).
9. Kirschfink, M. Controlling the complement system in inflammation. *Immunopharmacology* 38, 51–62 (1997).
10. Kirschfink, M. & Mollnes, T. E. Modern Complement Analysis. *Clinical and Vaccine Immunology* 10, 982–989 (2003).
11. Basta, M. Ambivalent effect of immunoglobulins on the complement system: Activation versus inhibition. *Molecular Immunology* 45, 4073–4079 (2008).
12. Janeway, C. J., Travers, P. & Walport, M. The complement system and innate immunity. in *Immunobiology: The Immune System in Health and Disease.* (ed. Janeway, C. J.) (Garland Science, 2001).
13. Dunkelberger, J. R. & Song, W.-C. Complement and its role in innate and adaptive immune responses. *Cell Res* 20, 34–50 (2010).
14. Mortensen, S. A. *et al.* Structure and activation of C1, the complex initiating the classical pathway of the complement cascade. *Proc Natl Acad Sci USA* 114, 986–991 (2017).
15. Ritchie, G. E. *et al.* Glycosylation and the Complement System. *Chem. Rev.* 102, 305–320 (2002).
16. Roos, A. *et al.* Human IgA Activates the Complement System Via the Mannan-Binding Lectin Pathway. *J Immunol* 167, 2861–2868 (2001).
17. Basta, M. Activation and Inhibition of Complement by Immunoglobulins. in *The Complement System* (ed. Szebeni, J.) 517–529 (Kluwer Academic Publishers, 2004).
18. Wallis, R., Mitchell, D. A., Schmid, R., Schwaeble, W. J. & Keeble, A. H. Paths reunited: Initiation of the classical and lectin pathways of complement activation. *Immunobiology* 215, 1–11 (2010).
19. Thurman, J. M. & Holers, V. M. The Central Role of the Alternative Complement Pathway in Human Disease. *J Immunol* 176, 1305–1310 (2006).
20. Hiemstra, P. S., Gorter, A., Stuurman, M. E., Van Es, L. A. & Daha, M. R. Activation of the alternative pathway of complement by human serum IgA. *Eur. J. Immunol.* 17, 321–326 (1987).
21. Trouw, L. A., Pickering, M. C. & Blom, A. M. The complement system as a potential therapeutic target in rheumatic disease. *Nat Rev Rheumatol* 13, 538–547 (2017).

22. Frank, M. M. & Fries, L. F. The role of complement in inflammation and phagocytosis. *Immunology Today* 12, 322–326 (1991).

23. Merle, N. S., Noe, R., Halbwachs-Mecarelli, L., Fremeaux-Bacchi, V. & Roumenina, L. T. Complement System Part II: Role in Immunity. *Front. Immunol.* 6, 257 (2015).

24. Basta, M. *et al.* F(ab)′2-mediated neutralization of C3a and C5a anaphylatoxins: a novel effector function of immunoglobulins. *Nat Med* 9, 431–438 (2003).

25. Ember, J. A. & Hugli, T. E. Complement factors and their receptors. *Immunopharmacology* 38, 3–15 (1997).

26. Pio, R., Ajona, D. & Lambris, J. D. Complement inhibition in cancer therapy. *Seminars in Immunology* 25, 54–64 (2013).

27. Markiewski, M. M. & Lambris, J. D. The Role of Complement in Inflammatory Diseases From Behind the Scenes into the Spotlight. *The American Journal of Pathology* 171, 715–727 (2007).

28. Burg, M. *et al.* IFN-gamma up-regulates the human C5a receptor (CD88) in myeloblastic U937 cells and related cell lines. 155, 4419–4426 (1995).

29. Ohta, R. *et al.* Serum concentrations of complement anaphylatoxins and proinflammatory mediators in patients with 2009 H1N1 influenza: Anaphylatoxins in the new influenza. *Microbiology and Immunology* 55, 191–198 (2011).

30. Coulthard, L. G. & Woodruff, T. M. Is the Complement Activation Product C3a a Proinflammatory Molecule? Re-evaluating the Evidence and the Myth. *J.I.* 194, 3542–3548 (2015).

31. Wu, M. C. L. *et al.* The receptor for complement component C3a mediates protection from intestinal ischemia-reperfusion injuries by inhibiting neutrophil mobilization. *Proc Natl Acad Sci USA* 110, 9439–9444 (2013).

32. Ricklin, D. & Lambris, J. D. Complement in Immune and Inflammatory Disorders: Pathophysiological Mechanisms. *J.I.* 190, 3831–3838 (2013).

33. Rubio-Perez, J. M. & Morillas-Ruiz, J. M. A Review: Inflammatory Process in Alzheimer's Disease, Role of Cytokines. *The Scientific World Journal* 2012, 1–15 (2012).

34. Ballanti, E. *et al.* Role of the complement system in rheumatoid arthritis and psoriatic arthritis: Relationship with anti-TNF inhibitors. *Autoimmunity Reviews* 10, 617–623 (2011).

35. Schmidt, C. Q., Lambris, J. D. & Ricklin, D. Protection of host cells by complement regulators. *Immunol Rev* 274, 152–171 (2016).

36. Noris, M. & Remuzzi, G. Overview of Complement Activation and Regulation. *Seminars in Nephrology* 33, 479–492 (2013).

37. Chonn, A., Hertig, S. & Frencht, L. E. Clusterin, the Human Apolipoprotein and Complement Inhibitor, Binds to Complement C7, CSP, and the b Domain of C9'. 151, 2159–2165 (1993).

38. Merle, N. S., Church, S. E., Fremeaux-Bacchi, V. & Roumenina, L. T. Complement System Part I - Molecular Mechanisms of Activation and Regulation. *Front. Immunol.* 6, 262 (2015).

39. Ricklin, D., Reis, E. S. & Lambris, J. D. Complement in disease: a defence system turning offensive. *Nat Rev Nephrol* 12, 383–401 (2016).

40. Ricklin, D. & Lambris, J. D. Complement-targeted therapeutics. *Nat Biotechnol* 25, 1265–1275 (2007).

41. Schroeder, H. W. & Cavacini, L. Structure and function of immunoglobulins. *Journal of Allergy and Clinical Immunology* 125, 41–52 (2010).

42. Justiz Vaillant, A. & Ramphul, K. Immunoglobulin. *StatPearls Publishing* (2020).

43. Palma, J., Tokarz-Deptuła, B., Deptuła, J. & Deptuła, W. Natural antibodies – facts known and unknown. *cejoi* 43, 466–475 (2018).

44. Burton, D. R. Antibody: the flexible adaptor molecule. *Elsevier Science Publishers Ltd* 2, 64–69 (1990).

45. Janeway, C. *Immunobiology: The immune system in health and disease*. (Garland Publ., 2001).

46. Vidarsson, G., Dekkers, G. & Rispens, T. IgG Subclasses and Allotypes: From Structure to Effector Functions. *Front. Immunol.* 5, 1–17 (2014).

47. Kapur, R., Einarsdottir, H. K. & Vidarsson, G. IgG-effector functions: "The Good, The Bad and The Ugly". *Immunology Letters* 160, 139–144 (2014).

48. van Erp, E. A., Luytjes, W., Ferwerda, G. & van Kasteren, P. B. Fc-Mediated Antibody Effector Functions During Respiratory Syncytial Virus Infection and Disease. *Front. Immunol.* 10, 548 (2019).

49. Ferrante, A., Beard, L. & Feldman, R. IgG subclass distribution of antibodies to bacterial and viral antigens. *The Pediatric Infectious Disease Journal* 9, 516–524 (1990).

50. van Helden, P. M. W. *et al.* IgG subclasses of anti-FVIII antibodies during immune tolerance induction in patients with hemophilia A: Anti-factor VIII IgG Subclasses During ITI. *British Journal of Haematology* 142, 644–652 (2008).

51. Woof, J. M. & Kerr, M. A. The function of immunoglobulin A in immunity. *J. Pathol.* 208, 270–282 (2006).

52. Woof, J. M. & Russell, M. W. Structure and function relationships in IgA. *Mucosal Immunol* 4, 590–597 (2011).

53. Snoeck, V., Peters, I. R. & Cox, E. The IgA system: a comparison of structure and function in different species. *Vet. Res.* 37, 455–467 (2006).

54. Mantis, N. J., Rol, N. & Corthésy, B. Secretory IgA's complex roles in immunity and mucosal homeostasis in the gut. *Mucosal Immunol* 4, 603–611 (2011).

55. Hansen, I. S., Baeten, D. L. P. & den Dunnen, J. The inflammatory function of human IgA. *Cell. Mol. Life Sci.* 76, 1041–1055 (2019).

56. de Sousa-Pereira, P. & Woof, J. M. IgA: Structure, Function, and Developability. *Antibodies* 8, 57 (2019).

57. Lopez, E., Shattock, R. J., Kent, S. J. & Chung, A. W. The Multifaceted Nature of Immunoglobulin A and Its Complex Role in HIV. *AIDS Research and Human Retroviruses* 34, 727–738 (2018).

58. Russell, M. W., Reinholdt, J. & Kilian, M. Anti-inflammatory activity of human IgA antibodies and their Fabα fragments: inhibition of IgG-mediated complement activation. *Eur. J. Immunol.* 19, 2243–2249 (1989).

59. Petrušić, V. *et al.* Hexameric immunoglobulin M in humans: Desired or unwanted? *Medical Hypotheses* 77, 959–961 (2011).

60. Racine, R. & Winslow, G. M. IgM in microbial infections: Taken for granted? *Immunology Letters* 125, 79–85 (2009).

61. Boes, M. Role of natural and immune IgM antibodies in immune responses. *Molecular Immunology* 37, 1141–1149 (2000).

62. Kubagawa, H. *et al.* Identity of the elusive IgM Fc receptor (Fc$\mu$R) in humans. *Journal of Experimental Medicine* 206, 2779–2793 (2009).

63. Kubagawa, H. *et al.* Functional Roles of the IgM Fc Receptor in the Immune System. *Front. Immunol.* 10, 945 (2019).

64. Meryk, A. *et al.* Fc$\mu$ receptor as a Costimulatory Molecule for T Cells. *Cell Reports* 26, 2681–2691 (2019).

65. Liu, J. *et al.* Role of the IgM Fc Receptor in Immunity and Tolerance. *Front. Immunol.* 10, 529 (2019).

66. Brandtzaeg, P. & Prydz, H. Direct evidence for an integrated function of J chain and secretory component in epithelial transport of immunoglobulins. *Nature* 311, 71–73 (1984).

67. Lu, L. L., Suscovich, T. J., Fortune, S. M. & Alter, G. Beyond binding: antibody effector functions in infectious diseases. *Nat Rev Immunol* 18, 46–61 (2018).

68. Mayadas, T. N., Cullere, X. & Lowell, C. A. The Multifaceted Functions of Neutrophils. *Annu. Rev. Pathol. Mech. Dis.* 9, 181–218 (2014).

69. Rosales, C. Neutrophil: A Cell with Many Roles in Inflammation or Several Cell Types? *Front. Physiol.* 9, 113 (2018).

70. Rosales, C. & Uribe-Querol, E. Neutrophil Activation by Antibody Receptors. in *Neutrophils* (ed. Khajah, M.) (IntechOpen, 2019).

71. Pham, C. T. N. Neutrophil serine proteases: specific regulators of inflammation. *Nat Rev Immunol* 6, 541–550 (2006).

72. Fuchs, T. A. *et al.* Novel cell death program leads to neutrophil extracellular traps. *Journal of Cell Biology* 176, 231–241 (2007).

73. Tamassia, N. *et al.* Cytokine production by human neutrophils: Revisiting the “dark side of the moon”. *Eur J Clin Invest* 48, e12952 (2018).

74. Forthal, D. Functions of Antibodies. *Microbiol Spectr.* 2, 1–17 (2014).

75. VanBlargan, L. A., Goo, L. & Pierson, T. C. Deconstructing the Antiviral Neutralizing-Antibody Response: Implications for Vaccine Development and Immunity. *Microbiol. Mol. Biol. Rev.* 80, 989–1010 (2016).

76. Khan, M. N. & Pichichero, M. E. Vaccine candidates PhtD and PhtE of Streptococcus pneumoniae are adhesins that elicit functional antibodies in humans. *Vaccine* 30, 2900–2907 (2012).

77. Cartron, G., Watier, H., Golay, J. & Solal-Celigny, P. From the bench to the bedside: ways to improve rituximab efficacy. *Blood* 104, 2635–2642 (2004).

78. Zhou, X., Hu, W. & Qin, X. The Role of Complement in the Mechanism of Action of Rituximab for B-Cell Lymphoma: Implications for Therapy. *The Oncol* 13, 954–966 (2008).

79. Baig, N. A. *et al.* Complement dependent cytotoxicity in chronic lymphocytic leukemia: ofatumumab enhances alemtuzumab complement dependent cytotoxicity and reveals cells resistant to activated complement. *Leukemia & Lymphoma* 53, 2218–2227 (2012).

80. Ricklin, D., Hajishengallis, G., Yang, K. & Lambris, J. D. Complement: a key system for immune surveillance and homeostasis. *Nat Immunol* 11, 785–797 (2010).

81. Bohanakashtan, O. Cell signals transduced by complement. *Molecular Immunology* 41, 583–597 (2004).

82. Bellosillo, B. *et al.* Complement-mediated cell death induced by rituximab in B-cell lymphoproliferative disorders is mediated in vitro by a caspase-independent mechanism involving the generation of reactive oxygen species. *Blood* 98, 2771–2777 (2001).

83. Al-Youssef, N. L., Ghobadloo, S. M. & Berezovski, M. V. Inhibition of complement dependent cytotoxicity by anti-CD20 aptamers. *RSC Adv.* 6, 12435–12438 (2016).

84. Rosales, C. & Uribe-Querol, E. Phagocytosis: A Fundamental Process in Immunity. *BioMed Research International* 2017, 1–18 (2017).

85. Stuart, L. M. & Ezekowitz, R. A. B. Phagocytosis. *Immunity* 22, 539–550 (2005).

86. Blach-Olszewska, Z. & Leszek, J. Mechanisms of over-activated innate immune system regulation in autoimmune and neurodegenerative disorders. *Neuropsychiatric Disease and Treatment* 3, 365–372 (2007).

87. Chen, L. *et al.* Inflammatory responses and inflammation-associated diseases in organs. *Oncotarget* 9, 7204–7218 (2018).

88. Brady, L. J. Antibody-Mediated Immunomodulation: a Strategy To Improve Host Responses against Microbial Antigens. *IAI* 73, 671–678 (2005).

89. Bayry, J. *et al.* Immunomodulation of Autoimmunity by Intravenous Immunoglobulin through Interaction with Immune Networks. *Vox Sanguinis* 83, 49–52 (2002).

90. Imbach, P. 30 years of immunomodulation by intravenous immunoglobulin. *Immunotherapy* 4, 651–654 (2012).

91. Sewell, W. A. C. & Jolles, S. Immunomodulatory action of intravenous immunoglobulin. *Immunology* 107, 387–393 (2002).

92. Nimmerjahn, F. & Ravetch, J. V. Anti-Inflammatory Actions of Intravenous Immunoglobulin. *Annu. Rev. Immunol.* 26, 513–533 (2008).

93. Prins, C., Gelfand, W. & French, L. E. Intravenous Immunoglobulin: Properties, Mode of Action and Practical Use in Dermatology. *Acta Derm Venereol* 87, 206–218 (2007).

94. Basta, M., Illa, I. & Dalakas, M. C. Increased in vitro uptake of the complement C3b in the serum of patients with Guillain–Barr6 syndrome, myasthenia gravis and dermatomyositis. 71, 227–22 (1996).

95. Basta, M., Langlois, P., Marques, M., Frank, M. M. & Fries, L. F. High-dose intravenous immunoglobulin modifies complement-mediated in vivo clearance. *Blood* 74, 326–333 (1989).

96. Basta, M. *et al.* F(ab)′2-mediated neutralization of C3a and C5a anaphylatoxins: a novel effector function of immunoglobulins. *Nat Med* 9, 431–438 (2003).

97. Roos, A. *et al.* Specific Inhibition of the Classical Complement Pathway by C1q-Binding Peptides. *J Immunol* 167, 7052–7059 (2001).

98. Roos, A., Rieben, R., Faber-Krol, M. C. & Daha, M. R. IgM-enriched human intravenous immunoglobulin strongly inhibits complement-dependent porcine cell cytotoxicity mediated by human xenoreactive antibodies. *Xenotransplantation* 10, 596–605 (2003).

99. Rieben, R. *et al.* Immunoglobulin M–Enriched Human Intravenous Immunoglobulin Prevents Complement Activation In Vitro and In Vivo in a Rat Model of Acute Inflammation. *Blood* 93, 942–951 (1999).

100. Spycher, M. *et al. In vitro* comparison of the complement-scavenging capacity of different intravenous immunoglobulin preparations. *Vox Sanguinis* 97, 348–354 (2009).

101. Frank, M. M., Basta, M. & Fries, L. F. The effects of intravenous immune globulin on complement-dependent immune damage of cells and tissues. *Clinical Immunology and Immunopathology* 62, 82–86 (1992).

102. Miletic, V. D., Hester, C. G. & Frank, M. M. Regulation of Complement Activity by Immunoglobulin. *The Journal of Immunology* 156, 749–757 (1996).

103. Mollnes, T. E. *et al.* Inhibition of Complement-Mediated Red Cell Lysis by Immunoglobulins is Dependent on the IG Isotype and its Cl Binding Properties. *Scand J Immunol* 41, 449–456 (1995).

104. Arumugam, T. V. *et al.* Intravenous immunoglobulin (IVIG) protects the brain against experimental stroke by preventing complement-mediated neuronal cell death. *Proceedings of the National Academy of Sciences* 104, 14104–14109 (2007).

105. Esen, F. *et al.* Neuroprotective effects of intravenous immunoglobulin are mediated through inhibition of complement activation and apoptosis in a rat model of sepsis. *ICMx* 5, 1 (2017).

106. Troeger, C. *et al.* Estimates of the global, regional, and national morbidity, mortality, and aetiologies of lower respiratory tract infections in 195 countries: a systematic analysis for the Global Burden of Disease Study 2015. *The Lancet Infectious Diseases* 17, 1133–1161 (2017).

107. Lanata, C. & Black, R. Acute Lower Respiratory Infections. in *Nutrition and Health in Developing Countries* (Humana Press, 2008).

108. Mahashur, A. Management of lower respiratory tract infection in outpatient settings: Focus on clarithromycin. *Lung India* 35, 143–149 (2018).

109. Mizgerd, J. P. Acute Lower Respiratory Tract Infection. *N Engl J Med* 358, 716–727 (2008).

110. Wang, H. *et al.* Global, regional, and national life expectancy, all-cause mortality, and cause-specific mortality for 249 causes of death, 1980–2015: a systematic analysis for the Global Burden of Disease Study 2015. *The Lancet* 388, 1459–1544 (2016).

111. Jain, S. *et al.* Community-Acquired Pneumonia Requiring Hospitalization among U.S. Adults. *N Engl J Med* 373, 415–427 (2015).

112. Wunderink, R. G. & Waterer, G. Advances in the causes and management of community acquired pneumonia in adults. *BMJ* 358, j2471 (2017).

113. Morgan, A. & Glossop, A. Severe community-acquired pneumonia. *BJA Education* 16, 167–172 (2016).

114. Morris, A. C. Management of pneumonia in intensive care. *J Emerg Crit Care Med* 2, 101–101 (2018).

115. Steel, H. C., Cockeran, R., Anderson, R. & Feldman, C. Overview of Community-Acquired Pneumonia and the Role of Inflammatory Mechanisms in the Immunopathogenesis of Severe Pneumococcal Disease. *Mediators of Inflammation* 2013, 1–18 (2013).

116. Siljan, W. W. *et al.* Cytokine responses, microbial aetiology and short-term outcome in community-acquired pneumonia. *Eur J Clin Invest* 48, e12865 (2018).

117. Peiris, J. S. M., Guan, Y. & Yuen, K. Y. Severe acute respiratory syndrome. *Nat Med* 10, 88–97 (2004).

118. Giamarellos-Bourboulis, E. J. *et al.* Kinetics of circulating immunoglobulin M in sepsis: relationship with final outcome. *Crit Care* 17, R247 (2013).

119. Pandya, P. H. & Wilkes, D. S. Complement System in Lung Disease. *Am J Respir Cell Mol Biol* 51, 467–473 (2014).

120. Müller-Redetzky, H., Lienau, J., Suttorp, N. & Witzenrath, M. Therapeutic strategies in pneumonia: going beyond antibiotics. *Eur Respir Rev* 24, 516–524 (2015).

121. Song, Y. *et al.* XueBiJing Injection Versus Placebo for Critically Ill Patients With Severe Community-Acquired Pneumonia: A Randomized Controlled Trial. *Critical Care Medicine* 47, 735–743 (2019).

122. Ferrer, M. *et al.* Severe community-acquired pneumonia: Characteristics and prognostic factors in ventilated and non-ventilated patients. *PLoS ONE* 13, e0191721 (2018).

123. Müller-Redetzky, H. *et al.* Neutralizing Complement C5a Protects Mice with Pneumococcal Pulmonary Sepsis. *Anesthesiology* 132, 795–807 (2020).

124. Kreymann, K. G., de Heer, G., Nierhaus, A. & Kluge, S. Use of polyclonal immunoglobulins as adjunctive therapy for sepsis or septic shock*: *Critical Care Medicine* 35, 2677–2685 (2007).

125. Harapan, H. *et al.* Coronavirus disease 2019 (COVID-19): A literature review. *Journal of Infection and Public Health* 13, 667–673 (2020).

126. Gorbalenya, A. E. *et al.* Severe acute respiratory syndrome-related coronavirus: The species and its viruses – a statement of the Coronavirus Study Group. *bioRxiv* Published ahead of print, (2020).

127. Wang, C., Horby, P. W., Hayden, F. G. & Gao, G. F. A novel coronavirus outbreak of global health concern. *The Lancet* 395, 470–473 (2020).

128. Chauhan, S. Comprehensive review of coronavirus disease 2019 (COVID-19). *Biomedical Journal* Published ahead of print, (2020).

129. Singhal, T. A Review of Coronavirus Disease-2019 (COVID-19). *Indian J Pediatr* 87, 281–286 (2020).

130. Drosten, C. *et al.* Identification of a Novel Coronavirus in Patients with Severe Acute Respiratory Syndrome. *N Engl J Med* 348, 1967–1976 (2003).

131. Zaki, A. M., van Boheemen, S., Bestebroer, T. M., Osterhaus, A. D. M. E. & Fouchier, R. A. M. Isolation of a Novel Coronavirus from a Man with Pneumonia in Saudi Arabia. *N Engl J Med* 367, 1814–1820 (2012).

132. Huang, C. *et al.* Clinical features of patients infected with 2019 novel coronavirus in Wuhan, China. *The Lancet* 395, 497–506 (2020).

133. Salje, H. *et al.* Estimating the burden of SARS-CoV-2 in France. *Science* 369, 208–211 (2020).

134. Dhama, K. *et al.* Coronavirus Disease 2019–COVID-19. *Clinical Microbiology Reviews* 33, e00028-20 (2020).

135. Mehta, P. *et al.* COVID-19: consider cytokine storm syndromes and immunosuppression. *The Lancet* 395, 1033–1034 (2020).

136. Matricardi, P. M., Dal Negro, R. W. & Nisini, R. The first, holistic immunological model of COVID-19: Implications for prevention, diagnosis, and public health measures. *Pediatr Allergy Immunol* 31, 454–470 (2020).

137. Song, P., Li, W., Xie, J., Hou, Y. & You, C. Cytokine storm induced by SARS-CoV-2. *Clinica Chimica Acta* 509, 280–287 (2020).

138. Gralinski, L. E. *et al.* Complement Activation Contributes to Severe Acute Respiratory Syndrome Coronavirus Pathogenesis. *mBio* 9, e01753-18 (2018).

139. Gao, T. *et al.* Highly pathogenic coronavirus N protein aggravates lung injury by MASP-2-mediated complement over-activation. *medRxiv* Published ahead of print, (2020).

140. Cugno, M. *et al.* Complement activation in patients with COVID-19: A novel therapeutic target. *Journal of Allergy and Clinical Immunology* 146, 215–217 (2020).

141. Magro, C. *et al.* Complement associated microvascular injury and thrombosis in the pathogenesis of severe COVID-19 infection: A report of five cases. *Translational Research* 220, 1–13 (2020).

142. Ritis, K. *et al.* A Novel C5a Receptor-Tissue Factor Cross-Talk in Neutrophils Links Innate Immunity to Coagulation Pathways. *J Immunol* 177, 4794–4802 (2006).

143. Øvstebø, R. *et al.* Microparticle-associated tissue factor activity is reduced by inhibition of the complement protein 5 in *Neisseria meningitidis* -exposed whole blood. *Innate Immun* 20, 552–560 (2014).

144. Tang, N., Li, D., Wang, X. & Sun, Z. Abnormal coagulation parameters are associated with poor prognosis in patients with novel coronavirus pneumonia. *J Thromb Haemost* 18, 844–847 (2020).

145. Cao, W. *et al.* High-Dose Intravenous Immunoglobulin as a Therapeutic Option for Deteriorating Patients With Coronavirus Disease 2019. *Open Forum Infectious Diseases* 7, ofaa102 (2020).

146. Lanza, M. *et al.* Successful intravenous immunoglobulin treatment in severe COVID-19 pneumonia. *IDCases* 21, e00794 (2020).

147. Mastaglio, S. *et al.* The first case of COVID-19 treated with the complement C3 inhibitor AMY-101. *Clinical Immunology* 215, 108450 (2020).

148. Sakoulas, G. *et al.* Intravenous Immunoglobulin (IVIG) Significantly Reduces Respiratory Morbidity in COVID-19 Pneumonia: A Prospective Randomized Trial. *medRxiv* Published ahead of print, (2020).

149. Laursen, I. A. *et al.* Development, Manufacturing and Characterization of a Highly Purified, Liquid Immunoglobulin G Preparation from Human Plasma. *Transfus Med Hemother* 41, 205–212 (2014).

150. Späth, P. J., Schneider, C. & von Gunten, S. Clinical Use and Therapeutic Potential of IVIG/SCIG, Plasma-Derived IgA or IgM, and Other Alternative Immunoglobulin Preparations. *Arch. Immunol. Ther. Exp.* 65, 215–231 (2017).

151. Shah, S. Pharmacy considerations for the use of IGIV therapy. *American Journal of Health-System Pharmacy* 62, 5–11 (2005).

152. Gelfand, E. W. Differences between IGIV products: Impact on clinical outcome. *International Immunopharmacology* 6, 592–599 (2006).

153. Siegel, J. Safety considerations in IGIV utilization. *International Immunopharmacology* 6, 523–527 (2006).

154. Kempf, C., Stucki, M. & Boschetti, N. Pathogen inactivation and removal procedures used in the production of intravenous immunoglobulins. *Biologicals* 35, 35–42 (2007).

155. Ballow, M. The IgG molecule as a biological immune response modifier: Mechanisms of action of intravenous immune serum globulin in autoimmune and inflammatory disorders. *Journal of Allergy and Clinical Immunology* 127, 315–323 (2011).

156. Dwyer, J. Manipulating the immune system with immune globulin. *New England Journal of Medicine* 326, 107–114 (1992).

157. Debre, M., Bonnet, M., Fridman, W. & Carosella, E. Infusion of Fc-gamma fragments for treatment of children with acute immune thrombocytopenic purpura. *The Lancet* 342, 945–949 (1993).

158. Kreuz, W. *et al.* A multi-centre study of efficacy and safety of Intratect®, a novel intravenous immunoglobulin preparation: A multi-centre study on Intratect. *Clinical & Experimental Immunology* 161, 512–517 (2010).

159. Colovic, M., Dimitrijevic, M., Sonnenburg, C. & Suvajdzic, N. Clinical efficacy and safety of a novel intravenous immunoglobulin preparation in adult chronic ITP. *Hematol J.* 4, 358–362 (2003).

160. Bauhofer, A., Dietrich, R. L. J. & Schmeidl, R. Safety monitoring of the intravenous immunoglobulin preparation Intratect® in primary and secondary immunodeficiencies: a prospective non-interventional study. *CP* 53, 21–30 (2015).

161. Ehrenstein, M. R. & Notley, C. A. The importance of natural IgM: scavenger, protector and regulator. *Nat Rev Immunol* 10, 778–786 (2010).

162. Schwab, I. & Nimmerjahn, F. Intravenous immunoglobulin therapy: how does IgG modulate the immune system? *Nat Rev Immunol* 13, 176–189 (2013).

163. Welte, T. *et al.* Efficacy and safety of trimodulin, a novel polyclonal antibody preparation, in patients with severe community-acquired pneumonia: a randomized, placebo-controlled, double-blind, multicenter, phase II trial (CIGMA study). *Intensive Care Med* 44, 438–448 (2018).

164. Sproston, N. R. & Ashworth, J. J. Role of C-Reactive Protein at Sites of Inflammation and Infection. *Front. Immunol.* 9, 754 (2018).

165. Duerr, C. *et al.* The novel polyclonal Ab preparation trimodulin attenuates *ex vivo* endotoxin-induced immune reactions in early hyperinflammation. *Innate Immun* 25, 374–388 (2019).

166. Rieben, R. Preclinical study with Prof. Rieben. Data not published. (2008).

167. Nolte, M. T., Pirofsky, B. & Gerritz, G. A. Intravenous immunoglobulin therapy for antibody deficiency. 36, 237–243 (1979).

168. Soderstrom, T., Soderstrom, R. & Enskog, A. Immunoglobulin subclasses and prophylactic use of immunoglobulin in immunoglobulin g subclass deficiency. 68, 1426–1429 (1991).

169. Tuomanen, E. I., Austrian, R. & Masure, H. R. Pathogenesis of Pneumococcal Infection. *The New England Journal Of Medicine* 332, 1280–1284 (1995).

170. Klein, G., Giovanella, B., Westman, A., Stehlin, J. & Mumford, D. An EBV-genome-negative cell line established from an American Burkitt lymphoma; receptor characteristics. EBV infectibility and permanent conversion into EBV-positive sublines by in vitro infection. *Intervirology* 5, 319–34 (1975).

171. Benjamin, D. *et al.* Immunoglobulin secretion by cell lines derived from African and American undifferentiated lymphomas of Burkitt's and non-Burkitt's type. *J Immunol* 129, 1336–1342 (1982).

172. Dorvignit, D. *et al.* Expression and biological characterization of an anti-CD20 biosimilar candidate antibody: A case study. *mAbs* 4, 488–496 (2012).

173. Gillissen, M. A. *et al.* The modified FACS calcein AM retention assay: A high throughput flow cytometer based method to measure cytotoxicity. *Journal of Immunological Methods* 434, 16–23 (2016).

174. Flavell, D. J. *et al.* The anti-CD20 antibody rituximab augments the immunospecific therapeutic effectiveness of an anti-CD19 immunotoxin directed against human B-cell lymphoma. *Br J Haematol* 134, 157–170 (2006).

175. Collins, S. J., Gallo, R. C. & Gallagher, R. E. Continuous growth and differentiation of human myeloid leukaemic cells in suspension culture. *Nature* 270, 347–349 (1977).

176. Breitman, T. R., Selonick, S. E. & Collins, S. J. Induction of differentiation of the human promyelocytic leukemia cell line (HL-60) by retinoic acid. *Proceedings of the National Academy of Sciences* 77, 2936–2940 (1980).

177. Collins, S. J., Ruscetti, F. W., Gallagher, R. E. & Gallo, R. C. Terminal differentiation of human promyelocytic leukemia cells induced by dimethyl sulfoxide and other polar compounds. *Proceedings of the National Academy of Sciences* 75, 2458–2462 (1978).

178. Nakayasu, M., Hecker, E. & Sugimura, T. Induction of differentiation in human promyelocytic leukemia cells by tumor promoters. *J Cancer Res Clin Oncol* 103, 17–29 (1982).

179. Birnie, G. D. The HL60 cell line: A model system for studying human myeloid cell differentiation. *Br. J. Cancer* 58, 41–45 (1988).

180. Berg, R. The indigenous gastrointestinal microflora. *Trends in Microbiology* 4, 430–435 (1996).

181. Bentley, R. & Meganathan, R. Biosynthesis of vitamin K (menaquinone) in bacteria. *Microbiological Reviews* 46, 241–280 (1982).

182. Sears, H. J., Brownlee, I. & Uchiyama, J. K. Persistence Of Individual Strains Of Escherichia Coli In The Intestinal Tract Of Man. *Journal of Bacteriology* 59, 293–301 (1950).

183. Kaper, J. B., Nataro, J. P. & Mobley, H. L. T. Pathogenic Escherichia coli. *Nat Rev Microbiol* 2, 123–140 (2004).

184. Tenaillon, O., Skurnik, D., Picard, B. & Denamur, E. The population genetics of commensal Escherichia coli. *Nat Rev Microbiol* 8, 207–217 (2010).

185. Hardwick, J. Blood processing. *ISBT Science Series* 3, 148–176 (2008).

186. Leeman, M., Choi, J., Hansson, S., Storm, M. U. & Nilsson, L. Proteins and antibodies in serum, plasma, and whole blood—size characterization using asymmetrical flow field-flow fractionation (AF4). *Anal Bioanal Chem* 410, 4867–4873 (2018).

187. Sadagopan, N. P. *et al.* Investigation of EDTA anticoagulant in plasma to improve the throughput of liquid chromatography/tandem mass spectrometric assays. *Rapid Commun. Mass Spectrom.* 17, 1065–1070 (2003).

188. Vercauteren, K. O. A., Lambrecht, S. & Delanghe, J. Preanalytical classical and alternative complement pathway activity loss. *Biochem. med. (Online)* 29, 498–505 (2019).

189. Fearon, D. T. & Austen, K. F. Activation of the alternative complement pathway due to resistance of zymosan-bound amplification convertase to endogenous regulatory mechanisms. *Proc. Natl. Acad. Sci. USA* 74, 1683–1687 (1977).

190. Di Carlo, F. J. & Fiore, J. V. On the Composition of Zymosan. *Science* 127, 756–757 (1958).

191. Bornstein, G. G. *et al.* Development of a new fully human anti-CD20 monoclonal antibody for the treatment of B-cell malignancies. *Invest New Drugs* 28, 561–574 (2010).

192. Carner, K. *et al.* Depletion of B Cells In Vivo by a Chimeric MouseHuman Monoclonal Antibody toCD20. *Blood* 83, 435–445 (1994).

193. Nahm, M. H. & Burton, R. L. Protocol for opsonophagocytic killing assay for antibodies against Group B Streptococcus (UAB GBS OPA). (2016).

194. von Behring & Kitasato. Ueber das Zustandekommen der Diphtherie-immunität und der Tetanus-immunität bei Thieren. *Deutsche Medicinische Wochenschrift* 16, 1113–1114 (1890).

195. Hooper, J. A. The history and evolution of immunoglobulin products and their clinical indications. *LymphoSign Journal* 2, 181–194 (2015).

196. Kaveri, S. V. *et al.* Intravenous immunoglobulin and immune response: IVIg and immune response. *Clin Exp Immunol* 178, 94–96 (2014).

197. Cedzyński, M., Thielens, N. M., Mollnes, T. E. & Vorup-Jensen, T. Editorial: The Role of Complement in Health and Disease. *Front. Immunol.* 10, 1869 (2019).

198. Basta, M., Fries, L. F. & Frank, M. M. High Doses of Intravenous Ig Inhibit In Vitro Uptake of C4 Fragments Onto Sensitized Erythrocytes. *Blood* 77, 376–380 (1991).

199. Kasperska-Zajac, A. *et al.* Increased serum complement C3 and C4 concentrations and their relation to severity of chronic spontaneous urticaria and CRP concentration. *J Inflamm* 10, 22 (2013).

200. Sharp, T. H. *et al.* Insights into IgM-mediated complement activation based on in situ structures of IgM-C1-C4b. *Proc Natl Acad Sci USA* 116, 11900–11905 (2019).

201. Frank, M. & Fries, L. F. Complement. in *Fundamental Immunology* 686–687 (Raven Press, 1989).

202. Frank, M. M., Miletic, V. D. & Jiang, H. Immunoglobulin in the Control of Complement Action. *IR* 22, 137–146 (2000).

203. Güven, E. *et al.* Non-specific binding in solid phase immunoassays for autoantibodies correlates with inflammation markers. *Journal of Immunological Methods* 403, 26–36 (2014).

204. Näreoja, T., Määttänen, A., Peltonen, J., Hänninen, P. E. & Härmä, H. Impact of surface defects and denaturation of capture surface proteins on nonspecific binding in immunoassays using antibody-coated polystyrene nanoparticle labels. *Journal of Immunological Methods* 347, 24–30 (2009).

205. Péterfi, Z. & Kocsis, B. Comparison of Blocking Agents for an Elisa for Lps. *Journal of Immunoassay* 21, 341–354 (2000).

206. Xiao, Y. & Isaacs, S. N. Enzyme-linked immunosorbent assay (ELISA) and blocking with bovine serum albumin (BSA)—not all BSAs are alike. *Journal of Immunological Methods* 384, 148–151 (2012).

207. Klos, A. *et al.* The role of the anaphylatoxins in health and disease. *Molecular Immunology* 46, 2753–2766 (2009).

208. Tate, J. & Ward, G. Interferences in Immunoassay. *Clin Biochem Rev* 25, 105–120 (2004).

209. Nezlin, R., Freywald, A. & Oppermann, M. Proteins separated from human IgG molecules. *Molecular Immunology* 30, 935–940 (1993).

210. Wang, B. *et al.* Regulation of antibody-mediated complement-dependent cytotoxicity by modulating the intrinsic affinity and binding valency of IgG for target antigen. *mAbs* 12, e1690959 (2020).

211. Rogers, L. M., Veeramani, S. & Weiner, G. J. Complement in monoclonal antibody therapy of cancer. *Immunol Res* 59, 203–210 (2014).

212. Jilani, I. *et al.* Transient down-modulation of CD20 by rituximab in patients with chronic lymphocytic leukemia. *Blood* 102, 3514–3520 (2003).

213. Hiraga, J. *et al.* Down-regulation of CD20 expression in B-cell lymphoma cells after treatment with rituximab-containing combination chemotherapies: its prevalence and clinical significance. *Blood* 113, 4885–4893 (2009).

214. D'Auria, F. *et al.* Modulation of CD20 antigen expression after rituximab treatment: A retrospective study in patients with chronic lymphocytic leukemia. *Clinical Therapeutics* 32, 1911–1916 (2010).

215. Pickartz, T. Selection of B-cell chronic lymphocytic leukemia cell variants by therapy with anti-CD20 monoclonal antibody rituximab. *Experimental Hematology* 29, 1410–1416 (2001).

216. Klein, C. *et al.* Epitope interactions of monoclonal antibodies targeting CD20 and their relationship to functional properties. *mAbs* 5, 22–33 (2013).

217. Peschke, B., Keller, C. W., Weber, P., Quast, I. & Lünemann, J. D. Fc-Galactosylation of Human Immunoglobulin Gamma Isotypes Improves C1q Binding and Enhances Complement-Dependent Cytotoxicity. *Front. Immunol.* 8, 646 (2017).

218. Strasser, J. *et al.* Unraveling the Macromolecular Pathways of IgG Oligomerization and Complement Activation on Antigenic Surfaces. *Nano Lett.* 19, 4787–4796 (2019).

219. Sledgei, C. R. & Bing, H. Binding Properties of the Human Complement Protein Clq. *The Journal Of Biological Chemistry* 248, 2818–2823 (1973).

220. Scitiess, J. T. T. & Engel, J. Antigen-independent activation of the first component of complement C1 by chemically crosslinkend rabbit IgG-oligomers. *FEBS Letters* 112, 152–154 (1980).

221. Diebolder, C. A. *et al.* Complement Is Activated by IgG Hexamers Assembled at the Cell Surface. *Science* 343, 1260–1263 (2014).

222. Newman, S. & Mikus, L. Deposition Of C3b And iC3b Onto Particulate Activators Of The Human Complement System. *J. ExP. MED* 161, 1414–1431 (1985).

223. Rieben, R. *et al.* Immunoglobulin M–Enriched Human Intravenous Immunoglobulin Prevents Complement Activation In Vitro and In Vivo in a Rat Model of Acute Inflammation. *Blood* 93, 942–951 (1999).

224. Schroff, R. W., Foon, K. A., Beatty, S. M., Oldham, R. K. & Morgan, A. C. Human Anti-Murine Immunoglobulin Responses in Patients Receiving Monoclonal Antibody Therapy. *Cancer Research* 45, 879–885 (1985).

225. Hosono, M. *et al.* Human/mouse chimeric antibodies show low reactivity with human anti-murine antibodies (HAMA). *Br J Cancer* 65, 197–200 (1992).

226. Hwang, W. Y. K. & Foote, J. Immunogenicity of engineered antibodies. *Methods* 36, 3–10 (2005).

227. Andersson, J., Ekdahl, K. N., Larsson, R., Nilsson, U. R. & Nilsson, B. C3 Adsorbed to a Polymer Surface Can Form an Initiating Alternative Pathway Convertase. *J Immunol* 168, 5786–5791 (2002).

228. Hed, J., Johansson, M. & Lindroth, M. Complement activation according to the alternate pathway by glass and plastic surfaces and its role in neutrophil adhesion. *Immunology Letters* 8, 295–299 (1984).

229. Müller-Redetzky, H., Lienau, J., Suttorp, N. & Witzenrath, M. Therapeutic strategies in pneumonia: going beyond antibiotics. *Eur Respir Rev* 24, 516–524 (2015).

230. Calbo, E., Alsina, M., Rodriguez-Carballeira, M., Lite, J. & Garau, J. The impact of time on the systemic inflammatory response in pneumococcal pneumonia. *European Respiratory Journal* 35, 614–618 (2010).

231. Tian, W. *et al.* Predictors of mortality in hospitalized COVID-19 patients: A systematic review and meta-analysis. *J Med Virol* 92, 1875–1883 (2020).

232. Centurión, O. A., Scavenius, K. E., García, L. B., Torales, J. M. & Miño, L. M. Potential mechanisms of cardiac injury and common pathways of inflammation in patients with COVID-19. *Crit Pathw Cardiol.* Published ahead of print, (2020).

233. Jose, R. J. & Manuel, A. COVID-19 cytokine storm: the interplay between inflammation and coagulation. *The Lancet Respiratory Medicine* 8, 46–47 (2020).

234. Giudice, V. *et al.* Combination of Ruxolitinib and Eculizumab for Treatment of Severe SARS-CoV-2-Related Acute Respiratory Distress Syndrome: A Controlled Study. *Front. Pharmacol.* 11, 857 (2020).

235. Lam, L. M. *et al.* Erythrocytes Reveal Complement Activation in Patients with COVID-19. *medRxiv* Published ahead of print, (2020).

236. Diurno, F. *et al.* Eculizumab treatment in patients with COVID-19: preliminary results from real life ASL Napoli 2 Nord experience. *European Review for Medical and Pharmacological Sciences* 24, 4040–4047 (2020).

237. Lee, J. W. *et al.* Ravulizumab (ALXN1210) vs eculizumab in adult patients with PNH naive to complement inhibitors: the 301 study. *Blood* 133, 530–539 (2019).

238. CHINA National Health Commission. Diagnosis and Treatment of Pneumonia Infected by Novel Coronavirus (Trial Version 7). *Chinese Medical Journal* 133, 1087–1095 (2020).

239. Li, T. Diagnosis and clinical management of severe acute respiratory syndrome Coronavirus 2 (SARS-CoV-2) infection: an operational recommendation of Peking Union Medical College Hospital (V2.0): Working Group of 2019 Novel Coronavirus, Peking Union Medical College Hospital. *Emerging Microbes & Infections* 9, 582–585 (2020).

240. Worley, M. J. *et al.* Neutrophils mediate HIV-specific antibody-dependent phagocytosis and ADCC. *Journal of Immunological Methods* 457, 41–52 (2018).

241. Trayner, I. D. *et al.* Changes in antigen expression on differentiating HL60 cells treated with dimethylsulphoxide, all-trans retinoic acid, h1,25-dihydroxyvitamin D3 or 12-O-tetradecanoyl phorbol-13-acetate. *Leukemia Research* 22, 537–547 (1998).

242. Verbrugge, A. Differential expression of leukocyte-associated Ig-like receptor-1 during neutrophil differentiation and activation. *Journal of Leukocyte Biology* 79, 828–836 (2006).

243. Fleck, R. A., Romero-Steiner, S. & Nahm, M. H. Use of HL-60 Cell Line To Measure Opsonic Capacity of Pneumococcal Antibodies. *CVI* 12, 19–27 (2005).

244. Fabbrini, M. *et al.* A new flow-cytometry-based opsonophagocytosis assay for the rapid measurement of functional antibody levels against Group B Streptococcus. *Journal of Immunological Methods* 378, 11–19 (2012).

245. Romero-Steiner, S. *et al.* Standardization of an opsonophagocytic assay for the measurement of functional antibody activity against Streptococcus pneumoniae using differentiated HL-60 cells. *Clinical and diagnostic laboratory immunology* 4, 415–422 (1997).

246. Chang, H., Oh, P., Ingber, D. & Huang, S. Multistable and multistep dynamics in neutrophil differentiation. *BMC Cell Biol* 7, 11 (2006).

247. Golay, J. *et al.* Human neutrophils express low levels of FcγRIIIA, which plays a role in PMN activation. *Blood* 133, 1395–1405 (2019).

248. Nuutila, J. *et al.* Quantitative analysis of complement receptors, CR1 (CD35) and CR3 (CD11b), on neutrophils improves distinction between bacterial and viral infections in febrile patients: Comparison with standard clinical laboratory data. *Journal of Immunological Methods* 315, 191–201 (2006).

249. Boonlayangoor, P., Telischi, M., Boonlayangoor, S. & Sinclair, T. Cryopreservation of human granulocytes: study ofgranulocyte function and ultrastructure. *Blood* 56, 237–245 (1980).

250. Yaseen, R. *et al.* Antimicrobial activity of HL-60 cells compared to primary blood-derived neutrophils against Staphylococcus aureus. *J Negat Results BioMed* 16, 2 (2017).

251. Burton, R. L. & Nahm, M. H. Development and Validation of a Fourfold Multiplexed Opsonization Assay (MOPA4) for Pneumococcal Antibodies. *CVI* 13, 1004–1009 (2006).

252. Abbanat, D. *et al.* Development and Qualification of an Opsonophagocytic Killing Assay To Assess Immunogenicity of a Bioconjugated Escherichia coli Vaccine. *Clin. Vaccine Immunol.* 24, e00123-17 (2017).

253. Burton, R. L. & Nahm, M. H. Development of a Fourfold Multiplexed Opsonophagocytosis Assay for Pneumococcal Antibodies against Additional Serotypes and Discovery of Serological Subtypes in Streptococcus pneumoniae Serotype 20. *Clin. Vaccine Immunol.* 19, 835–841 (2012).

254. Okamoto, M. *et al.* Toll-like Receptors (TLRs) are expressed by myeloid leukaemia cell lines, but fail to trigger differentiation in response to the respective TLR ligands. *British Journal of Haematology* 147, 585–587 (2009).

255. Iwasaki, A. & Medzhitov, R. Toll-like receptor control of the adaptive immune responses. *Nat Immunol* 5, 987–995 (2004).

256. Hayashi, F., Means, T. K. & Luster, A. D. Toll-like receptors stimulate human neutrophil function. *Blood* 102, 2660–2669 (2003).

257. Sabroe, I., Dower, S. K. & Whyte, M. K. B. The Role of Toll-Like Receptors in the Regulation of Neutrophil Migration, Activation, and Apoptosis. *Clinical Infectious Diseases* 41, 421–426 (2005).

258. Beutler, B. Tlr4: central component of the sole mammalian LPS sensor. *Current Opinion in Immunology* 12, 20–26 (2000).

259. Chow, J. C., Young, D. W., Golenbock, D. T., Christ, W. J. & Gusovsky, F. Toll-like Receptor-4 Mediates Lipopolysaccharide-induced Signal Transduction. *J. Biol. Chem.* 274, 10689–10692 (1999).

260. Brouwer, N. *et al.* Mannose-Binding Lectin (MBL) Facilitates Opsonophagocytosis of Yeasts but Not of Bacteria despite MBL Binding. *J Immunol* 180, 4124–4132 (2008).

261. Perobelli, S. M. *et al.* Plasticity of neutrophils reveals modulatory capacity. *Braz J Med Biol Res* 48, 665–675 (2015).

262. Mladenov, R. *et al.* The Fc-alpha receptor is a new target antigen for immunotherapy of myeloid leukemia: Targeting and Elimination of Malignant Myeloid Cells. *Int. J. Cancer* 137, 2729–2738 (2015).

263. Aleyd, E. *et al.* IgA Enhances NETosis and Release of Neutrophil Extracellular Traps by Polymorphonuclear Cells via Fcα Receptor I. *J.I.* 192, 2374–2383 (2014).

264. Lutz, H., Stammler, P., Jelezarova, E., Nater, M. & Spath, P. High doses of immunoglobulin G attenuate immune aggregate-mediated complement activation by enhancing physiologic cleavage of C3b in C3bn- IgG complexes. *Blood* 88, 184–193 (1996).

265. Durandy, A. *et al.* Intravenous immunoglobulins - understanding properties and mechanisms. *Clinical & Experimental Immunology* 158, 2–13 (2009).

266. Molecular Probes. BioParticles Fluorescent Particles and Opsonizing Reagents (product information). (2001).

267. Leemans, J. C., Heikens, M., van Kessel, K. P. M., Florquin, S. & van der Poll, T. Lipoteichoic Acid and Peptidoglycan from Staphylococcus aureus Synergistically Induce Neutrophil Influx into the Lungs of Mice. *CVI* 10, 950–953 (2003).

268. Wang, J. E. *et al.* Peptidoglycan and Lipoteichoic Acid from Staphylococcus aureus Induce Tumor Necrosis Factor Alpha, Interleukin 6 (IL-6), and IL-10 Production in Both T Cells and Monocytes in a Human Whole Blood Model. *Infect. Immun.* 68, 3965–3970 (2000).

269. Fournier, B. The function of TLR2 during staphylococcal diseases. *Front. Cell. Inf. Microbio.* 2, 167 (2013).

270. Gelfand, E. W. Intravenous Immune Globulin in Autoimmune and Inflammatory Diseases. *N Engl J Med* 367, 2015–2025 (2012).

271. Galeotti, C., Kaveri, S. V. & Bayry, J. IVIG-mediated effector functions in autoimmune and inflammatory diseases. *International Immunology* 29, 491–498 (2017).

272. Shock, A., Humphreys, D. & Nimmerjahn, F. Dissecting the mechanism of action of intravenous immunoglobulin in human autoimmune disease: lessons from therapeutic modalities targeting Fcγ receptors. *Journal of Allergy and Clinical Immunology* 146, 492–500 (2020).

273. Nagelkerke, S. Q. *et al.* Inhibition of FcgR-mediated phagocytosis by IVIg is independent of IgG-Fc sialylation and FcgRIIb in human macrophages. *Blood* 124, 3709–3718 (2014).

274. Nagelkerke, S. Q. & Kuijpers, T. W. Immunomodulation by IVIg and the Role of Fc-Gamma Receptors: Classic Mechanisms of Action after all? *Front. Immunol.* 5, 674 (2015).

275. Walpen, A. J., Laumonier, T., Aebi, C., Mohacsi, P. J. & Rieben, R. Immunoglobulin M-enriched intravenous immunoglobulin inhibits classical pathway complement activation, but not bactericidal activity of human serum. *Xenotransplantation* 11, 141–148 (2004).

276. Wagner, E., Platt, J. L. & Frank, M. M. High Dose Intravenous Immunoglobulin Does Not Affect Complement-Bacteria Interactions. *The Journal of Immunology* 160, 1936–1943 (1998).

277. Gilbert, I. Dissociation in an Encapsulated Staphylococcus. *Journal of Bacteriology* 21, 157–160 (1931).

278. O'Riordan, K. & Lee, J. C. Staphylococcus aureus Capsular Polysaccharides. *CMR* 17, 218–234 (2004).

279. Hageman, J. C. *et al.* Severe Community-acquired Pneumonia Due to *Staphylococcus aureus* , 2003–04 Influenza Season. *Emerg. Infect. Dis.* 12, 894–899 (2006).

280. Self, W. H. *et al. Staphylococcus aureus* Community-acquired Pneumonia: Prevalence, Clinical Characteristics, and Outcomes. *Clin Infect Dis.* 63, 300–309 (2016).

281. de la Torre, M. C. *et al.* Serum levels of immunoglobulins and severity of community-acquired pneumonia. *BMJ Open Resp Res* 3, e000152 (2016).

282. Bermejo-Martín, J. F. *et al.* Immunoglobulins IgG1, IgM and IgA: a synergistic team influencing survival in sepsis. *J Intern Med* 276, 404–412 (2014).

283. Rice, T. W. *et al.* Critical illness from 2009 pandemic influenza A virus and bacterial coinfection in the United States*: *Critical Care Medicine* 40, 1487–1498 (2012).

284. Zahariadis, G. *et al.* Risk of Ruling out Severe Acute Respiratory Syndrome by Ruling in another Diagnosis: Variable Incidence of Atypical Bacteria Coinfection Based on Diagnostic Assays. *Canadian Respiratory Journal* 13, 17–22 (2006).

285. Arabi, Y. M. *et al.* Critically Ill Patients With the Middle East Respiratory Syndrome: A Multicenter Retrospective Cohort Study. *Critical Care Medicine* 45, 1683–1695 (2017).

286. Lansbury, L., Lim, B., Baskaran, V. & Lim, W. S. Co-infections in people with COVID-19: a systematic review and meta-analysis. *Journal of Infection* 81, 266–275 (2020).

287. Crotty, M. P. *et al.* Investigation of subsequent and co-infections associated with SARS-CoV-2 (COVID-19) in hospitalized patients. *medRxiv* Published ahead of print, (2020).

288. Chen, X. *et al.* Epidemiological and clinical features of 291 cases with coronavirus disease 2019 in areas adjacent to Hubei, China: a double-center observational study. *medRxiv* Published ahead of print, (2020).

289. Xing, Q., Li, G., Xing, Y. & Chen, T. Precautions are Needed for COVID-19 Patients with Coinfection of Common Respiratory Pathogens. *medRxiv* Online ahead of print, 24 (2020).

290. Chen, J., Wu, H., Yu, Y. & Tang, N. Pulmonary alveolar regeneration in adult COVID-19 patients. *Cell Res* 30, 708–710 (2020).

291. Zhou, F. *et al.* Clinical course and risk factors for mortality of adult inpatients with COVID-19 in Wuhan, China: a retrospective cohort study. *The Lancet* 395, 1054–1062 (2020).

292. Shao, W. *et al.* Epithelial cells are a source of natural IgM that contribute to innate immune responses. *The International Journal of Biochemistry & Cell Biology* 73, 19–29 (2016).

## List of abbreviations

| | |
|---|---|
| ADCC | Antibody-dependent cell-mediated cytotoxicity |
| ADCP | Antibody-dependent cellular phagocytosis |
| ANOVA | Analysis of variance |
| APC | Allophycocyanin |
| ARDS | Acute respiratory distress syndrome |
| ATCC | American Type Culture Collection |
| BCR | B-cell receptor |
| C1INH | C1 inhibitor |
| CAP | Community-acquired pneumonia |
| CDC | Complement-dependent cytotoxicity |
| CFH | Complement factor H |
| CFI | Complement factor I |
| CFU | Colony-forming units |
| CH | Constant domain heavy chain |
| CIDP | Chronic inflammatory demyelinating polyneuropathy |
| CL | Constant domain light chain |
| COVID-19 | Coronavirus disease 2019 |
| CR1 | Complement receptor 1 |
| CR3 | Complement receptor 3 |
| CRP | C-reactive protein |
| DMF | Dimethylformamide |
| DMSO | Dimethyl sulfoxide |
| D-PBS | Dulbecco's PBS |
| *E. coli* | Escherichia coli |
| EDTA | Ethylenediaminetetraacetic acid |
| e.g. | Exempli gratia |
| FACS | Fluorescence-activated cell sorter |
| FB | Formulation buffer |
| FBS | Fetal bovine serum |
| Fc$\mu$R | Fc$\mu$ receptor |
| FcαRI | Fcα receptor I |
| FcγR | Fcγ receptor |
| FcγRIIB | Fcγ receptor II B |
| FITC | Fluorescein isothiocyanate |
| FSC | Forward scatter |

| | |
|---|---|
| $GVB^{++}$ | Gelatin Veronal Buffer with $Mg^{2+}$ and $Ca^{2+}$ |
| h | Hour |
| HACA | Human anti-chimeric antibodies |
| HAMA | Human anti-murine antibodies |
| HBSS | Hanks' Balanced Salt Solution |
| hi | Heat-inactivated |
| HRP | Horseradish peroxidase |
| ICU | Intensive care unit |
| Ig | Immunoglobulin |
| IgA | Immunoglobulin A |
| IgG | Immunoglobulin G |
| IgM | Immunoglobulin M |
| IL-1β | Interleukin-1β |
| IL-6 | Interleukin-6 |
| IV | Intravenous |
| IVIg | Intravenous immunoglobulin |
| kDa | Kilo Dalton |
| LB | Lysogeny broth |
| LPS | Lipopolysaccharide |
| LRI | Lower respiratory tract infections |
| LTA | Lipoteichoic acid |
| MAC | Membrane attack complex |
| MASP | MBL-associated serine proteases |
| MBL | Mannose-binding lectin |
| MERS | Middle East respiratory syndrome |
| min | Minute |
| MMN | Multifocal motor neuropathy |
| MoA | Mode of Action |
| MW Marker | Molecular weight marker |
| N | Nucleocapsid |
| NADPH | Nicotinamide adenine dinucleotide phosphate |
| NET | Neutrophil extracellular traps |
| NHS | Normal human serum |
| NHS minus | Normal human serum depleted of IgG and IgM |
| NK cell | Natural killer cell |
| OB | Opsonization buffer |

| | |
|---|---|
| OD | Optical density |
| OPA | Opsonophagocytosis assay |
| PAMP | Pathogen-associated molecular patterns |
| PBS | Phosphate-buffered saline |
| PE | Phycoerythrin |
| PI | Propidiumiodid |
| PID | Primary immunodeficiency |
| pIgR | Polymeric Ig receptor |
| PMN | Polymorphonuclear |
| PMT | Photomultiplier tube |
| RBC | Red blood cell |
| ROS | Reactive oxygen species |
| RT | Room temperature |
| *S. aureus* | *Staphylococcus aureus* |
| SARS | Severe acute respiratory syndrome |
| SARS-CoV-2 | Severe acute respiratory syndrome coronavirus 2 |
| sCAP | Severe community-acquired pneumonia |
| SDS-PAGE | Sodium dodecyl sulfate polyacrylamide gel electrophoresis |
| SEM | Standard error of the mean |
| SID | Secondary immunodeficiency |
| sIgA | Secretory IgA |
| SSC | Sideward scatter |
| TBS-T | Tris-buffered saline with tween 20 |
| TLR | Toll-like receptor |
| TMB | Tetramethylbenzidine substrate |
| TNF | Tumor necrosis factor |
| TPA | 12-O-tetradecanoylphorbol-13-acetate |
| U | Round bottom |
| VH | Variable domain heavy chain |
| VL | Variable domain light chain |
| w/o | Without |

## List of figures

## List of tables

## Acknowledgements

An dieser Stelle möchte ich mich bei allen Personen bedanken, die zum Gelingen meiner Dissertation beigetragen und mich während dieser besonderen Zeit unterstützt haben.

Zu Beginn bedanke ich mich bei meinem Doktorvater, Prof. Dr. Harald Kolmar, für die problemlose Betreuung meiner externen Promotion und für das Interesse an meinem Thema. Unsere Gespräche und Treffen haben mich immer ein Stückchen weitergebracht und mir viele hilfreiche Anregungen gegeben. Für diese Unterstützung, vor allem auch in der Endphase der Promotion, bedanke ich mich sehr.

Weiterhin gilt mein Dank meinem Korreferenten PD Dr. med. Dr. med. habil. Jörg Schüttrumpf, der es mir möglich machte, meine Doktorarbeit bei der Biotest AG anzufertigen und bei aufkommenden Fragen stets für mich da war. Vielen Dank für die Übernahme des Zweitgutachtens und für die Betreuung während meiner Promotion.

Bedanken möchte ich mich ebenso bei Prof. Dr. Katja Schmitz und apl. Prof. Dr. Zoe Waibler, dass sie meine Fachprüfer waren.

Ein ganz besonderer Dank gilt meinen Kollegen bei der Biotest AG, ohne die diese Arbeit nicht möglich gewesen wäre. Bei meinem internen Betreuer, Dr. Martin König, bedanke ich mich sehr für die vielen hilfreichen Meetings, Gespräche und konstruktiven Ratschläge. Unsere Diskussionsrunden in den Laborbesprechungen (mit Kaffee und Süßigkeiten) haben mir immer sehr geholfen neue Ideen zu entwickeln und mich somit meinem Ziel ein Stückchen weiter entgegengebracht. Danke auch für die Korrektur meiner Dissertation. Ein ganz herzlicher Dank gilt ebenso Dr. Sabrina Weißmüller, die jederzeit für mich da war und von der ich sehr viel lernen konnte. Sowohl auf menschlicher, als auch auf fachlicher Ebene war es mir immer eine Freude mit ihr zusammenzuarbeiten. Das Korrekturlesen meiner Arbeit und die vielen ermutigenden Gespräche haben mir sehr geholfen. Danke für diese besondere Unterstützung und für die unerlässliche sowie intensive Betreuung. Weiterhin möchte ich mich bei Dr. Corina Cornelia Heinz für ihre vielen Anregungen, Ideen und Hilfestellungen während meiner Promotion bedanken. Ihr großes Interesse und ihr Fachwissen begeisterten mich ausgesprochen und bereicherten meine Arbeit. Ich konnte mich stets auf sie verlassen und unsere vielen Meetings sowie Diskussionen waren immer sehr wertvoll für den Fortschritt der Dissertation. Danke für die intensive Hilfsbereitschaft und die vielen nützlichen Tipps, vor allem in stressigen und schwierigen Situationen.

Weiterhin möchte ich mich ebenso bei Dr. Matthias Germer für die Unterstützung und Hilfestellungen währen meiner gesamten Promotion bedanken. Dr. Tobias Roeser gilt ein Dank für die Beratung in patentrechtlichen Fragestellungen und Alexander Staus für die Hilfe in der statistischen Auswertung meiner Arbeit.

Ebenso möchte ich mich bei der Abteilung Bioanalytik bedanken, die es mir ermöglichte ihre Labore mitzubenutzen und stets ein offenes Ohr bei aufkommenden Fragen für mich hatte. Die Zusammenarbeit war ausgesprochen angenehm und ich konnte sehr viele tolle Menschen kennenlernen, die mich in schwierigen Zeiten immer unterstützt und mir wieder ein Lächeln auf das Gesicht gezaubert haben.

Außerdem bedanke ich mich bei Fabian Bohländer, mit dem ich jederzeit über die Schwierigkeiten des Doktorandenalltags diskutieren, lachen und konstruktive Lösungen erarbeiten konnte. Ohne ihn wäre unsere Zellkultur so nicht möglich gewesen.

Ein Dank gilt ebenso Dr. Karina Winterling und Dr. Peter Herbener, die stets ein offenes Ohr für mich hatten, sich immer Zeit für mich nahmen und mir in vielen Situationen mit Rat und Tat zur Seite standen.

Herrn Prof. Dr. Kirschfink danke ich für seine hilfreichen Anregungen zu meiner Doktorarbeit und seinem Team für die Unterstützung bei der Komplementanalytik.

Außerdem möchte ich mich ganz besonders bei meinen Eltern bedanken, die mich stets mit aller Kraft unterstützen und mir mit ihrer liebevollen Fürsorge sowie Hilfsbereitschaft diese Zeit um ein Vielfaches erleichtert haben. Ich konnte mich immer bedingungslos auf sie verlassen, was mir sehr viel Kraft gespendet und zum Gelingen dieser Promotion beigetragen hat.

Schließlich danke ich von ganzem Herzen meinem Freund, für seine Liebe und Geduld während dieser Zeit sowie in den vergangenen Jahren. Seine Hilfe, Gelassenheit und seine positive Art haben mich gerade in Zeiten der Erschöpfung immer wieder motiviert und mir die Kraft gegeben weiterhin meine Träume zu verfolgen. Danke für diese liebevolle und wichtige Unterstützung.